Impactos del desarrollo del riego en la calidad de agua en la cuenca del río San Salvador: modelación e implementación de escenarios en SWAT

Florencia Hastings Viñas

Magíster en Ciencias Agrarias
Opción Ciencias del Suelo

Febrero 2024

Impactos del desarrollo del riego en la calidad de agua en la cuenca del río San Salvador: modelación e implementación de escenarios en SWAT

Florencia Hastings Viñas

Magíster en Ciencias Agrarias
Opción Ciencias del Suelo

Febrero 2024

Tesis aprobada por el tribunal integrado por el PhD. Valentín Picasso, el Dr. Christian Chreties y la Dra. Lorena Rodríguez el 14 de diciembre de 2023. Autora: Ing. Civil Hidr. Amb. Florencia Hastings Viñas. Director: PhD. Mario Pérez-Bidegain. Codirectora: PhD. Angela Gorgoglione. Codirector: PhD. Rafael Navas.

AGRADECIMIENTOS

A mi familia y amigos, por el apoyo incondicional.

A mis tutores, por la guía y la dedicación.

A los colegas que aportaron información y discusiones valiosas.

A todos los que de alguna forma u otra formaron parte de esta etapa.

A la Agencia Nacional de Investigación e Innovación y a la Dirección de Recursos Naturales del Ministerio de Ganadería, Agricultura y Pesca, que aportaron en la financiación de la investigación.

RESUMEN

En el contexto global de aumento en la demanda de alimentos, la intensificación agrícola sostenible y la adaptación climática son desafíos cruciales. El riego se posiciona como una estrategia clave para la intensificación agrícola. No obstante, es importante abordar los impactos ambientales de la intensificación agrícola y el riego. La tesis de maestría se enfocó en cuantificar el impacto del desarrollo del riego suplementario de cultivos de verano en la cuenca del río San Salvador mediante el uso del modelo SWAT y se documentó en tres artículos científicos. En el primer artículo, se utilizaron herramientas de código abierto para mapear la cobertura del suelo en 1990, proporcionando una base para la conceptualización del modelo a lo largo del tiempo. El segundo artículo se centró en la implementación del modelo SWAT y la caracterización de flujos en la cuenca del río San Salvador. Se realizó la calibración y validación del caudal y se obtuvieron resultados satisfactorios. También se validó la capacidad del modelo para representar procesos biofísicos y la calidad del agua. El tercer artículo evaluó escenarios de desarrollo del riego, mostrando impactos positivos en rendimientos, pero también aumentos en la exportación de sedimentos y nutrientes. Las zonas *buffer* ribereñas se identificaron como efectivas para mejorar la calidad del agua, aunque se requerirían medidas adicionales para lograr un escenario ambientalmente sostenible. Se alcanzaron con éxito los objetivos propuestos para la tesis. El modelo SWAT se implementó, calibró y validó en la cuenca del río San Salvador, y fue comprobada su capacidad para representar procesos biofísicos y la calidad del agua. Además, se identificaron oportunidades y limitaciones para la aplicación del modelo en Uruguay, destacando la necesidad de mejorar los datos de caudales y calidad del agua. Es importante considerar la incertidumbre asociada a los resultados del modelo: para disminuirla son necesarios mayores esfuerzos de monitoreo. En resumen, la tesis contribuye significativamente al entendimiento de la relación entre el uso del suelo y la calidad del agua en la cuenca del río San Salvador. Además, proporciona una herramienta práctica para la planificación y gestión de recursos naturales en la cuenca.

Palabras clave: intensificación agrícola sostenible, riego, SWAT, calidad de agua, cuenca del río San Salvador

IMPACTS OF IRRIGATION DEVELOPMENT ON WATER QUALITY IN THE SAN SALVADOR WATERSHED: MODELING AND IMPLEMENTATION OF SCENARIOS IN SWAT

SUMMARY

In the global context of rising food demand, sustainable agricultural intensification and climate adaptation emerge as crucial challenges. Irrigation is identified as a crucial strategy for agricultural intensification. This master's thesis focused on quantifying the impact of supplementary irrigation development for summer crops in the San Salvador River basin using the SWAT model, documented across three scientific articles. In the first article, open-source tools were used to map land use in 1990, forming the model's conceptual basis. The second article focused on implementing the SWAT model and characterizing the streamflow and nutrient balance in the San Salvador River basin. Calibration and validation of the flow were conducted, obtaining satisfactory results. Additionally, the model's capacity to represent biophysical processes and water quality was validated. The third article evaluated irrigation development scenarios, revealing positive crop yield impacts alongside increased sediment and nutrient export. Riparian buffer zones were identified as effective in improving water quality, though additional measures would be needed for environmental sustainability. The thesis successfully achieved its objectives, implementing, calibrating, and validating the SWAT model in the San Salvador River basin. It identified opportunities and limitations for model application in Uruguay, emphasizing the need to enhance streamflow and water quality data. Recognizing uncertainty in model results, addressing it requires increased monitoring efforts. In summary, the thesis significantly contributes to understanding the relationship between land use and water quality in the San Salvador River basin. Furthermore, it provides a practical tool for planning and managing natural resources in the basin.

Keywords: sustainable agricultural intensification, irrigation, SWAT, water quality, San Salvador River basin

TABLA DE CONTENIDO

1 INTRODUCCIÓN GENERAL

1.1 CONTEXTO

En el contexto actual, caracterizado por una creciente demanda global de alimentos y bajo la premisa de alcanzar el segundo objetivo de desarrollo sostenible para lograr la seguridad alimentaria y promover la agricultura sostenible (Naciones Unidas, 2018), la intensificación agrícola y la adaptación a la variabilidad climática constituyen desafíos de suma importancia. De acuerdo con algunas proyecciones, se estima un aumento de la demanda global de alimentos que oscilará entre un 35 % y un 56 % para el período comprendido entre 2010 y 2050 (van Dijk et al., 2021). En este sentido, se promueve una agricultura sostenible adaptada al clima, la cual busca incrementar la productividad de manera sostenible, mejorar la resiliencia, reducir o eliminar las emisiones de gases de efecto invernadero y promover el desarrollo y la seguridad alimentaria (FAO, 2013). Se estima que la expansión del riego sostenible en áreas actualmente dedicadas a la agricultura de secano podría disminuir hasta un 80 % de la brecha existente entre la disponibilidad y la demanda global de alimentos (Beltran-Peña et al., 2020). En este marco, el riego se posiciona como una estrategia clave para la intensificación agrícola (Foley et al., 2011). Además, el almacenamiento de agua con fines de riego ha demostrado ser un componente crucial para aumentar la capacidad de adaptación a la variabilidad climática (Rosa, 2022, Hansen et al., 2011).

En el ámbito local, existe una política pública orientada al desarrollo del riego: Estrategia de Fomento del Desarrollo de la Agricultura Regada en Uruguay (MGAP, 2015). Esta estrategia reconoce al riego suplementario de cultivos (cereales y oleaginosos de verano) y pasturas, como una herramienta clave para mitigar la vulnerabilidad climática en los sistemas agrícolas, incrementar los rendimientos potenciales de los cultivos y mejorar la eficiencia en el uso del agua. Se señala que las posibilidades de utilizar fuentes subterráneas o captar agua directamente de los cursos de agua son limitadas en varias regiones del país, por lo tanto, se fomenta la construcción de reservas de agua asociativas con fines de riego. En lo que respecta al marco normativo, se promulgó la ley 19.553 en 2017, acompañada por el Decreto Reglamentario N° 366 de 2018, los cuales modifican las disposiciones anteriores

vinculadas al riego agrícola. Este marco legal introduce conceptos clave, como los caudales ambientales, y establece un proceso explícito para la autorización ambiental en proyectos de riego.

No obstante, es importante abordar los impactos ambientales de la intensificación agrícola y el riego. La intensificación agrícola implica un aumento en el uso de fertilizantes (Scholz et al., 2013) lo cual puede conllevar a la eutrofización de los cuerpos de agua, y la degradación de los ecosistemas acuáticos (Goyenola et al., 2021, Aubriot et al., 2017, Barreto et al., 2017, Rodríguez-Gallego et al., 2017, Lizarralde et al., 2016, Goyenola et al., 2015, LeBlanc et al., 2009, Scanlon et al., 2007, Carpenter et al., 1998). Es importante resaltar que los impactos ambientales del riego dependen de numerosos factores, entre otros: del método de riego (superficie, aspersión, localizado), del manejo agrícola (dosis y método de aplicación de agroquímicos, densidad de plantas, sistematización de chacras, etc.), las condiciones climáticas (climas áridos a húmedos, variabilidad y cambio climático), clases de suelo, la calidad del agua utilizada para riego y los múltiples usos del agua. En cuencas donde se utilizan sistemas de riego de baja eficiencia (por ejemplo, riego por inundación) se generan flujos de retorno subsuperficial que aumentan los caudales en los cursos de agua cercanos, mientras que en otras cuencas donde se utilizan sistemas de riego de alta eficiencia (por ejemplo, riego por pivots), el área de riego no queda conectada hidrológicamente a los cursos de agua cercanos y el agua de riego sale efectivamente de la cuenca por la evapotranspiración de los cultivos (Ketchum et al, 2023).

Un manejo adecuado del riego y la fertilización disponibiliza nitrógeno y fósforo para alcanzar los rendimientos óptimos de los cultivos, minimizando las pérdidas de nutrientes, en contraste, una aplicación excesiva de riego puede causar pérdidas de nutrientes a los cursos de agua y acuíferos (Wang et al., 2021, Sigua et al., 2020, Smilovic et al., 2019, Sigua et al., 2017). La pérdida de fósforo soluble es un problema potencial solo a altas tasas de riego (Shuman, 2001), mientras que el nitrógeno se lixivia más fácilmente (Merchan et al., 2015, Pinardi et al., 2018). Por otra parte, los impactos ambientales del riego pueden variar según la escala de análisis. A escala predial, el riego puede aumentar los rendimientos, pero no necesariamente se detecta una diferencia en el balance de nutrientes en comparación con los cultivos de secano

(Darré et al., 2018). A menudo, los estudios a escala predial no reflejan las complejas interacciones que ocurren a escala de cuenca, donde factores como la configuración del paisaje, las prácticas agrícolas, el transporte de sedimentos y nutrientes, y los múltiples usos del suelo ejercen un impacto significativo en la calidad del agua (Merriman et al., 2009).

En particular, este trabajo contribuye al estudio de los impactos en la cantidad calidad del agua de una cuenca donde se planifica el desarrollo del riego suplementario mediante pivots de cultivos extensivos de verano. Este campo de estudio en Uruguay es aún incipiente (Darré et al. 2019).

1.2 MOTIVACIÓN

El estudio del impacto del uso y manejo del suelo en la calidad del agua emerge como un campo crítico de investigación científica contemporánea, con implicancias en la gestión de los recursos naturales y la planificación del uso del suelo. Para comprender mejor estos procesos y sus efectos en la calidad del agua a escala de cuenca, se recurre a modelos como el Soil & Water Assessment Tool (SWAT) (Arnold et al., 1998). Este modelo biofísico, desarrollado tras cuatro décadas de investigación conjunta entre el Servicio de Conservación de Recursos Naturales del Departamento de Agricultura de los Estados Unidos (USDA/NRCS) y la Universidad Texas A&M, permite predecir el impacto de las prácticas de uso y manejo del suelo en la cantidad y calidad del agua en cuencas con características complejas. SWAT se ha convertido en una herramienta interdisciplinaria ampliamente aceptada para la modelación de cuencas y cuenta con un sólido respaldo en la literatura científica. Para una representación precisa de los procesos biofísicos se consideran tanto datos cuantitativos (*hard data*) como información cualitativa (*soft data*) para la calibración y validación del modelo (Nelson et al., 2018). Los datos cuantitativos comprenden series temporales medidas a largo plazo, mientras que los datos cualitativos abarcan información relacionada con procesos específicos que no son medidos directamente, como estimaciones anuales promedio.

1.3 HIPÓTESIS

En este contexto, se plantean tres hipótesis fundamentales que orientan la investigación:

1. El modelo SWAT es adecuado para representar los procesos biofísicos y la calidad del agua en la cuenca del río San Salvador. Esta hipótesis se sustenta en la premisa de que SWAT, un modelo hidrológico ampliamente utilizado, puede ajustarse a las condiciones específicas de esta cuenca.
2. Se puede suplir la escasez de datos e implementar un modelo confiable que aborde la gestión en la cantidad y calidad del agua, teniendo en cuenta el impacto del uso del suelo. Esta hipótesis subraya la importancia de desarrollar métodos robustos para abordar problemas de datos limitados. Además de la calibración de caudales, se emplea la calibración blanda para validar los procesos biofísicos en el modelo.
3. Existe una combinación de buenas prácticas agrícolas y medidas de conservación que minimizan los impactos de la agricultura irrigada en la calidad del agua.

1.4 OBJETIVOS

El objetivo general del trabajo es implementar una herramienta que cuantifique el impacto del desarrollo del riego en la cantidad y calidad del agua a escala de cuenca en la cuenca del río San Salvador. Los objetivos específicos son:

1. Explorar el modelo SWAT: implementar, calibrar y validar el modelo en la cuenca del río San Salvador, evaluar su capacidad para representar los procesos hidrológicos y la calidad del agua.
2. Evaluar la idoneidad y el desempeño del modelo para ser aplicado en el contexto específico de Uruguay, e identificar oportunidades y limitaciones.
3. Evaluar los potenciales impactos en la cantidad y calidad del agua en la cuenca del río San Salvador bajo diferentes escenarios, que incluyen el desarrollo de la agricultura irrigada y la aplicación de buenas prácticas agrícolas y medidas de conservación, como zonas *buffer* y caudales ambientales.

1.5 APLICACIÓN DE LA INVESTIGACIÓN

Esta investigación tiene una aplicación práctica y relevante en la planificación y gestión del uso del suelo sustentable, así como en la toma de decisiones relacionadas con el desarrollo del riego en la cuenca del río San Salvador. La herramienta implementada permite evaluar e incorporar los impactos en la cantidad y calidad del agua en la toma de decisiones. Por ejemplo, podría contribuir como instrumento en una futura evaluación ambiental estratégica para un Programa de promoción del riego en la cuenca del río San Salvador (Decreto n° 366, 2018). Asimismo, en el ámbito de la gestión, podría facilitar la evaluación de medidas para un plan de acción para la protección de la calidad ambiental. De esta manera, esta investigación proporciona una base científica sólida para abordar los desafíos que enfrenta esta cuenca en su búsqueda de un desarrollo de la agricultura irrigada sostenible y la preservación de sus recursos hídricos.

1.6 ESTRUCTURA DEL DOCUMENTO

Esta tesis se presenta en formato de artículo científico e incorpora tres artículos (el primero publicado y los restantes aprobados para su publicación) que abordan las cuestiones mencionadas en el contexto de la cuenca del río San Salvador en Uruguay. Los artículos se centran en (1) la identificación del uso del suelo mediante imágenes satelitales para la conceptualización del modelo (Hastings et al., 2020), (2) la implementación del modelo y la caracterización de flujos (Hastings et al., 2023a) y (3) la aplicación del modelo en la simulación de escenarios (Hastings et al., 2023b).

La estructura del documento comprende los siguientes capítulos:

En el capítulo 1, se aborda la «Introducción general», donde se contextualiza el estudio, se justifica la motivación de la investigación y se delinean las hipótesis y objetivos del trabajo. Además, se exploran posibles aplicaciones prácticas derivadas de los resultados de la investigación.

En el capítulo 2, se presenta el primer artículo, titulado *Land-cover mapping of agricultural areas using machine learning in Google Earth Engine* (Hastings et al., 2020), el cual se centra en generar un mapa de cobertura/uso del suelo para el año 1990

en la cuenca del río San Salvador. Se utilizaron imágenes satelitales Landsat 5 y técnicas de *machine learning* en la plataforma Google Earth Engine (GEE). El mapa generado se verifica y muestra concordancia con el censo agropecuario de 1990 (MGAP-DIEA, 1994). Se destaca el uso de GEE, que facilita el acceso a datos satelitales en la nube y proporciona capacidad de procesamiento gratuita. Este mapa se utiliza luego como dato de entrada para definir la conceptualización del modelo a través de las unidades de respuesta hidrológica.

En el capítulo 3, se presenta el segundo artículo, titulado *Impactos del desarrollo del riego en la calidad de agua en la cuenca del río San Salvador (Parte 1): Análisis de la exportación y transporte de nutrientes actual mediante SWAT* (Hastings et al., 2023a), el cual tiene como objetivo principal caracterizar los procesos hidrológicos y los procesos de exportación y transporte de sedimentos y nutrientes en esta cuenca mediante el uso del modelo SWAT. Además, se aplica metodología de US EPA (2007) para analizar, mediante curvas de frecuencia, las cargas de nutrientes simuladas con relación a las cargas admisibles y caracterizar las fuentes de nutrientes para las diferentes zonas de frecuencia de caudal.

En el capítulo 4, se presenta el tercer artículo, titulado *Impactos del desarrollo del riego en la calidad de agua en la cuenca del río San Salvador (Parte 2): Implementación de escenarios en SWAT* (Hastings et al., 2023b), el cual se enfoca en evaluar los impactos del desarrollo del riego en la cantidad y calidad del agua, y en la búsqueda de alternativas de buenas prácticas de manejo en el contexto de la intensificación agrícola sostenible. Se utiliza el modelo SWAT previamente calibrado y validado para la cuenca de San Salvador. El escenario implementado se basa en un estudio previo que considera criterios económicos, sociales y ambientales para seleccionar la opción más interesante para el desarrollo del riego en la cuenca del río San Salvador (BRLI y SIGMAPLUS, 2017). Este escenario implica la construcción de un embalse (26,5 hm^3) en un afluente del río San Salvador, que proporcionaría agua para el riego suplementario de 6.950 ha de cultivos de verano, lo que representa un aumento de 2,5 veces la superficie regada en comparación con en el año 2018. También se considera un segundo escenario en el que se incorporan zonas *buffer* ribereñas con el fin de retener nutrientes y mejorar la calidad de agua en la cuenca.

En el capítulo 5, se discuten los principales resultados y se exponen las conclusiones generales de la tesis, incluyendo las contribuciones particulares de cada artículo. Finalmente, en el capítulo 6 se presentan las referencias bibliográficas.

2 LAND-COVER MAPPING OF AGRICULTURAL AREAS USING MACHINE LEARNING IN GOOGLE EARTH ENGINE[1]

Florencia Hastings [*1;2] [0000-0002-7861-4702], Ignacio Fuentes [3] [0000-0001-7066-7482], Mario Perez-Bidegain [1] [0000-0002-5501-064X], Rafael Navas [4] [0000-0001-8559-9523], and Angela Gorgoglione [5] [0000-0002-2476-2339]

[1] *School of Agronomy, Universidad de la República, Av. Gral. Eugenio Garzón 780, Uruguay*
[2] *Directorate of Natural Resources, Ministry of Agriculture, Livestock and Fisheries, Av. Gral. Eugenio Garzón 456, Uruguay*
[3] *School of Life and Environmental Sciences, University of Sydney, New South Wales 2006, Australia*
[4] *Programa Nacional de Investigación en Producción y Sustentabilidad Ambiental, Instituto Nacional de Investigación Agropecuaria, Uruguay*
[5] *School of Engineering, Universidad de la República, Julio Herrera y Reissig 565, Uruguay*

*Correspondence: ing.fhastings@gmail.com

RESUMEN

Los mapas de cobertura de suelo son de gran utilidad para la planificación del uso del suelo y el desarrollo de políticas, así como también son inputs esenciales de los modelos hidrológicos. Google Earth Engine (GEE) es una plataforma gratuita que ofrece online datos satelitales con procesadores de alta capacidad. En este artículo se examinaron las capacidades de GEE para su aplicación en el desarrollo de un mapa de cobertura del suelo. Con este propósito se aplicó un procedimiento dividido en 5 etapas: (1) selección de imágenes y pre-procesamiento, (2) selección de las clases y las muestras de entrenamiento, (3) proceso de clasificación, (4) proceso de post-clasificación, (5) validación. La región de estudio se localiza en la cuenca del río San Salvador (Uruguay) la cual se encuentra bajo un proceso de intensificación agrícola. Como resultado, se construye un mapa de cobertura del suelo para el año 1990. El mapa muestra buena concordancia con el Censo Agropecuario y revela el cambio de cobertura del suelo de pasturas a cultivos durante el período 1990–2018.

Palabras clave: mapa cobertura de suelo, clasificación supervisada, Google Earth Engine, región agrícola.

[1] Publicado en: Gervasi O, et al. (Eds.) Computational Science and Its Applications – ICCSA 2020: 20th International Conference, Cagliari, Italy, July 1–4, 2020, Proceedings, Part IV. Springer, Cham. 721–736. doi: 10.1007/978-3-030-58811-3_52.

SUMMARY

Land-cover mapping is critically needed in land-use planning and policy making. Compared to other techniques, Google Earth Engine (GEE) offers a free cloud of satellite information and high computation capabilities. In this context, this article examines machine learning with GEE for land-cover mapping. For this purpose, a five-phase procedure is applied: (1) imagery selection and pre-processing, (2) selection of the classes and training samples, (3) classification process, (4) post classification, and (5) validation. The study region is located in the San Salvador basin (Uruguay), which is under agricultural intensification. As a result, the 1990 land-cover map of the San Salvador basin is produced. The new map shows good agreements with past agriculture census and reveals the transformation of grassland to cropland in the period 1990–2018.

Keywords: Land-cover map, Supervised classification, Google Earth Engine, Agricultural region.

2.1 INTRODUCTION

Land-use/land-cover (LULC) change plays a critical role in the global change study. Often, land cover is the result of human actions to modify the natural environment into a "customized environment". Such customization takes place to increase agriculture production, satisfy domestic needs, or restore ecosystem services. In the last decade, several studies have demonstrated that environmental problems are often related to LULC change [1][2]. LULC and human/natural modification have impacted negatively on the degradation of water quality, loss of biodiversity, deforestation, and global warming [3]. Therefore, characterizing and mapping land cover is essential for planning and managing natural resources, including agricultural fields [4]. Furthermore, LULC is a major data source of hydrologic models [5][6]. For this purpose, the implementation of effective land-cover mapping requires advanced remote-sensing methodologies able to provide accurate, inexpensive, and on-demand

land-cover products using free cloud-based data processing platforms and free and open-access information.

Based on these considerations, it is essential to process big earth data (e.g., satellite images) in the classification procedure over a large watershed. Numerous platforms, such as Google Earth Engine (GEE), Amazon's Web Services, Microsoft's Azure, and National Aeronautics and Space Administration (NASA) Earth Exchange have been created to tackle this issue and support processing and analysis of big earth data [7][8]. In particular, GEE is an application that processes big geospatial data and classifies land cover over vast areas [9]. In this platform, the open-source satellite images can be efficiently imported and processed in the cloud without the need for downloading the data to local computers. Furthermore, many remote-sensing algorithms (e.g., classification algorithms and cloud masking techniques) and several image-driven products are available in this platform and are included and editable in user-defined algorithms [10][9]. To date, numerous studies about classifications using GEE in large areas have been conducted. Belgiu et al. investigated the ability of a machine learning technique in land-cover mapping in different agro-ecological areas of the world [11]. Many efforts with remote sensing have been carried out to overcome the challenges of producing less costly (or free) and more time-efficient land-cover mapping around the world [12]. Project MapBiomas is a good example; it shows how collections of LULC maps could be integrated into a web platform to aid planning and managing natural resources in Brazil [13].

Based on these considerations, this study explores a methodology that uses a cloud-based free open-source database to contribute to current land-cover mapping efforts. Particularly in Uruguay, only LULC maps for the years 2000, 2008, 2011, 2015 [14] and 2018 [15] are available (online). The primary objective is to explore machine learning in GEE and its accuracy for historical land-cover mapping of areas mainly characterized by agricultural land use. The specific objectives of this study are: i) evaluate the utilization of GEE for feature extraction, with its advantages and disadvantages; ii) assess the performance of supervised machine-learning techniques to classify the land surface; iii) obtain a historical land-cover map for an agricultural watershed by coupling GEE and machine learning methods. This methodology was

applied to the San Salvador watershed, an agricultural basin located in Uruguay (South America).

2.2 MATERIALS

This section first presents a description of the study area, and then the data used to develop the land-cover map. The data used includes satellite data and field data from the General Census of Agriculture (GCA). The phenological data of the surveyed crops is also presented.

2.2.1 Study area

The San Salvador basin is located in Uruguay, in the Soriano department, and it covers an area of 2,390km2 (Figure 2-1).

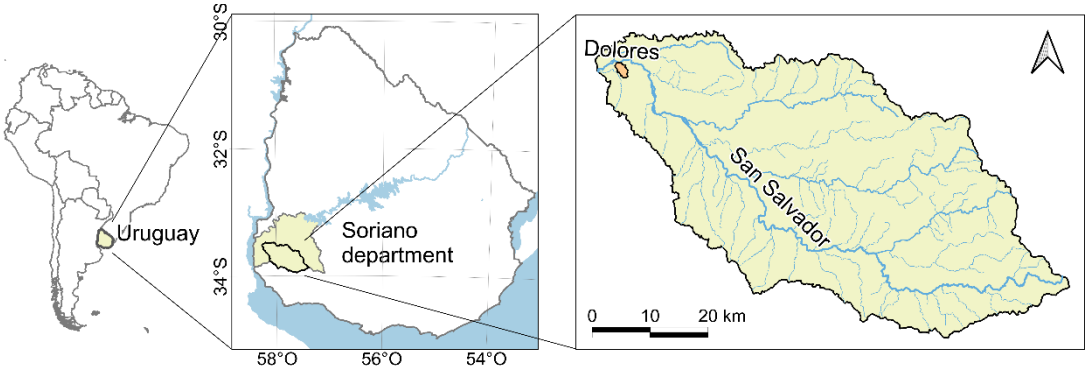

Figure 2-1: Location of San Salvador basin (Soriano department, Uruguay). Coordinate Reference System: World Geodetic System 1984 (WGS84).

Uruguay has a humid subtropical climate. According to the Köppen climate classification, it is Cfa, C = temperate, moderate, rainy, f = fully humid, a = mean temperature in the warmest month is 22. or higher [16]. The mean total annual precipitation is 1100 mm and the temperature can range between -7.9. and 40.4 °C [16]. The region is characterized by a landscape of smooth hills and, the study area, has an average slope equal to 2.3%.

The San Salvador basin is located in the west part of the country where the most suitable soils for agriculture are [17]. In the decade of 1990, the agriculture practices included crop-pasture rotation, associated with livestock, with tillage practices [18]. Since the 21st century, agriculture suffered important changes due the incorporation

of no-tillage practices, transgenic, continuous cropping, and economic freedom [18]. In a short period, soybean become the main grain crop, increasing the planted area from 12,000 ha in 2000/2001 to 1,300,000 ha in 2014/2015, total cropland extension were 426,000 ha and 1,500,000 ha respectively [19]. Also, production forest had an important increase from 186,277 ha planted in 1990 [20] to 1,000,190 ha in 2018 [21] because of the development in the forestwood sector. Land-cover map of 2018 shows that 68% of Uruguay surface is covered with native grassland associated with livestock and 18% with croplands [15]. It is worth to mention that the 8.4% of the national gross domestic product (GDP) (2018) is from agricultural products and associated industries [22].

The above-mentioned increase in cropland also took place in the San Salvador basin. The land-cover map of 2018 shows that 62.4% of the basin is covered by cropland. Figure **2-2** and Table **2-1** show the basin land-cover of 2018.

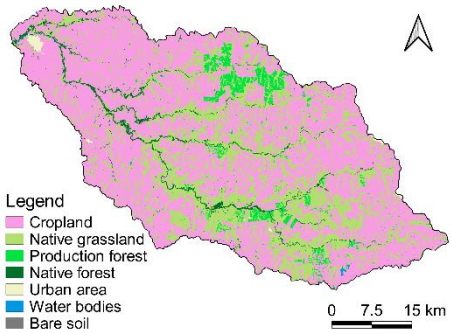

Figure 2-2 Land-cover map of San Salvador basin in 2018, classification of Sentinel-2 Level 2A scenes (resolution 10m/pixel) [15]

Table 2-1 Area of land-cover classes in 2018 in the San Salvador basin

Class	**Area (ha)**	**%**
Cropland	149,255	62.4%
Native grassland	74,845	31.3%
Production forest	7,943	3.3%
Native forest	5,691	2.4%
Urban area	927	0.4%
Water bodies	361	0.2%
Bare soil	27	0.0%
Total	**239,047**	**100%**

Taking into account the strategic importance of San Salvador watershed for the economy of the country, it is fundamental to have accurate historical landcover mapping of this area to detect any land-cover change that can affect the agricultural production. Furthermore, it is worth mentioning the importance of the distribution of croplands in 1990 to study the land-cover change in this area. Based on these considerations, we selected San Salvador and the year 1990 as our case study.

2.3.1 Satellite and field data

Surface Reflectance Tier 1 dataset, which represents the atmospherically corrected surface reflectance from the Landsat 5 Enhanced Thematic Mapper (ETM) sensor, was used in this study. Landsat 5 was operational in the ’90s (launched in 1984 and decommissioned in 2013) and its images are freely available. The satellite had a 16-day repeat cycle and a spatial resolution of 30 meters.

The field data available for 1990 is the database from the General Census of Agriculture (GCA) that provides aggregated data to validate the results of the imagery classification. Furthermore, the phenological data of the surveyed crops were used for the visual interpretation of the satellite images.

2.2.1.1 General Census of Agriculture

In Uruguay, the GCA is conducted by the Ministry of Agriculture, Livestock and Fisheries (MGAP) every ten years. Census data is reported, to preserve people´s privacy, in aggregated geographical units called census tracts (CTs).

In 1990, for the Soriano department, the census registered an area dedicated to winter crops six times larger than the one dedicated to summer crops. The main crops are wheat in winter and sorghum in summer. Among winter crops, wheat covers 72% of the planted area, barley covers 21%, and oat (grain) 7%. The main winter forage crop is oat (sowed pasture), 80% of the oat area is for grazing (sowed pasture) and 20% is for grain. In summer sorghum, corn, and soybean cover 54%, 33% and 12% of the planted area respectively.

The data from GCA disaggregated per CTs was obtained from the GCA database facilitated by agricultural statistics of MGAP. The database showed that some CTs had under-coverage and over-coverage of the total area. For this reason, only were considered those CTs that had a difference smaller than ±15% in the coverage-area. So, even though the San Salvador watershed has 12 CTs in common with the Soriano department, only 6 CTs were taken into account. The selected CTs and the land-cover area obtained from GCA is presented in Figure **2-3** and Table **2-2**.

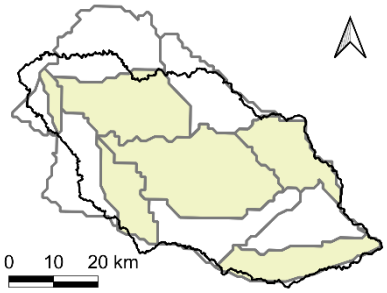

Figure 2-3: Selected census tracts of the General Census of Agriculture 1990

Table 2-2: Land-cover area of the selected census tracts of the General Census of Agriculture 1990.

Class	Area (ha)	%
Native grassland	73,525	51.7%
Cropland	34,563	24.3%
Sowed pasture	30,856	21.7%
Native forest	2,490	1.7%
Production forest	923	0.6%
Total	**142,357**	**100%**

2.2.1.2 Phenological data

The phenological data used was taken from two sources. For wheat, barley, and oat, phenological data was obtained from the reports on the evaluation of cultivars (results of 2003) [23]. In the case of sorghum, corn, and soybean, a phenologic model developed on the base of experimental data ran in 1990 [24] was considered. Table 2-3 presents the phenology of crops surveyed in the 1990 census. The phenological phases considered were the early growth stage (between emergence and flowering) and peak on leaf area index season (after flowering).

2.3 METHODS

This section outlines the conceptualization of the methodology approach and the phases implemented to develop the land-cover map.

2.3.1 Conceptualization of the methodology approach

According to the major steps of image classification identified by Lu and Weng [25], in this study, five phases were implemented: (1) imagery selection and preprocessing, (2) selection of the classes and training samples, (3) classification process, (4) post-classification process, and (5) validation. An overall flowchart of the methodology approach showing each phase is presented in Figure 2-4.

Table 2-3: Average dates of phenological phases. *Average date of harvest. **Average.

Crop	Sowing	Emergence	Flowering	Maturity
Wheat [23]	13-Jun	23-Jun	22-Oct	12-Dec*
Barley [23]	10-Jul	19-Jul	10-Oct	2-Dec*
Oat [23]	12-mar	18-mar		17-nov**
Sorghum [24]	15-Oct	26-Oct	9-Jan	13-Feb
Corn [24]	7-Oct	17-Oct	24-Dec	24-Feb
Soybean [24]	21-Oct	2-Nov	31-Dec	16-Apr

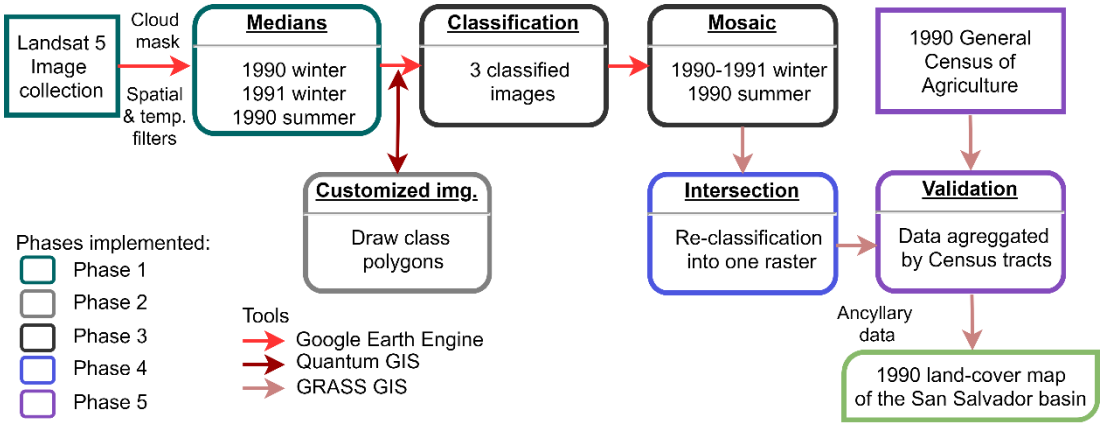

Figure 2-4: Conceptualization of the methodology approach.

GEE is a cloud-based platform that includes a wide geospatial dataset, as well as the entire Landsat archive, and algorithms that facilitate spatial analysis [10]. Image selection and supervised classification techniques were implemented in GEE which was coupled with Geographic Information Systems (GIS) environment. Quantum GIS 3.4.15 (QGIS) was used to customize images and create the polygons classes and GRASS GIS 7.4.2 was adopted for the post-classification phase.

2.3.2 Phase 1: Imagery selection and pre-processing

The satellite images were collected between December 1989 and August 1991. The criterium adopted for imagery selection was to cover completely the study area considering the crop peak growth phenological stage of winter and summer crops. According to the wheat phenology, the main winter crop, winter peak growing season ranges from October 22nd to December 12th. Sorghum and corn were the main crops for summer season, so, in average, peak growing season ranges from December 15th to February 15th. Furthermore, a quality filter was applied to mask pixels with clouds,

cloud shadows or high reflectance (reflectance greater than 6000). Considering the scarcity of quality scenes that covers the entire study area, scenes acquired in different dates were used. To minimize the phenology variation among the scenes, a period smaller than a month was chosen within each growing season. To perform the classification, the images selected were reduced to one per season by the median. Thus, when images had overlapping pixels, the median was computed independently in each band.

2.3.3 Phase 2: Selection of classes and training samples

The supervised classification approach uses the training samples signatures to classify the image and define the land-cover categories [25]. A successful classification depends on a proper class selection and its representative sampling [25]. Considering that the classes are defined by visual interpretation of satellite images, discernible land-cover units were selected as native grasslands, croplands, and water. Cropland class was also disaggregated into a hierarchical system of subclasses by the post-classification process. Three spectral bands (red, green and near infrared) of surface reflectance were used for the class-visual interpretation.

Some other classes as urban area, production forest, and native forest were considered. These classes were not included in the classification because of mixed pixel problems in remote sensing technology within non-cropland [26]. Instead, some ancillary data were used. For urban area, from the land-cover map of Uruguay of 2000 was used [14]. For production forest, data were mapped from Landsat imagery as there were only four polygons of this class. For native forest, data from the national forest inventory (2018) [21] was used. A visual comparison between the data of the national forest inventory (2018) and aerial photos, taken in 1966 by the Military Geographic Service [27] was made, and no substantial difference was observed. Furthermore, native forest represents about 2% of the study area according to 1990 census data, so it does not represent a significant contribution to the land-cover map.

2.3.4 Phase 3: Classification process

A supervised classification approach was performed using a Classification and Regression Tree (CART) classifier implemented in GEE. CART is a binary decision tree. It uses a sample of training data for which the correct classification is known. It recursively splits the data based on a statistical test ending in terminal nodes associated with entities correctly classified [28][29]. One advantage of selecting non-parametric classifiers, like decision trees, is that they do not suppose a normal distribution of the dataset, which is difficult to achieve especially in complex landscapes [25]. Furthermore, visual interpretation-sampling data were considered.

The polygons with data classes of 1990 winter and 1990 summer were randomly split keeping on average 70% of the polygons for training and 30% for validating the classifier. Also, were consider polygons with data classes of 1991 winter and 1991 summer to perform a cross-year validation. As a result, two classified images were obtained representing 1990 winter and 1990 summer. All spectral bands were used as inputs to classification, four visible and near-infrared (VNIR) bands, two short-wave infrared (SWIR) bands processed to orthorectified surface reflectance, and one thermal infrared (TIR) band processed to orthorectified brightness temperature.

An error matrix was employed to assess the accuracy of the classification and cross-year validation. The overall accuracy (OA), Kappa coefficient (K), consumer's accuracy (CA), and producer's accuracy (PA) coefficients were calculated from the error matrix. OA is the rate of the total correctly classified field samples [30]. K is a measure of overall statistical agreement of an error matrix, which takes into account non-diagonal elements [30]. CA is the conditional probability that the pixels classified as category *i* was assigned as category *i* by the reference data [30]. PA is the conditional probability that the pixels assigned as category *j* by the reference data are classified as category *j* [30].

2.3.5 Phases 4 and 5: Post-classification process and validation

The post-classification process consisted of observing the sequence winter-summer land cover and making a re-assignation of classes resulting in the final land-cover map. For that, the two classified images were imported as a raster image into GRASS GIS. Then, the two raster images were intersected, creating a new cross raster map representing all unique combinations of classes and its associated cross-matrix. Finally, the classes were re-assigned.

After the classes re-assignation, a comparison to census data was made to evaluate the accuracy of the resulting map. The map validation is performed since training and validating data were not surveyed in the field [25].

2.4 RESULTS AND DISCUSSION

In this section, the results of each methodological phase to develop the landcover map are presented. Furthermore, a discussion of the main findings of the study reported in this article is included.

2.4.1 Phase 1 results: Imagery selection and pre-processing

To create a cloud-free image of 1990, winter scenes corresponding to the early growth stage of winter crops were selected due to the lack of scenes during the phenological phase of peak growth of winter crops. However, due to the quality filters (to mask pixels with clouds, cloud shadows, or high reflectance) applied to the images, the coverage of the studied area was 83%. Thus, to complete the coverage of the entire study area, images of 1991 winter were used. For summer period, scenes during the phenological phase of the peak growth of summer crops were selected. Also, images of 1991 winter and 1991 summer were selected to perform a cross-year validation. A summary of the considered scenes for each season, its cloud coverage, and acquisition date is presented in Table 2-4. In Figure 2-5, the selected scenes, reduced by the median, representing (a) 1990 winter, (b) 1991 winter, and (c) 1990 summer are shown.

Table 2-4: Scenes used from Landsat 5 (Enhanced Thematic Mapper sensor, Surface Reflectance Tier 1 dataset). *Scene ID refers to path, row, and acquisition date from the complete ID.

	ID*	Cloud cover	Acquisition date
1990 winter	224083_19900804_20170129	0%	8/4/1990
	224084_19900804_20170129	0%	8/4/1990
	225083_19900811_20170130	28%	8/11/1990
	225084_19900811_20170130	41%	8/11/1990
	224083_19900820_20170130	0%	8/20/1990
	224084_19900820_20170128	0%	8/20/1990
	225084_19900827_20170129	58%	8/27/1990
1991 winter	224084_19910807_20170125	96%	8/7/1991
	225083_19910814_20170125	0%	8/14/1991
	225084_19910814_20170125	0%	8/14/1991
1990 summer	224083_19891223_20170201	1%	12/23/1989
	224084_19891223_20170201	0%	12/23/1989
	225083_19891230_20170201	7%	12/30/1989
	225084_19891230_20170201	27%	12/30/1989
	225084_19900115_20170131	4%	1/15/1990
	225083_19900115_20170131	0%	1/15/1990
1991 summer	224083_19910111_20170129	10%	1/11/1991
	224084_19910111_20170127	12%	1/11/1991
	225083_19910102_20170129	5%	1/2/1991
	225084_19910102_20170128	3%	1/2/1991

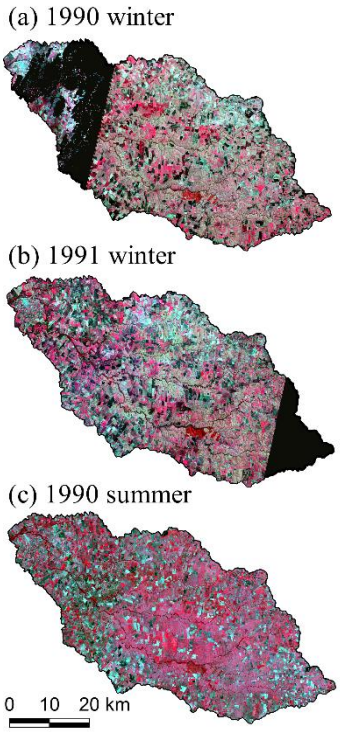

Figure 2-5: Landsat median images of 1990 winter, 1991 winter and 1990 summer (false colour composite Bands 4, 3, 2)

2.4.2 Phase 2 results: Selection of classes and training samples

A first search was made in USGS Landsat look to recognize how crops looked during August and define the land-cover units [31]. A 1989 sequence of images showing the different phenologic phases of winter crops was found. Wheat and barley (winter crops) are discern in May image (Figure 2-6a) respectively highlighted in red and yellow but not distinguished in the image from August onward (Figure 2-6b - 6d). Figure 2-6c shows that winter crops achieved peak growth and Figure 2-6d shows they were harvested. From August image (Figure 2-6a) oat was recognized, highlighted in green, this enables to assign a subclass of winter crops to oat. Native grasslands were recognized and showed in black with no significant variation observed into the four images.

(a) Date 5/20/1989. (b) Date 8/1/1989. (c) Date 10/27/1989. (d) Date 11/28/1989.

Figure 2-6: Landsat 5 images showing the evolution of winter crops (red circle: wheat, yellow square: barley, green square: sowed pasture, black circle: grassland)

Table 2-5: Land-cover classification classes.

1st level	2nd level	Descriptions
Water bodies	WATB	Streams, rivers, lakes and reservoirs.
Grassland	GRAS	Native grasslands or improved grasslands.
	FLDP	Native grasslands placed in floodplains.
Cropland	PAST, PAST2	Sowed pasture in two phenological phases (only for winter images)
	CRPw	Winter cropland. Includes: wheat and barley.
	CRPs, CRPs2	Summer croplands. Includes: sorghum, corn and soybean.
	FLLW	Summer fallow.
	BARE	Bare or tilled soil.

In this study, ten classes were defined to perform the classification. For floodplains (FLDP) a new class was added, as it was observed that grassland kept misclassified as cropland. A list of the defined classes with their description is presented in Table 2-5.

2.4.3 Phase 3 results: Classification process

For each image, an average of 20 polygons were defined per class, and area used to train and validate the classifiers. This resulted in an average of 1500 ha for training, 500 ha for validation, and 1000 ha for cross-year validation (6). The supervised classification was applied to the three median images described in Section 4.1. Finally, in the case of winter images, a mosaic was made to couple the missing area of the winter image of 1990 with data of the winter image of 1991.

The statistical accuracy assessment was applied to train and validate datasets of each image. Table 2-6 presents the results of statistics OA, K, CA and PA calculated. For the training, validating and cross-year validating dataset, OA and K vary in a range of 0.96 to 1.00 and 0.95 to 1.00 respectively. These results indicate that the three classified images achieved high overall accuracies. Furthermore, CA and PA

coefficients show the performance per class. In general, PA and CA vary in a range of 0.83 to 1.00. However, floodplain class had low accuracy, PA and CA vary in a range of 0.44 to 1.00. As mentioned before, it was detected by visual inspection that grassland was misclassified as cropland by the classifier in this area. The post-classification process allowed separating cropland and grassland from the floodplain class.

Table 2-6: Classification performance and area used for training and validation.

	Winter						**Summer**					
	1990				**1991**		**1990**				**1991**	
	Training		Validation		Validation		Training		Validation		Validation	
	CA	PA	CA	PA	CA	PA	CA	PA	CA	PA	CA	PA
Water bodies	1.00	1.00	1.00	1.00	---	---	1.00	0.99	0.83	0.99		
Native grassland	1.00	1.00	0.99	0.98	0.99	0.95	1.00	0.97	0.99	0.97	0.99	1.00
Floodplains	1.00	0.98	1.00	0.95	0.62	0.97	0.98	0.90	0.44	0.90	1.00	0.94
Sowed pasture	1.00	1.00	0.99	1.00	0.99	0.87	---	---	---	---	---	---
Sowed pasture2	1.00	1.00	1.00	1.00	1.00	0.99	---	---	---	---	---	---
Winter cropland	1.00	1.00	1.00	0.99	0.96	1.00	---	---	---	---	---	---
Fallow	---	---	---	---	---	---	1.00	0.99	1.00	0.99	1.00	1.00
Summer cropland	---	---	---	---	---	---	1.00	0.99	1.00	0.99	1.00	0.99
Bare soil	1.00	1.00	0.97	1.00	0.96	0.98	1.00	1.00	1.00	1.00	1.00	1.00
OA =	1.00		0.99		0.96		1.00		0.98		1.00	
Kappa=	1.00		0.99		0.95		1.00		0.98		0.99	
Area (ha)	1548		454		1016		1411		615		1066	

2.4.4 Phase 4 results: Post-classification process

The seasonal variation of each class was taken into account to better distinguish the class of interest and do the class re-assignation. The intersection of the two classified images (winter and summer) resulted in a cross-raster map and its associated cross-matrix. The five classes considered to construct the final map are water bodies, native grassland, sowed pasture, winter croplands, summer croplands and double cropping lands.

In Table 2-7, the cross-matrix shows the area (ha) distribution of the intersection between the classified winter image and the classified summer image. Each row represents the area of winter classes desegregated into summer classified classes.

Similarly, each column represents the area classified on summer image desegregated into winter classified classes.

The cross-matrix, presented in Table 2-7, shows that 84% of the area classified as GRAS on winter image stayed as GRAS on the final map, and the remaining 16% was assigned to a cropland class. Furthermore, 76% of the area classified as FLDP on winter was re-assigned to the class GRAS and the remaining 24% was re-allocated to a cropland class (CRPw). This was the main reason for defining the specific FLDP class, as discussed in Section 4.3.

Table 2-7: Cross-matrix expressing the area (ha) distribution of the intersection of the classified winter image with the classified summer image.

		Area (ha) classified on summer					
	Class	Native grassland	Floodplain	Fallow	Summer cropland	Bare soil	Total
Area (ha) classified on winter	Native grassland	63,942	25,435	6,772	3,835	6,565	106,549
	Floodplain	12,228	29,703	9,279	5,001	5,147	61,358
	Sowed pasture	1,814	5,208	3,033	678	1,843	12,576
	Sowed pasture2	2,625	5,613	2,594	1,846	1,917	14,595
	Winter cropland	2,703	3,384	5,077	706	7,033	18,903
	Bare soil	7,203	5,174	4,634	1,405	5,551	23,967
	Total	**90,515**	**74,517**	**31,389**	**13,471**	**28,056**	**237,948**

2.4.5 Phase 5 results: Validation

A comparison between 1990 GCA and the new land-cover map was made to validate the results of the final land-cover map. GCA data was grouped into classes of interest. So, the total area surveyed in GCA as vegetables, row crops, tilled soil, and fallow was compared with the total area of CRPw, CRPs and CRPWs classes; native forest was compared with MONT class area; production forest surface was compared with the FRST surface; the total area covered by pasture and annual forages was compared with the PAST area; and the total area dedicated to improved grassland and native grassland was compared with the GRAS area. The area of the six CTs selected was aggregated to reduce the geographic resolution errors and compared with the same extension of the land-cover map.

The area of the land-cover map classes is very similar to surface reported in the GCA. In Table 2-8 is presented the areas per class obtained from the land-cover map and from the GCA, and the difference between the two areas. In general, the area of the new-defined categories is greater than the GCA area due to the difference between the surveyed and the measured area that is equal to 6,574 ha. This difference is not valid for pasture and production forest classes. The challenge in classifying pasture class is represented by the fact that perennial pastures can be confused with grasslands. Furthermore, dairy production land use occupies an area where there are mixed portions of pasture and crop that are difficult to separate. About production forest area, an error in the CTs borders may explain the misclassified area since an area of production forest was identified next to the CTs borders.

Table 2-8: Comparison of the areas per class of the land-cover map and the General Census of Agriculture 1990 (GCA)

Class	Classified (ha)	%	Census (ha)	%	Difference (ha)
Native grassland	84,097	57%	73,525	52%	10,572
Native forest	3,520	2%	2,490	2%	1,030
Cropland	43,805	29%	34,563	24%	9,242
Sowed pasture	17,509	12%	30,856	21%	-13,347
Production forest	0	0%	923	1%	-923
Total	**148,931**	**100%**	**142,357**	**100%**	**6,574**

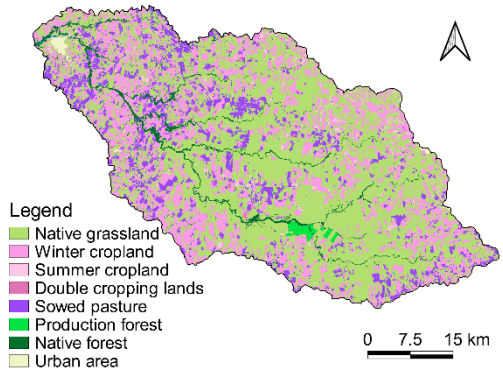

Figure 2-7: Land-cover map of San Salvador basin in 1990.

Table 2-9: Area of land-cover classes of San Salvador basin in 1990

Class	Area (ha)	%
Native grassland	135,826	56.8%
Winter cropland	66,830	28.0%
Summer cropland	4,314	1.8%
Double cropping	662	0.3%
Sowed pasture	23,452	9.8%
Native forest	5,683	2.4%
Production forest	1,185	0.5%
Urban area	991	0.4%
Water bodies	127	0.0%
Total	**239,071**	**100%**

Figure 2-7 shows the final land-cover map of the San Salvador basin in 1990 and, Table 2-9 presents the area covered by each class. The three main land covers identified in the basin were native grasslands (GRAS) with a surface equal to 56.8%, croplands (CRPw, CRPws and CRPs) with a total area of 30.0%, and sowed pastures with a surface of 9.8%.

As expected, the results showed a significant land-cover change between 1990 and 2018. Cropland surface increased from 95,258 ha to 149,255 ha (57%) and grassland reduced from 135,826 ha to 74,845 ha (45%). Also, the production forest area increased from 1,185 ha to 7,943 ha (570%). The observed trends are related to agriculture and forestry expansion since 1990. Uruguay met a challenge for sustainable intensification as committed, in 2015, in the 21st Session of the Conference of the Parties (COP21) [32]. Since 2013, a public policy towards soil conservation, based on the Universal Soil Loss Equation (USLE), is being implemented [32]. This policy, designed by the MGAP, is recognized as a good example by the Food and Agriculture Organization (FAO) [33].

The main source of error identified in this study might be related to the scarcity of scenes on the dates and area of interest. For instance, the winter crop season was characterized only based on the available images in August, when winter crops were on an early growth stage. Another source of error may be introduced by the training and validation polygons created by the visual interpretation of images and its sampling design. The low accuracy achieved on the floodplain class may occur due to: (1) reflectance similarities between vegetation on floodplains and crops, especially in the summer season, and (2) the heterogeneity of the vegetation on the surface this class represents. However, the low accuracy in the floodplain class was improved, based on visual validation, by using a multi-seasonal post-classification approach.

The methodology of this study can be used to develop a series of historical annual land-cover maps and might be applied for mapping other basins with similar surface features. Landsat scenes are freely available since 1984. Yet, their frequency increase since 1987-1988, so temporal series from this period to the present can be achieved. For validation, data from GCA is available every ten years and data of agricultural annual surveys (DIEA-MGAP) can also be employed. Furthermore, since

2000 onwards other satellite missions, such as MODIS (2000), CEBERS-4 (2014) and Sentinel (2014), provide free satellite imagery. Therefore, the presented methodology might be improved using a multi-satellite approach.

2.5 CONCLUSIONS

This study presented an efficient approach to estimate the land-cover of an agricultural basin, using free open-source tools. GEE showed excellent potential in land cover mapping with high processing efficiency. Machine-learning algorithms developed in GEE are easily applied and a wide range of free satellite imagery is available.

As a case study, we estimated the land-cover in the San Salvador basin in 1990 based on Landsat 5 imagery and GEE processing platform. High accuracy was achieved in the supervised classification according to the error matrix analysis. Additionally, map validation showed good agreements with GCA data. The methodology presented was capable to deal with the scarcity of historical quality scenes.

The methodology presented in this article can be improved by a multi satellite approach. Temporal map series of the same watershed can be developed as well as other catchments. The above mentioned are issues that can be explored in future research.

Map availability. The San Salvador basin land-cover map of 1990 can be freely downloaded from https://www.gub.uy/ministerio-ganaderia-agriculturapesca/politicas-y-gestion/mapa-cobertura-utilizando-google-earthengine-cuenca-del-rio-san-salvador-1990.

Acknowledgements. We thank DIEA-MGAP that kindly made available the GCA data and DGRN-MGAP for their comments and suggestions.

Funding. This research was supported by the National Research and Innovation Agency (ANII) under contract number FSA_PI_2018_1_148628.

2.6 REFERENCES

1. Giri, S., Qiu, Z.: Understanding the relationship of land uses and water quality in Twenty First Century: A review. J. Environ. Manage. 173, 41–48 (2016).
2. Rodríguez, J., Rico, A., Mendoza-Martínez, E., Gómez-Ruiz, A., Sedeño-Diaz, J., López-López, E.: Impact of Changes of Land Use on Water Quality, from Tropical Forest to Anthropogenic Occupation: A Multivariate Approach. Water 10, 1–16 (2018).
3. Dwivedi, R., Kandrika, S., Ramana, K.: Land-use/land-cover change analysis in part of Ethiopia using Landsat Thematic Mapper Data. Int. J. Remote Sens. 26, 1285–1287 (2005).
4. Gomez, C., White, J., Wulder, M.: Optical remotely sensed time series data for land cover classification: A review. ISPRS J. Photogramm. 116, 55–72 (2016)
5. Figorito, B., Tarantino, E., Balacco, G., Fratino, U.: An object-based method for mapping ephemeral river areas from WorldView-2 satellite data. Proc. SPIE 8531, 85310B (2012).
6. Aquilino, M., Tarantino, E., Fratino, U.: Multi-temporal land use analysis of an ephemeral river area using an artificial neural network approach on Landsat imagery. ISPRS - Int. Arch. Photogramm. XL-5/W3, 167–173 (2013).
7. Amani, M., Brisco, B., Afshar, M., Mirmazloumi, S., Mahdavi, S., Mirzadeh, S.M.J., Huang, W., Granger, J.: A generalized supervised classification scheme to produce provincial wetland inventory maps: an application of Google Earth Engine for big geo data processing. Big Earth Data p. 378–394 (2019).
8. Xiong, J., Thenkabail, P., Gumma, M., Teluguntla, P., Poehnelt, J., Congalton, R., Yadav, K., Thau, D.: Automated cropland mapping of continental Africa using Google Earth Engine cloud computing. ISPRS J. Photogramm. 126, 225–244 (2017).
9. Kumar, L., Mutanga, O.: Google Earth Engine Applications Since Inception: Usage, Trends, and Potential. Remote Sensing 10, 1509 (2018).
10. Gorelick, N., Hancher, M., Dixon, M., Ilyushchenko, S., Thau, D., Moore, R.: Google Earth Engine: Planetary-scale geospatial analysis for everyone. Remote Sens. Environ. 202, 18–27 (2017).

11. Belgiu, M., Csillik, O.: Sentinel-2 cropland mapping using pixel-based and object based time-weighted dynamic time warping analysis. Remote Sens. Environ. 204, 509–523 (2018).
12. Mumby, P., Green, E., Edwards, A., Clark, C.: The cost-effectiveness of remote sensing for tropical coastal resources assessment and management. J. Environ. Manage. 55, 157–166 (1999).
13. MapBiomas Project - Collection v4.0 of the Annual Land Use Land Cover Maps of Brazil, http://mapbiomas.org, last accessed February 7th, 2020.
14. National Directorate of Land-use Planning - Ministry of Housing, Land Planning and Environment (DINOT-MVOTMA): Land-cover map of Uruguay. Tech. rep., Montevideo, Uruguay (2014), (in spanish).
15. Petraglia, C., Dell'Acqua, M., Pereira, G., Yussim, E.: Integrated land cover/use map of Uruguay of 2018. Gráfica Mosca, Montevideo, Uruguay (2019), (in spanish).
16. Uruguay Meteorological Institute (INUMET), https://www.inumet.gub.uy/index.php/clima, last accessed January 3rd, 2020.
17. Agricultural Statistics - Ministry of Agriculture, Livestock and Fisheries (DIEAMGAP): Agricultural Regions of Uruguay. Tech. rep., Montevideo, Uruguay (2015), (in spanish).
18. Arbeletche, P., Coppola, M., Paladino, C.: Analysis of agro-business as a form of business management in South America: the Uruguayan case. Agrociencia Uruguay 16, 110–119 (2012), (in spanish).
19. Couto, P.: Recent trends in rainfed agriculture. Plan agropecuario 161, 64–68 (2017), (in spanish).
20. Agricultural Statistics - Ministry of Agriculture, Livestock and Fisheries (DIEA-MGAP): General Census of Agriculture of 1990. Editorial MGAP, Montevideo, Uruguay (1994), (in spanish).
21. Forestry Directorate - Ministry of Agriculture, Livestock and Fisheries (DGF-MGAP): Results of the national forest mapping 2018. Tech. rep., Montevideo, Uruguay (2018), (in spanish).

22. Agricultural Statistics - Ministry of Agriculture: Agricultural Statistical Yearbook 2019. Tech. rep., Montevideo, Uruguay (2019), (in spanish).
23. Castro, M., Pereyra, S., Stewart, S., Germán, S., Vázquez, D.: Experimental results of the national cultivar evaluation. Tech. rep., National Institute of Agricultural Research (INIA) and National Institute of Seeds (INASE), Montevideo, Uruguay (2003), (in spanish).
24. Fassio, A., Ibáñez, W., Rodríguez, M., Ceretta, S., Pérez, O., Rabaza, C., Vergara, G., Cesán, A., Restaino, E.: Prediction of phenological states for Soy, Sunflower, Corn, Sorghum (grain, forage, sweet and silage). Tech. rep., National Institute of Agricultural Research (INIA), Montevideo, Uruguay (2014), (in spanish).
25. Lu, D., Weng, Q.: A Survey of Image Classification Methods and Techniques for Improving Classification Performance. Int. J. Remote Sens. 28, 823–870 (2007).
26. Liu, J., Liu, M., Tian, H., Zhuang, D., Zhang, Z., Zhang, W., Tang, X., Deng, X.: Spatial and temporal patterns of China's cropland during 1990-2000: An analysis based on Landsat TM data. Remote Sens. Environ. 98, 442–456 (2005).
27. Military Geographic Service (SGM): Aerial photographs of Uruguay 1966/67, scale 1/40,000, http://visualizador.sgm.gub.uy/gmaps/index.html, last accessed January 3rd, 2020 (in spanish).
28. Bittencourt, H., Clarke, R.T.: Use of classification and regression trees (CART) to classify remotely-sensed digital images. In: IGARSS 2003. 2003 IEEE International Geoscience and Remote Sensing Symposium. Proceedings (IEEE Cat. No.03CH37477). vol. 6, pp. 3751–3753 (2003).
29. Friedl, M., Brodley, C.: Decision tree classification of land cover from remotely sensed data. Remote Sens. Environ. 61(3), 399–409 (1997).
30. Stehman, S.: Selecting and interpreting measures of thematic classification accuracy. Remote Sens. Environ. 62, 77–89 (1997).
31. U.S. Geological Survey (USGS) Landsatlook, https://landsatlook.usgs.gov/viewer.html, last accessed January 15th, 2020.

32. Ministry of Agriculture, Livestock and Fisheries (MGAP): Uruguay agribusiness. The challenges for sustainable development. Tech. rep., Montevideo, Uruguay (2017), (in spanish).
33. Food and Agriculture Organization of the United Nations and Intergovernmental Technical Panel on Soils: Status of the World's Soil Resources – Main Report. Tech. rep., Rome, Italy (2015).

3 IMPACTS OF IRRIGATION DEVELOPMENT ON WATER QUALITY IN THE SAN SALVADOR WATERSHED (PART 1): ASSESSMENT OF CURRENT NUTRIENT DELIVERY AND TRANSPORT USING SWAT.[2]

IMPACTOS DEL DESARROLLO DEL RIEGO EN LA CALIDAD DE AGUA EN LA CUENCA DEL RÍO SAN SALVADOR (PARTE 1): ANÁLISIS DE LA EXPORTACIÓN Y TRANSPORTE DE NUTRIENTES ACTUAL MEDIANTE SWAT.

IMPACTOS DO DESENVOLVIMENTO DA IRRIGAÇÃO NA QUALIDADE DA ÁGUA NA BACIA HIDROGRÁFICA DE SAN SALVADOR (PARTE 1): ANÁLISE DA EXPORTAÇÃO E DO TRANSPORTE ATUAIS DE NUTRIENTES USANDO O SWAT.

Hastings, Florencia[1]; Perez-Bidegain, Mario[1]; Navas, Rafael[2]; Gorgoglione, Angela[3]

[1]Universidad de la República, Facultad de Agronomía, Montevideo, Uruguay. ORCID F.H. https://orcid.org/ 0000-0002-7861-4702, M.P-B. https://orcid.org/ 0000-0002-5501-064X .
[2]Universidad de la República, Centro Universitario Regional Norte, Departamento del Agua, Salto, Uruguay. ORCID https://orcid.org/0000-0001-8559-9523.
[3]Universidad de la República, Facultad de Ingeniería, Montevideo, Uruguay. ORCID https://orcid.org/0000-0002-2476-2339.

ABSTRACT

The development of irrigation involves a change in land use and management and has implications for water quality and quantity. Is critical to design conservation practices and best management practices consistent with sustainable agricultural intensification. The objective of this work was to understand and characterize key processes affecting hydrology, nutrient export and trans-port, and quantify impacts in the San Salvador watershed. For this purpose, the Soil & Water Assessment Tool (SWAT) was implemented, calibrated for water quantity, and water quality was adjusted using soft calibration techniques. The model reproduces water quantity and nutrient balance, and aids in characterizing the nutrient delivery and transport in the watershed. The magnitude of runoff affects the balance of nutrients. In high flows, diffuse sources are more prevalent, while in low flows, point sources and direct livestock manure to the river are more significant. The main outcomes of this work contribute to the design of strategies to achieve sustainable agricultural intensification.

[2] Publicado en: Agrociencia Uruguay [Internet], 27(NE1):e1198. Doi: 10.31285/AGRO.27.1198.

It also describes a new modeling tool freely available that could be used in further studies.

Keywords: sustainable agriculture, water quality, SWAT.

RESUMEN

El desarrollo del riego implica un cambio en el uso y manejo del suelo e impacta en la calidad y cantidad de agua, es fundamental diseñar prácticas de conservación y buenas prácticas agrícolas que respondan al paradigma de intensificación agrícola sostenible. El objetivo de este trabajo fue comprender y caracterizar los procesos claves que afectan la hidrología, la exportación y transporte de nutrientes y cuantificar los impactos en la cuenca del río San Salvador. Se implementó el modelo Soil & Water Assessment Tool, se calibró la cantidad de agua y la calidad de agua fue ajustada utilizando técnicas de calibración blanda. El modelo reproduce adecuadamente la cantidad de agua y el balance de nutrientes y permite caracterizar los procesos de exportación y transporte de nutrientes en la cuenca. La magnitud del escurrimiento afecta el balance de nutrientes. En condiciones de caudales altos las fuentes difusas predominan, mientras que en caudales bajos las cargas puntuales y excreciones directas del ganado a cursos de agua son las principales fuentes. Los resultados de este trabajo contribuyen al diseño de estrategias para alcanzar una intensificación agrícola sostenible. También se documenta una nueva herramienta de modelación que queda disponible y puede utilizarse en estudios posteriores.

Palabras clave: agricultura sostenible, calidad de agua, SWAT.

RESUMO

O cenário de desenvolvimento da agricultura resulta em mudanças no uso e gestão do solo e impacta a disponibilidade e qualidade da água. É fundamental projetar práticas de conservação e boas práticas agrícolas que atendam ao paradigma da intensificação agrícola sustentável. O objetivo deste trabalho foi compreender e caracterizar os processos-chave que afetam a hidrologia, a exportação e transporte de

nutrientes, e quantificar os impactos na bacia do rio San Salvador. O modelo Soil & Water Assessment Tool (SWAT) foi implementado, a quantidade de água foi calibrada a qualidade de água foi ajustada utilizando técnicas de calibração suave. O modelo reproduz adequadamente a quantidade de água e o balanço de nutrientes na bacia, permitindo caracterizar os processos de exportação e transporte de nutrientes na bacia. A magnitude do escoamento afeta o balanço de nutrientes. Com escoamento elevado, fontes difusas de nutrientes são mais significativas, enquanto em baixos níveis de escoamento, fontes pontuais e excrementos vacunos que escoam direto aos canais de drenagem prevalecem. Os resultados deste trabalho contribuem para o desenvolvimento de estratégias para uma intensificação agrícola sustentável. Também se descreve uma nova ferramenta de modelagem que fica disponível e pode ser usada em futuros trabalhos.
Palavras chave: agricultura sustentável, qualidade de água, SWAT.

3.1 INTRODUCTION

Intensive agricultural activities are one of the primary non-point sources of pollution that menace the quality of water bodies and the ecosystem's health[(1)]. Hence, sustainable land management and conservation practices have been increasingly implemented to reduce such types of pollution. For instance, one widely used conservation practice is riparian buffer zones[(2)]. Previous studies have demonstrated the positive effects of riparian buffer zones on water quality at the local field level[(3)]. However, such an effect should be evaluated at a watershed scale to aid river basin management programs. Therefore, hydrologic and water quality models at a basin scale are valuable tools for this purpose[(4-5)]. For decades, they have been used to assess streamflow and non-point source pollution along with the impacts (short- and long-term) of alternative management practices[(6-7)]. They are also valuable for determining the feasibility of water quality objectives at different budget levels, prioritizing sub-basins for watershed plan implementation, and identifying optimal conservation measures[(8)].

In the scientific literature, there are several types of models based on physical hypotheses that simulate precipitation-runoff and pollutant delivery and transport processes. Lumped models consider the watershed as a single unit, averaging the spatial features related to the model response[9]. Distributed models divide the catchment into elementary units, such as grid cells, and flows are routed from one cell to another as water drains through the basin. This allows the representation of watershed heterogeneity. The grid resolution is usually chosen to be of the appropriate size to represent the spatial variation of the main water quantity and quality processes. There are also semi-distributed models, which discretize the watershed into homogeneous sub-areas or sub-basins depending on the topography, the physical characteristics of the basin or the drainage area. Infiltration or precipitation parameters are treated as homogeneous within each sub-basin[10]. The Soil & Water Assessment Tool (SWAT)[11] model is one of the most widely adopted semi-distributed models in Uruguay[12-17]. It can generate precise results in the simulation of precipitation-runoff processes and pollutant delivery and transport.

A crucial aspect of modeling is understanding the key characteristics and processes of the watershed under study (water, sediment, nutrient, and carbon budgets)[17]. Although there is no universal method for calibrating and validating models, the use of soft data and various model performance criteria is increasingly recommended to ensure that models capture the main hydrologic and water quality processes[17-19]. Hard data are long-term, measured time series, while soft data are information about specific processes that may not be directly measured, such as an average annual estimate[17]. Studies show the importance of constraining model parameters to obtain reasonable crop yields and water balances and to simulate realistic scenarios with different management practices[19].

This study considered the San Salvador watershed, an agricultural basin in Uruguay. This basin is representative of the agricultural expansion process of the country[20] and now has the potential to intensify its production through supplementary irrigation[21-22]. The irrigation development changes land use and management and affects the water quality and quantity of the San Salvador River. In this investigation, the specific focus is on nutrients and sediments; however, pollutants encompass a

broader range, including fertilizers, herbicides, insecticides, chemicals, sediments and metals. Understanding the fundamental processes affecting the delivery, transport, and transformation of nutrient and sediment and quantifying the impacts at the watershed scale is critical to evaluate and suggest best management practices consistent with sustainable agricultural intensification.

Based on these considerations, the main objective of this study is to implement a SWAT model able to represent the streamflow and pollutant (nutrient and sediment) delivery and transport for the San Salvador watershed. This model will support sustainable land use strategies in a scenario of irrigation development. The specific objective is four-fold: i) evaluate the applicability of the SWAT model in a data-scarce region based on well-known model performance indicators; ii) reproduce spatially distributed flows and assess the water balance at the sub-basin level; iii) simulate spatially distributed pollutant delivery and transport; iv) let the model available to enable further studies and scenario modeling.

This study represents the first part of a master's thesis with the goal of constructing a modeling tool to support sustainable land use and planning in an agriculture irrigation development scenario. The scenario implementation and analysis were reported in the paper "Impacts of irrigation development on water quality in the San Salvador watershed (Part 2): Implementation of scenarios in SWAT"[(23)].

3.2 MATERIALS AND METHODS

3.2.1 Study area

In this study, the watershed of the San Salvador River in the department of Soriano, Uruguay, is considered (Figure 3-1). The main river flows northwesterly until it joins the Uruguay River. The watershed has an extension of 2,413 km^2 and an average slope of 2.3%. The city of Dolores is the main city in the watershed. It has 19,135 inhabitants[(24)] and is located at the watershed outlet. The average annual temperature and total precipitation during the period 1961-1990 are 17.5 °C and 1100 mm, respectively[(25)].

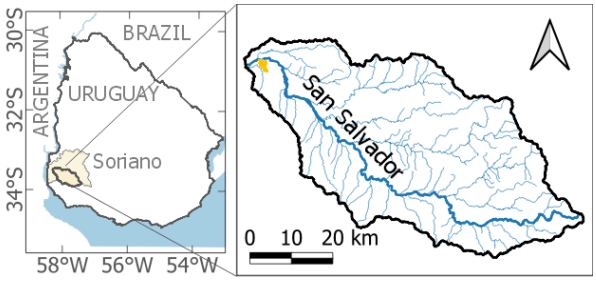

Figure 3-1: Location of the San Salvador watershed (Soriano department, Uruguay). Coordinate Reference System: World Geodetic System 1984 (WGS84).

Between 1990 and 2018, a remarkable change in land use was registered in the San Salvador basin (

Table 3-1 and Figure 3-2)[20]: cropland increased from 953 to 1,495 km^2 (57%), grassland decreased from 1,358 to 749 km^2 (45%), and production forest increased from 12 to 78 km^2 (570%). Land management also changed: in 1990, cropping with grazing combined with livestock and till practices prevailed, while in 2018, continuous cropping, no-till, and transgenic crops prevailed[26]. In 1990, winter crops in Soriano were three times larger than summer crops, and the main crops were winter wheat, barley, and sunflower[27]. However, in 2018, summer crops were twice as long as winter crops, and soybeans were the main crop[28].

Table 3-1: Area (km^2) of land use (LU) classes in 1990 and 2018 in the San Salvador watershed. LU classes were simplified by Hastings and others[20] and Petraglia and others[29], respectively.

Class	LU 1990	%	LU 2018	%
Native grassland	1,358	56.9%	749	31.0%
Rain-fed cropland	953	39.8%	1495	62.0%
Native forest	57	2.4%	57	2.4%
Production forest	12	0.5%	78	3.2%
Urban area	10	0.4%	5	0.2%
Irrigated cropland	---	---	28	1.2%

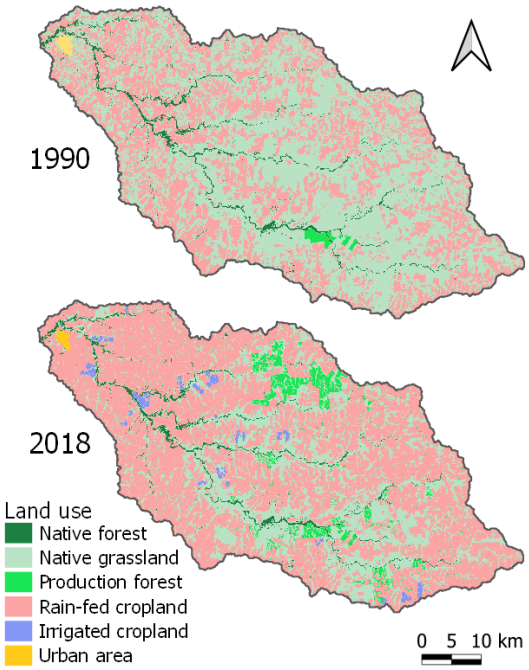

Figure 3-2: Land use maps of the San Salvador watershed: in 1990 (on top) and 2018 (bottom). Maps were simplified by Hastings and others[20] and Petraglia and others[29], respectively.

3.2.2 Data availability

SWAT requires specific data about weather, soil properties, topography, vegetation, and land management practices of the watershed[30]. An overview of the input data used in this study is provided in Table S 3-1 in the Supplementary Materials. Geospatial input data include digital elevation model[31] (DEM) (Figure 3-3), 1990 and 2018 Land Use / Land Cover (LULC) maps[20][29] (Figure 3-2), and soil map[32] (scale 1:40,000).

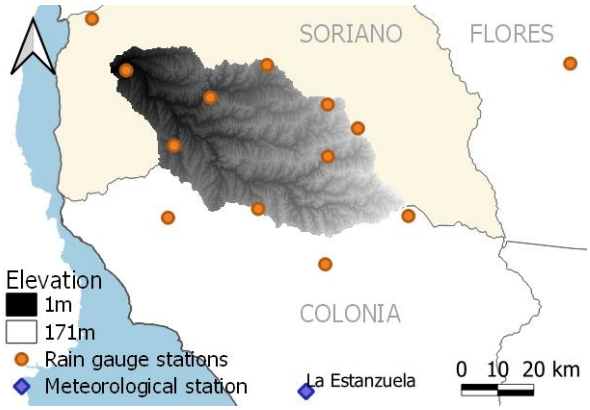

Figure 3-3: Elevation digital model[31], rain gauge stations[33], and meteorological station[34].

According to the soil map, there are 37 units in the watershed. The predominant soil type is Vertic Argiudoll (90%), which has high natural fertility and agricultural productivity in Uruguay. At SWAT, soil data are divided into physical and chemical characteristics. For the physical characteristics, the data are sourced from soil profiles linked to each map unit[32] or computed using the Soil-Plant-Air-Water (SPAW) model[35]. The soil units were classified into hydrological groups (HG) using the methodology proposed in the documentation of SWAT[30] and validated with the work of Durán[36] with very good agreement. The results show that HG classes D and C are predominant in the basin, with 70% and 21%, respectively (Figure 3-4). Regarding chemical characteristics, the contents of total nitrogen (TN) and Bray I phosphorus are reported for the soil profiles associated with each map unit. Nitrogen content was assumed to be 98% organic and 2% inorganic[37]; total phosphorus (TP) content was determined by a regression based on clay content and assumed to be 50% organic and 50% inorganic[38].

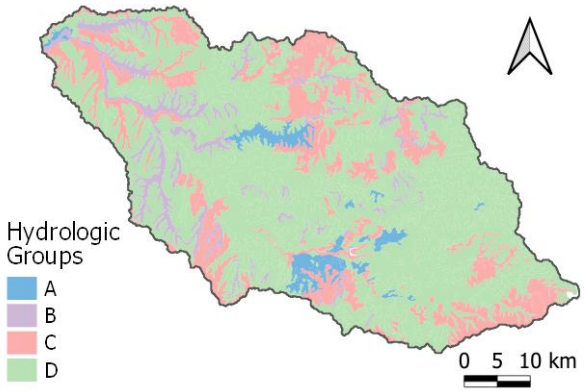

Figure 3-4: Hydrologic groups estimated from Soil Map, esc.: 1:40.000[32].

Daily precipitation data from 1987 to 2021 are from 14 rain gauging stations[25][33] in and around the watershed. Daily weather data (minimum and maximum air temperature, wind speed, relative humidity, and solar radiation) from 1987 to 2021 were recorded from the nearest meteorological station[34]. Figure 3-3 shows the location of the meteorological station and rain gauges. As the weather conditions within each sub-basin are homogeneous, the daily mean areal precipitation

was calculated for each sub-basin using the inverse distance weighting method[39] and then employed as input data for SWAT.

In the watershed, there is a single gauging station situated at Paso Ramos (outlet of sub-basin 12, Figure 3-5) (58° 09' 49" W, 33° 33' 15" S), which pertain to the National Water Directorate of the Ministry of Environment (DINAGUA-MA)[40]. Water levels at this station were manually recorded from 1985 to 2006, and discharges were computed using a rating curve. Although data is available until 2006, according to DINAGUA, only measurements up to 2000 are considered reliable. Rating curves are utilized to compute flow time series from water levels. These curves are derived empirically through field measurements and can introduce notable uncertainties that impact the calibration procedure of the hydrological model[41]. According to the station data quality analysis[42], the error is 33% for low flows (1.4 - 6.8 m^3/s) and 20% for medium flows (6.8 - 86 m^3/s). The peak and low flows (86 - 2000 m^3/s and 0 to 1.4 m^3/s, respectively) are ranges that were not recorded, so they were extrapolated from the rating curve and are subject to bigger uncertainties.

There are ten water quality stations in the watershed, seven along the San Salvador River that have been in operation since 2014, and four stations on tributaries that have been in operation since 2019 (Figure 3-5). The station designated SS50 is in Paso Ramos, where the streamflow station is. Monitoring has been conducted once every two months by State Sanitary Works Administration (OSE) and National Directorate for Quality and Environmental Assessment of the Ministry of Environment (DINACEA-MA) since 2016 and at a lower frequency since 2014. In addition, five campaigns were carried out in 2020-2021 as part of the INNOVAGRO project[39]. For this study, of the 44 parameters analyzed regularly, TN, TP, and total suspended solids (TSS) are considered. Table S 3-7 shows the number of samples and the mean, minimum and maximum values measured for TN, TP, and SST.

Point sources of pollution are domestic sewage in the city of Dolores and intensive livestock production (fattening farms and dairies). Dolores has a total population of 19,135 and discharges its domestic wastewater directly into the San Salvador River. Nutrient loads from domestic sewage are estimated using population size and bibliographic coefficients[43]. Nutrient load from fattening farms and dairies

is calculated using the estimated number of cattle in each sub-basin[44] and the calculations proposed by DINAMA[45]. According to the National Livestock Information System Livestock and the Livestock Comptroller´s Division of the Ministry of Livestock, Agriculture, and Fisheries (SNIG and DICOSE-MGAP)[44], the stock of cattle in fattening farms and dairies in the study area in 2018 was 12,595 and 6,646 cattle units, respectively. Another direct source of nutrients is the free access of cattle to watercourses. In Uruguay, this is a common management practice related to grazing on native grasslands and seeded pastures[46]. In the absence of information on the proportion of the area where this practice is applied and the proportion of manure directly deposited by cattle, it is assumed that 5% of cattle manure directly enters watercourses. According to SNIG and DICOSE[44], the stock of cattle grazing native grasslands and seeded pastures in the study area in 2018 was 58,972 and 3,905 cattle units, respectively.

SWAT includes scheduled management practices such as crop rotation, planting, harvesting, irrigation, fertilization, and tillage. Crop rotations for 1990 are based on information from the 1990 General Census of Agriculture, where two rotations of cropping with grazing combined with livestock are considered (Table S 3-2). For 2018, rotations are based on interviews with technicians of the General Directorate of Natural Resources of the MGAP (DGRN-MGAP), where four rotations of continuous cropping and one rotation of cropping with grazing combined with livestock are considered (Table S 3-3). Additionally, Table S 3-4 shows the cropping cycle and annual fertilizer rates.

The reference data for erosion rates was provided by DGRN and correspond to the annual averages obtained for Uruguay during 2000-2020 using the Revised Universal Soil Loss Equation (RUSLE)[47].

3.2.3 Model description and set up

The Soil & Water Assessment Tool (SWAT) is a model for predicting the effects of land use, land management, and climate change on water resources[11]. It is widely used to assess nutrient loading and soil erosion in agricultural basins. The model allows the simulation of various biophysical processes such as runoff, infiltration,

water storage, routing, crop yield, sediment transport, and nutrient cycling. The version of the model used is SWAT 2012, including SWAT Editor (2020 Revision 681) and QSWAT interface (version 1.9), available for QGIS (version 2.6.1).

Geospatial data were processed using QGIS (version 3.16.11), converting maps to raster format and projecting to the WGS 84 / UTM Zone 21S coordinate reference system. Thirteen sub-basins were delineated using the QSWAT interface, considering that outlets coincide with hydrometric and water quality stations (Figure 3-5). The sub-basins range from 47 to 341 km^2, sub-basins 4 and 11 were also delineated to subdivide a large one.

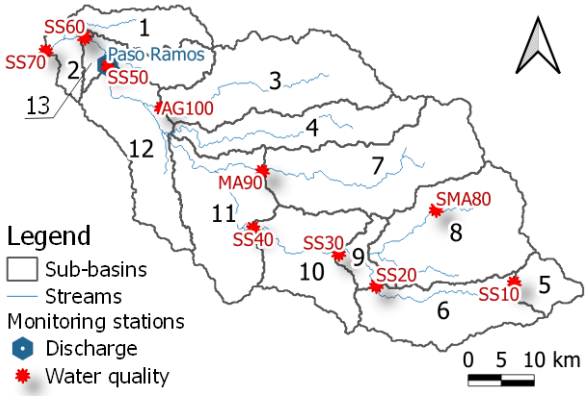

Figure 3-5: Monitoring stations (DINAGUA and DINACEA-MA) and SWAT sub-basins.

Due to the lack of accompanying observations on streamflow (1988-2006) and water quality (2014 to present), two models based on LULC and crop rotations from 1990 and 2018 were implemented; the first model was used to calibrate streamflow and the second model was used to verify water quality. The Split Land Use tool of SWAT was used to divide the rain-fed cropland, considering the main crop rotations and their relative extension (Table S 3-2 and Table S 3-3): two rotations for 1990 and five for 2018.

Hydrological response units (HRUs) are the basic computational unit of the model, and the number of HRUs depends on the heterogeneity of the input maps and the number of sub-basins. Given the computational limitations, it was necessary to reduce the initial number of HRUs. SWAT allows the application of filters based on the proportion of land use, soil, and slope to reduce the number of HRUs, but simulated water quality is sensitive to information loss[48]. Following the recommendations of

Her and others[48], we simplified the input maps to reduce the number of HRUs rather than applying filters. In this sense, we (1) reduced the original resolution of the maps (Table S 3-1) resulting in a pixel size of 120x120 m; (2) simplified the LULC maps, eliminating two minor classes (water 0.15% and bare soil 0.02%), noted that water bodies in SWAT are modeled by channels (streams) and reservoirs. Note that the number of HRUs with agricultural land use increased due to the representation of crop rotations, but the split allows for a detailed spatial distribution of the main crop rotations; (3) simplified the soil map, considering a maximum of 5 soil classes for each land use in each sub-basin, and reassigning minority classes according to hydrologic group and texture. These changes reduced the number of HRUs to 487 and 1354 for LULC 1990 and 2018, respectively.

The delivery of sediment and nutrients from the soil to water results from weathering acting on landforms[30]. SWAT uses the Modified Universal Soil Loss Equation (MUSLE)[49] to determine sediment yield daily:

$$sed = 11.8 \times \left(Q_{surf} \times q_{peak} \times area_{HRU}\right)^{0.56} \times K_{USLE} \times C_{USLE} \times P_{USLE} \times LS_{USLE}$$

Where *sed* is the sediment yield on a given day (Mg/ha/day); Q_{surf} is the surface runoff volume (mm); q_{peak} is the peak runoff rate (m^3/s); $area_{HRU}$ is the area of HRU (ha); K_{USLE} is the soil erodibility determined from soil data; C_{USLE} is the cover and management factor obtained from local research (Table 3-2); P_{USLE} is the support practice factor and is set equal to 1; LS_{USLE} is the topographic factor and is obtained from the slope length and average slope of the sub-basin (both calculated from DEM)[30]. RUSLE predicts the mean annual erosion rate and involves the consideration of a sediment delivery ratio for the computation of sediment yield[50]. On the other hand, MUSLE substitutes the rainfall energy factor with a runoff factor, allowing the equation to be applied to individual storm events for the calculation of sediment yield[30].

Table 3-2: USLE cover and management factor[51].

Land use	**C_{USLE}**
Native grassland	0.02
Production forest	0.006
Cropland with pastures, no till	0.02
Cropland, no till	0.036

SWAT simulates the transformation and movement of nitrogen and phosphorus in various organic and inorganic pools[30]. Soil N cycling has five different organic and inorganic pools; N transformation includes mineralization, decomposition and immobilization, nitrification, denitrification, and ammonia volatilization. Other N processes include plant uptake, biological N fixation, and NO_3-N movement in the water. The P cycle in the soil has six different organic and inorganic pools; the transformation of P in soil includes mineralization, decomposition, immobilization, and other processes such as plant uptake. Nitrates and soluble P are removed from the topsoil layer by surface and subsurface runoff. The amount of organic N and P transported with sediments is a function of organic N and P in the topsoil layer and sediment yield. In this study, nutrient yields are the total N or P loading delivered from HRU to stream.

SWAT can model in-stream processes that affect nutrient and sediment transformation and transport using QUAL2E[52] algorithms. The data used for in-stream water quality correspond to sediment and nutrient yields from HRUs and point sources.

3.2.4 Hard and soft model calibration

The calibration approach included hard and soft data[17]. Discharge data from the Paso Ramos gauging station were used for discharge calibration and validation. Due to the low sampling frequency (every three months), water quality was soft-calibrated. Crop yields, sediment yields, and nutrient cycling were also soft-calibrated using local data.

3.2.4.1 Crop soft-calibration

In SWAT, the processes involving crops, water, and nutrients are interconnected. The initial stage of model calibration focused on a soft calibration of crop growth. This calibration approach results in improved water and nutrient budgets compared to traditional approaches (without crop calibration)[53].

The model was soft-calibrated by comparing the annual average of simulated to observed (Uruguayan Federation of Crea Groups, FUCREA and Uruguay United Irrigators Association, RUU) crop yields for soybeans, corn, winter wheat, and barley.

For native grasslands, native forests, and production forests, biomass was compared using available data (Table S 3-1).

3.2.4.2 Flow calibration and validation

The steps to calibrate the flow discharge were: (1) performing a sensitivity analysis using extendedFourier amplitude sensitivity testing (eFAST)[54], after which were selected the parameters with the highest sensitivity index for calibration (the indices are calculated as the ratio of each partial variance to variance of the model output); (2) performing several calibration tests, including two methods for calculating evapotranspiration (Penman-Monteith and Hargreaves), two methods for streamflow routing (variable storage and Muskingum), and two algorithms for calibration (Sequential Uncertainty Fitting, SUFI2[55], and Particle Swarm Optimization, PSO[56]), with one option selected after the tests; (3) based on the initial calibration results, the baseflow was manually adjusted varying the groundwater parameters; (4) with the groundwater parameters fixed, the surface runoff parameters were calibrated; (5) the flow validation was performed.

The parameters included in eFAST analysis were selected based on the literature[57-58]. A brief description of each parameter, the process in which it is involved, the default values in the model, and the range of values considered are shown in Table S 3-7. In addition, some parameters were divided into two groups according to the land use: (A) native grassland, rainfed agriculture, and rainfed agriculture with pasture; (B): production forest and native forest.

Discharge was calibrated for 1990-1998 and validated for 1999-2000 with a daily time step, and a three-year warm-up period 1987-1989 was used to stabilize the model's initial conditions. The SWATrunR package[59] in R was used to perform sensitivity analysis, calibration, and validation. Nash-Sutcliffe efficiency (NSE)[60] was used as the objective function for model simulation optimization. Additionally, percent bias (PBIAS) and Kling-Gupta efficiency (KGE)[61] were calculated to evaluate model performance. NSE determines the relative magnitude of residual variance compared to measured data variance and has its optimum at 1[62]. PBIAS indicates the average tendency of the simulated data to be larger or smaller than the observed data; its

optimal value is 0, and positive or negative values of PBIAS indicate bias as underestimation or overestimation, respectively[62]. Streamflow simulation can be considered satisfactory if NSE > 0.50 and PBIAS is in the range [-15%, 25%][62]. KGE is a combination of the correlation coefficient, bias ratio, and variability ratio that allows optimization based on multiple criteria; its optimum is 1, and values in the range [-0.41, 1] can be considered satisfactory performance[63].

3.2.4.3 Sediment yield verification

For verification, the 2000-2020 annual average of simulated sediment yield was compared to the erosion rates provided by DGRN.

3.2.4.4 Phosphorus and nitrogen yields verification

Nutrient yields were soft-calibrated by comparing the annual average of simulated values with values from a literature review commonly used in Uruguay[64]. Additionally, the P index[65] soft data was recently estimated in Uruguay to assess the risk of P delivery from agricultural lands to surface waters. The values of P index were also compared to annual average of simulated nutrient yields.

3.2.4.5 Water quality verification

A global sensitivity analysis was conducted using eFAST, and the most sensitive parameters were adjusted. The goal of this soft-calibration was to align the average observed TN and TP values with those from a subset of simulations. To make a more accurate comparison, as the sampling is once every two months but simulations are daily, a subset of twenty-one days centered around the sampling day was employed instead of considering the entire set of simulations.

For this analysis, the SWATrunR package[49] in R was employed, utilizing the PSO algorithm to enhance the optimization of water quality simulations.

3.2.5 Analysis of nutrient delivery and transport

The approach of duration curve from U.S. Environmental Protection Agency (US EPA)[66] was used to analyze nutrient delivery and transport in the San Salvador watershed. This approach allows the characterization of water quality data under

different flow regimes. It can be used as a diagnostic tool to determine the magnitude and frequency of exceedances of water quality standards under all flow regimes.

The discharge duration curve relates daily discharge values to the percentage of the time those values were equaled or exceeded. Five hydrologic condition zones are distinguished: high flows (0-10%), moist conditions (10-40%), mid-range flows (40-60%), dry conditions (60-90%), and low flows (90-100%).

In this study, load-duration curves were generated by multiplying simulated flow by water quality concentrations. Analysis was performed for TN and TP. The curve compares three loads: observed, simulated, and targeted[67] during 2014-2021 in Paso Ramos (sub-basin 12). Targeted load refers to the allowable, considering the concentration levels specified in the local water quality guidelines[67]. Further, a source-duration curve was created to determine the contributions from the different sources to the nutrient load, using daily cumulative nutrient yields and point source loading up to Paso Ramos. It is worth noting that the observed load was calculated with simulated flow data since the observed flow is unavailable for this period. As previously discussed (Section 2.2), the zones of high and low flow have greater uncertainty, this uncertainty extends to the load curves within these specific zones.

A fundamental premise of this approach is the correlation of nutrient sources and water quality with flow conditions. These curves link water quality impairments to major sources. However, they do not account for processes such as sedimentation, plant uptake, or chemical transformations.

3.3 RESULTS AND DISCUSSION

3.3.1 Hard and soft model calibration

3.3.1.1 Crop soft-calibration

Soft-calibrated parameters and fitted values are summarised in the Table S 3-5 and Table S 3-6. Table 3-3 shows the average annual yield and biomass for observed and simulated data. After streamflow calibration, biomass and yield differed slightly; the results presented are the final values. However, this was the first step in calibrating the model because plant growth, especially perennial plants, was poorly represented.

Since the difference between simulated and observed annual averages was less than 20%, we assumed good agreement between simulated and observed data.

Table 3-3: Crop yield and plant biomass soft-calibration results 2010–2021.

Plant	Observed	Simulated	(%)
Yields (kg/ha)			
Corn 1st	6,133	6,938	13%
Corn 1st irrigated	11,060	11,591	5%
Soybean 1st	2,625	2,794	6%
Soybean 2nd	2,159	2,552	18%
Soybean 1st irrigated	4,052	3,814	-6%
Winter Wheat	3,805	3,728	-2%
Barley	3,737	3,395	-9%
Biomass (kg/ha)			
Native grasses	5,031	4,175	-17%
Pasture	6,600	6,179	-6%
Native forest	122,000	103,000	-16%
Production forest	240,000	228,000	-5%

3.3.1.2 Flow calibration and validation

Five steps are involved in the flow calibration and validation process (section 2.3). The first step was the sensitivity analysis performed using eFAST[57-58]. According to the analysis, the most sensitive parameter was CN2(A), with a sensitivity index of 0.55, while the index for the other parameters was less than 0.06 (Figure 3-6). The ten parameters with the highest sensitivity were considered for flow calibration: CN2(A), ALPHA_BF, CH_N2, ESCO_A, CH_L2, GWQMN, SOL_AWC, SLSUBBSN, OV_N_A, CH _S2.

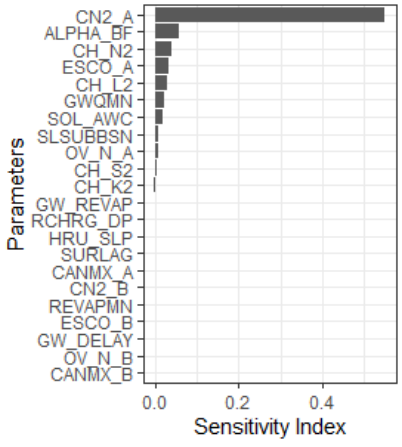

Figure 3-6: Results of the flow sensitivity analysis.

Some calibration tests were performed with two methods for evapotranspiration calculation, two methods for flow routing, and two algorithms for calibration. The configurations tested did not significantly improve the results as NS, PBIAS, and KGE that varied from 0.51 to 0.55, -14% to -19%, and 0.47 to 0.52, respectively. The selected configuration includes the Penman-Monteith and Variable Storage methods for calculating evapotranspiration and flow routing, respectively. The PSO algorithm was chosen because it has the highest NS and acceptable PBIAS and KGE. Based on the initial calibration results, groundwater flow was adjusted manually by varying the parameters ALPHA_BF and GW_DELAY, with GW_DELAY included because it appeared sensitive. Once fixed the groundwater parameters, the surface runoff was automatically calibrated by the PSO algorithm; the resulting parameters are listed in Table 3-5. Afterward, the flow validation was performed.

Table 3-4 shows the performance results of the calibration and validation and Figure 3-7 show the flow duration curves, simulated and observed (1990-2000). According to Moriasi and others[62], the performance of the calibration was satisfactory. In the validation period, NSE decreased to an unsatisfactory level, and KGE and PBIAS remained satisfactory. Therefore, the hydrologic submodel performance is considered adequate, according to the available data. The guidelines for quantification of accuracy[62] suggest a comparison metric for the simulations. However, it is important to note that the guidelines do not consider the uncertainty of climatological forcing[68] and/or hypothetical scenarios[69]. To account and adjust for different sources of errors in the hydrological model output, error models could be used[70].

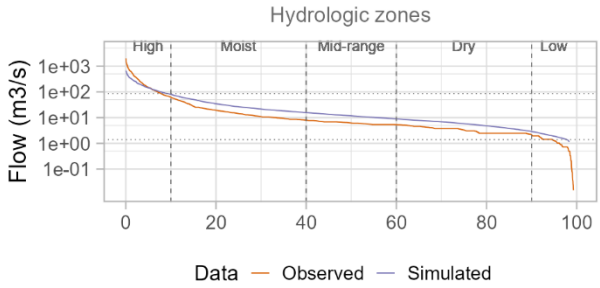

Figure 3-7: Flow duration curves, simulated and observed, 1990-2000.

Table 3-4: The SWAT model performance metrics during the calibration and validation of daily streamflow.

	NS	KGE	PBIAS
Calibration	0.55	0.47	-9
Validation	0.37	0.5	-12.5

Table 3-5: The most sensitive parameters and the adjusted values after flow calibration.

Parameter	Table	Unit	Change	Final
CN2 (A)	Mgt	---	Relative	8.5%
ALPHA_BF	Gw	1/day	Absolute	0.85
CH_N2	Rte	---	Absolute	0.03
ESCO	Hru	---	Absolute	0.87
CH_L2	Rte	Km	Relative	-13.1%
GW_DELAY	Gw	Days	Absolute	70.37
SOL_AWC	Sol	mmH_2O/mm soil	Relative	64.0%
SLSUBBSN	Hru	M	Relative	75.1%
OV_N	Hru	---	Relative	-22.2%
CH_S2	Rte	m/m	Relative	41.4%

3.3.1.3 Sediment yield verification

Table 3-6 compares the reference erosion rate for each land use with the average annual sediment yield for 2000-2020. The simulated averages are of the same order of magnitude as the reference values. Moreover, they are generally within the reference range, except for agriculture, where the simulated value is slightly higher. Additionally, Table S 3-9 presents sediment yield mean values (2014-2021) per sub-basin and land use category.

Table 3-6: Mean sediment yield simulated with SWAT and erosion rates reported by DGRN, standard deviations are enclosed within parenthesis, 2010-2020.

Land use	Erosion rate DGRN (Mg/ha/yr)	Sediment yield SWAT (Mg/ha/yr)
Irrigated cropland	---	4.29 (2.55)
Rainfed cropland	2.74 (1.57)	4.34 (2.56)
Rainfed cropland with pastures	---	2.13 (1.35)
Production forest	0.89 (0.5)	0.43 (0.32)
Native forest	0.99 (0.86)	0.19 (0.14)
Native grassland	1.86 (1.49)	2.49 (1.42)

3.3.1.4 Phosphorus and nitrogen yield verification

Table 3-7 presents the average annual yields of TN and TP in 2014-2021, along with corresponding bibliographic references[64] for each land use category. Additionally, Table S 3-9 presents TN and TP mean values per sub-basin and land use category. The simulated averages are in the same range as the reference values, except for production and native forests, where the simulations show lower TN yields. Additionally, the P-index (2014-2018) holds a slightly higher value compared to the simulated average TP. However, it is worth noting that the P-index was calculated over different period and for the entire Uruguay.

Table 3-7: Simulated (2014-2021) mean and standard deviation of yields from Total Nitrogen (NT) and Total Phosphorus (kg/ha/year), soft data from the scientific literature (min.-max.) [64], and P index [65].

Land use	**Bibliography**	**Sim. mean**	**Sim. sd**	
NT (kg/ha/yr)				
Irrigated cropland	---	17.25	8.75	
Rain-fed cropland	15.4 (3.2-47.7)	12.96	6.47	
Cropland with grazing	7.0 (1.5-21.1)	9.78	3.82	
Production forest	1.9 (0.8-3.7)	0.25	0.14	
Native forest	0.4	0.02	0.01	
Native grassland	1.3 (0.4-3.3)	2.26	0.93	
PT (kg/ha/yr)				**P_{Index}**
Irrigated cropland	---	2.93	1.34	
Rain-fed cropland	4.11 (0.32-16.71)	2.54	1.15	3.46
Cropland with grazing	1.79 (0.15-7.06)	2.7	0.98	
Production forest	0.29 (0.03-0.65)	0.18	0.11	1.79
Native forest	0.01	0.08	0.05	
Native grassland	0.24 (0.03-0.62)	1.14	0.48	2.35

3.3.1.5 Water quality verification

Table 3-8 presents the most sensitive parameters and the adjusted values after water quality calibration. Figure 3-8 shows boxplots comparing the simulated and observed concentrations of TN and TP. The simulated values upstream (small sub-basin extension) overestimated the concentrations of TN and TP. However, the

concentrations at stations SS40 to SS70 show good agreement (see location of stations in Figure 3-5).

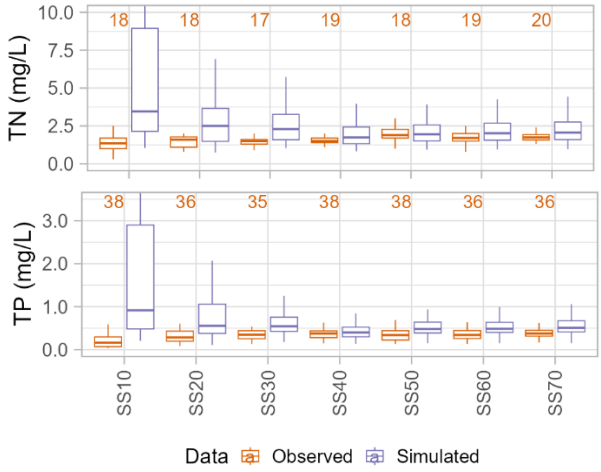

Figure 3-8: Simulated and observed concentrations of Total Nitrogen (TN) and Total Phosphorus (TP) (mg/L), 2014-2021. The orange numbers represent the number of observations at each monitoring station.

Table 3-8: The most sensitive parameters and the adjusted values after water quality calibration.

Parameter	Table	Unit	Final	Description
SPCON	Rte	---	0.0002	Linear parameter for calculating the maximum amount of sediment that can be reentrained during channel sediment routing.
ERORGP	Hru	---	0.638	Organic P enrichment ratio for loading with sediment.
P_UPDIS	Bsn	---	13.344	Phosphorus uptake distribution parameter.
NPERCO	Bsn	---	0.000 1335	Nitrogen percolation coefficient.
BIOMIX	Mgt	---	0.2	Biological mixing efficiency.
ERORGN	Hru	---	3.267	Organic N enrichment ratio for loading with sediment.

3.3.2 Analysis of nutrient delivery and transport

Load-duration curves for the 2014-2021 period in Paso Ramos (sub-basin 12) were generated for TN and TP (Figure 3-9 and Figure 3-10). Overall, there is a good agreement between observed and simulated nutrient loads (Figure 3-9 and Figure 3-10, Part C). However, under dry and low-flow conditions, the simulation overestimates the loads. As shown, the pattern of nutrient impairment occurs under all flow

conditions as the observed and simulated nutrient loads exceed the target loads[67]. It is worth noting that the load results in zones of high and low flow exhibit higher uncertainty, as discussed in Section 2.5.

The source-duration curves (Figure 3-9 and Figure 3-10) (Part A) and their relative contribution by source and hydrologic zone (Part B) showed that between mid-range and low flows, the main loads come from direct livestock excreta into waterbodies and point sources from feedlots and dairies. In addition, under wet and high-flow conditions, diffuse sources associated with land use mainly affect water quality.

For moist to high-flow conditions, the major source is diffuse loading associated with land use. The nutrient diffuse contribution is about 98% and 73% for high and moist conditions, respectively. Within the diffuse loadings, the main contributors in order of importance are rain-fed agriculture, agriculture with grazing, and natural grassland with grazing. Table S 3-12 shows the proportional contribution of each source type by hydrologic condition zones. Moreover, within Table S 3-9, Table S 3-10 and Table S 3-11, the average contribution of each source type per sub-basin are presented.

For low to mid-range flow conditions, the major sources of nutrients are direct excretions from cattle to water bodies and point sources. The direct loading contribution is about 65% for TN and 51% for TP. Within the total direct load (TN and TP), the load from natural grassland is 1.7 times higher than from agriculture with grazing. In addition, the contribution from point sources is about 32% for TN and 47% for TP. Within point sources, the load from dairies is higher than from fattening farms, with a value of 1.8 times for TN and 2.4 times for TP.

During dry and low flow conditions, simulations showed an overestimation of TN and TP loads. In the model, these input loads were not evaluated from measures but were calculated from the number of cattle, 84,849 cattle units[44] in the watershed in 2018. The amount of direct excretion of cattle into water bodies was an assumption based on the knowledge that this practice exists. Besides, wastewater discharges from fattening farms and dairies are assumed to be constant over time but may fluctuate

with runoff because wastewater is typically stored in lagoons. Therefore, further research is needed to improve information on excreta input loads.

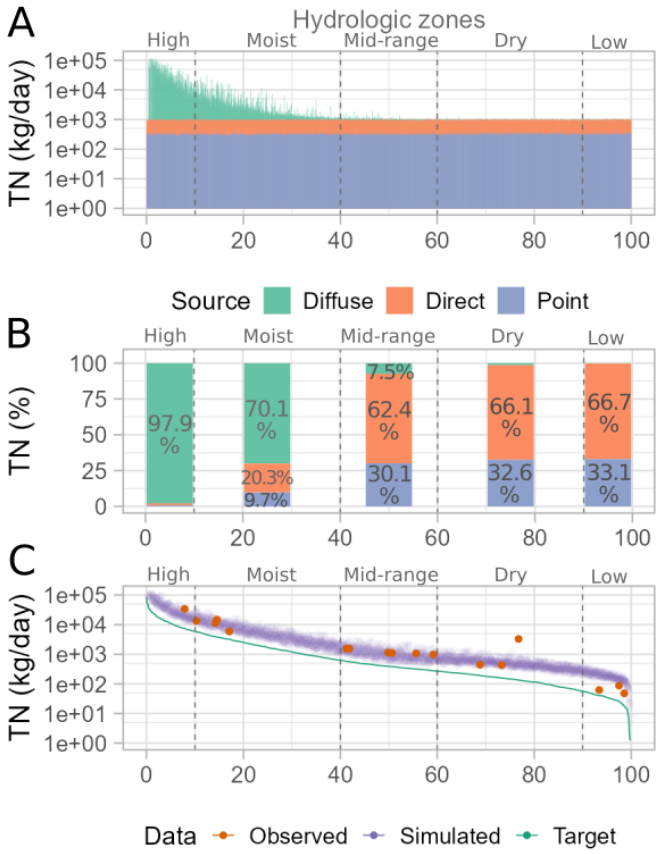

Figure 3-9: Total Nitrogen (TN) loads from 2014 to 2021 in Paso Ramos. (A) Load duration curve showing contributions from various sources; in this case, loads include cumulative yields from TN and point source loads in Paso Ramos. (B) The relative contribution of sources by hydrologic zone. (C) Load duration curves comparing observed and simulated data to the target curve.

Considering all flow conditions, diffuse loading from cropland was the main source of nutrient loading (77% and 71% of total loading from TN and TP, respectively, during 2014-2021). However, the load-duration curve approach showed that diffuse loading explained nutrient impairment only 40% of the time during high and wet flow conditions. For low to mid-range flow conditions (the remaining 60% of the time), water quality can be explained primarily by the contribution of direct excretions from cattle to water bodies and point sources (dairies and fattening farms). This characterization of nutrient budgets indicates that: (1) nutrient balance impairment occurs under all flow conditions; (2) to achieve sustainable agricultural intensification a range of conservation measures and best management practices

(BMPs) should be implemented. Diffuse sources pose a significant challenge because nutrients enter surface waters through various mechanisms (e.g., runoff, groundwater infiltration)[1][11][30]. Best management practices (BMPs)[2][4][8] generally focus on source control (practices to reduce erosion) or delivery reduction (e. g. riparian buffers to intercept nutrients[3]). Direct loading control includes measures to prevent animal access to waterbodies, restore banks, and prevent excess nutrients from entering the water. Point source control includes the treatment and management of wastewater from dairy and fattening farms[4][8].

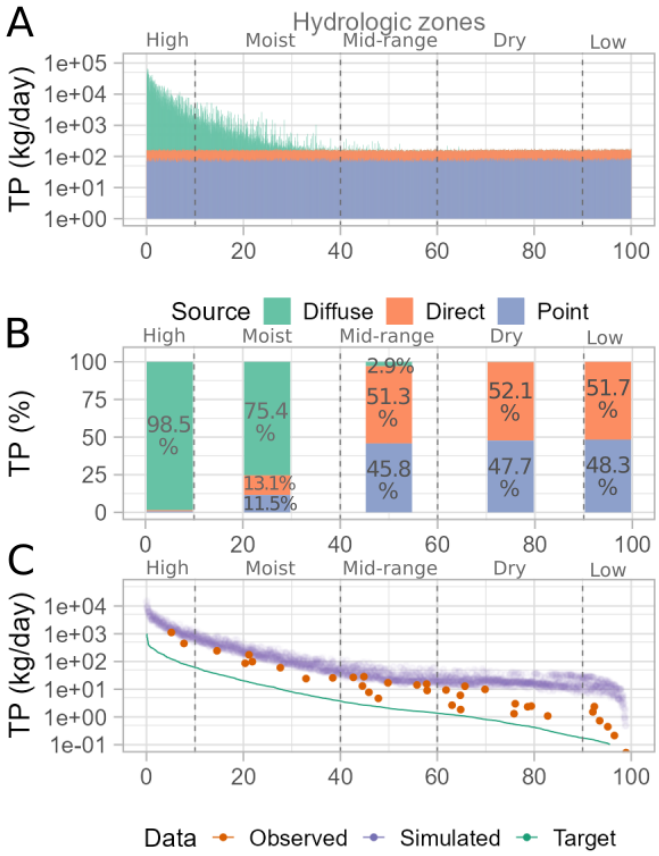

Figure 3-10: Tolal Phosphorus (TP) loads from 2014 to 2021 in Paso Ramos. (A) Load duration curve showing contributions from various sources; in this case, loads include cumulative yields from TP and point source loads in Paso Ramos. (B) The relative contribution of sources by hydrologic zone. (C) Load duration curves comparing observed and simulated data to the target.

3.4 CONCLUSIONS

In this study, a model SWAT was implemented that can characterize water quantity and quality in the San Salvador watershed. The main results obtained with such a model can be summarized as follows:

Calibration and validation of streamflow were successfully performed (NSE=0.55 and 0.37, PBIAS=-9 and -12.5, KGE=0.47, 0.5 for calibration and validation, respectively). Biomass, crop, sediment, nitrogen and phosphorus yields, and water quality showed good agreement with local soft data. The evaluation by hard and soft calibration and with available knowledge and data indicates that it is possible to fill the data shortage and build a reliable model.

The pattern of nutrient impairment occurs under all flow conditions as the observed and simulated nutrient loads exceed the target loads. Although diffuse loading from cropland was the primary source of nutrient loading (77% and 71% of total loading from TN and TP, respectively, during 2014-2021), the loading duration curve approach showed that this result was present in only 40% of the time during high and wet runoff conditions. For low to moderate runoff conditions (the remaining 60% of the time), water quality can be explained primarily by the contribution of direct excretions from cattle to water bodies and point sources (dairies and feedlots).

It is important to emphasize that the model developed in this study SWAT is suitable to represent the crops and land management practices typical of South America and the resulting sediment and nutrient fluxes. In addition, it represents a useful tool to facilitate informed decisions in the development of strategies to mitigate pollution impacts on receiving waters.

Acknowledgments

This study is part of the master's thesis of Florencia Hastings from FAGRO-UdelaR. It was partially supported by the National Research and Innovation Agency [grant numbers: POS_NAC_2020_1_164287 and FSA_PI_2018_1_148628].

We are sincerely grateful to colleagues who contributed significantly to the modeling decisions with information and/or discussions; they represented the following institutions (in alphabetical order): Integrated Watershed Modeling Group

(GMIC); Ministry of Livestock, Agriculture and Fisheries (MGAP); Ministry of Environment (MA); School of Agronomy, Universidad de la República (FAGRO-UdelaR); School of Engineering, Universidad de la República (FING-UdelaR), Uruguay United Irrigators Association (RUU).

Transparency of data

The model implemented in this work and the water quality data are freely available on the OSF platform: https://osf.io/ytn9g/

Author contribution statement

HF: Methodology, Software, Validation, Formal analysis, Investigation, Data Curation, Writing - Original Draft, Visualization, Funding acquisition.

PBM, NR and GA: Conceptualization, Methodology, Writing - Review & Editing, Supervision, Funding acquisition.

3.5 REFERENCES

1. Ullrich A, Volk M. Application of the Soil and Water Assessment Tool (SWAT) to predict the impact of alternative management practices on water quality and quantity. Agric Water Manag. 2009;96(8):1207-17.
2. United States Department of Agriculture, NRCService. Core4 conservation practices training guides: the common sense approach to natural resource conservation. Washington: USDA; 1999. 395p.
3. Calvo C. Rol ecosistémico de la zona riparia en sistemas dulceacuícolas en un escenario de cambio global [doctoral's thesis]. Montevideo (UY): Universidad de la República, Facultad de Agronomía; 2022. 146p.
4. Merriman KR, Gitau MW, Chaubey I. A tool for estimating best management practice effectiveness in Arkansas. Appl Eng Agric. 2009;25(2):199-213.
5. White MJ, Arnold JG. Development of a simplistic vegetative filter strip model for sediment and nutrient retention at the field scale. Hydrol Process. 2009;23(11):1602-16.

6. Osmond DL, Meals DW, Hoag DL, Arabi M, Luloff AE, Jennings GD, McFarland ML, Spooner J, Sharpley AN, Line DE. Synthesizing the experience of the 13 National Institute of Food and Agriculture-Conservation Effects Assessment Project Watershed Studies: present and future. In: Osmond DL, Meals DW, Hoag DLK, Arabi M, editors. How to build better agricultural conservation programs to protect water quality: The National Institute of Food and Agriculture-Conservation Effects Assessment Project Experience. Ankeny: Soil and Water Conservation Society; 2012. pp.151-67.
7. Plan de Acción Santa Lucía: medidas de segunda generación. Montevideo: GNA; 2018. 95p.
8. Tomer MD, Sadler EJ, Lizotte RE, Bryant RB, Potter TL, Moore MT, Veith TL, Baffaut C, Locke MA, Walbridge MR. A decade of conservation effects assessment research by the USDA Agricultural Research Service: Progress overview and future outlook. J Soil Water Conserv. 2014;69(5):365-73.
9. Brirhet H, Benaabidate L. Comparison of two hydrological models (Lumped And Distributed) over a pilot area of the Issen Watershed In The Souss Basin, Morocco. Eur Sci J. 2016;12(18):347. Doi: 10.19044/esj.2016.v12n18p347.
10. Paudel M, Nelson EJ, Downer CW, Hotchkiss R. Comparing the capability of distributed and lumped hydrologic models for analyzing the effects of land use change. J Hydroinformatics. 2011;13(3):461-73.
11. Arnold JG, Srinivasan R, Muttiah RS, Williams JR. Large area hydrologic modeling and assessment part I: model development. J Am Water Resour Assoc. 1998;34(1):73-89. Doi: 10.1111/j.1752-1688.1998.tb05961.x.
12. Mer F, Vervoort RW, Baethgen W. Building trust in SWAT model scenarios through a multi-institutional approach in Uruguay. SESMO. 2020;2:17892. Doi: 10.18174/sesmo.2020a17892.
13. Aznarez C, Jimeno-Sáez P, López-Ballesteros A, Pacheco JP, Senent-Aparicio J. Analyzing the impact of climate change on hydrological ecosystem services in Laguna del Sauce (Uruguay) using the SWAT Model and Remote Sensing Data. Remote Sens (Basel). 2021;13(10):2014. Doi: 10.3390/rs13102014.

14. Vilaseca F, Castro A, Chreties C, Gorgoglione A. Daily rainfall-runoff modeling at watershed scale: a comparison between physically-based and data-driven models. In: Computational Science and Its Applications – ICCSA 2021. Berlin: Springer-Verlag; 2021. pp. 18-33.
15. Gelós M, Neighbur N, Kok P, Badano L, Hastings F, Nervi E, Alonso J, Navas R, Vervoort W, Baethgen W. On the prediction of phosphorus fluxes in the Santa Lucía basin under different land use and management practices using SWAT model. In: Phosphorus in Soils and Plants Symposium towards a sustainable phosphorus utilization in agroecosystems. Montevideo: Facultad de Agronomía; 2022. pp. 81.
16. Hastings F, Kok P, Gelós M, Tejera Á. Implementación de un modelo de calidad de agua con la herramienta SWAT en la cuenca del Río Negro. In: XI Congreso Nacional de AIDIS [Internet]. Montevideo: AIDIS Uruguay; 2022 [cited 2023 Dec 19]. 8p. Available from: https://aidis.org.uy/wp-content/uploads/2022/11/Hastings-Florencia.pdf
17. Nervi E, Gelós M, Kok P, Alonso J, Navas R, Badano L, Neighbur N, Hastings F, Vervoort R W, Baethgen W. Evaluación de escenarios de uso del suelo en una subcuenca del río Santa Lucía utilizando el modelo SWAT. In: XI Congreso Nacional de AIDIS [Internet]. Montevideo: AIDIS Uruguay; 2022 [cited 2023 Dec 19]. 8p. Available from: https://aidis.org.uy/wp-content/uploads/2022/11/Nervi-Eliana-2.pdf
18. Arnold JG, Youssef MA, Yen H, White MJ, Sheshukov AY, Sadeghi AM, Moriasi AM, Steiner JL, Amatya D, Skaggs RW, Haney EB, Jeong J, Arabi M, Gowda PH. Hydrological processes and model representation: impact of soft data on calibration. Trans ASABE. 2015;58(6):1637-60.
19. Nelson AM, Moriasi DN, Talebizadeh M, Steiner JL, Gowda PH, Starks PJ, Tadesse HK. Use of soft data for multicriteria calibration and validation of Agricultural Policy Environmental eXtender: impact on model simulations. J Soil Water Conserv. 2018;73(6):623-36.
20. Hastings F, Fuentes I, Perez-Bidegain M, Navas R, Gorgoglione A. Land-cover mapping of agricultural areas using machine learning in Google Earth Engine.

In: International Conference on Computational Science and Its Applications. Cham: Springer; 2020. pp. 721-36.

21. Climate-Smart Agriculture in Uruguay [Internet]. Washington: The World Bank Group; 2015 [cited 2023 Dec 04]. Available from: https://climateknowledgeportal.worldbank.org/sites/default/files/2019-06/CSA%20in%20Uruguay.pdf
22. Ministerio de Ganadería, Agricultura y Pesca (UY). Uruguay agrointeligente: los desafíos para un desarrollo sostenible. Montevideo: MGAP; 2017. 161p.
23. Hastings F, Perez-Bidegain M, Navas R, Gorgoglione A. Impacts of irrigation development on water quality in the San Salvador watershed (Part 2): implementation of scenarios in SWAT. Agrociencia Uruguay [Internet]. 2023 [cited 2024 Feb 13];27(NE1):e1199. doi: 10.31285/AGRO.27.1199.
24. Instituto Nacional de Estadística. Resultados del Censo de Población 2011: población, crecimiento y estructura por sexo y edad. Montevideo: INE; 2012. 17p.
25. Instituto Uruguayo de Meteorología. Clasificación climática [Internet]. Montevideo: INUMET; [cited 2023 Jul 18]. Available from: https://www.inumet.gub.uy/clima/estadisticas-climatologicas/clasificacion-climatica
26. Pedro A, Macarena C, Cintia P. Análisis del agro-negocio como forma de gestión empresarial en América del Sur: el caso uruguayo. Agrociencia Uruguay. 2012;16(1):110-9. Doi: 10.31285/AGRO.17.546.
27. Ministerio de Ganadería, Agricultura y Pesca (UY). Censo General Agropecuario 1990. Montevideo: DCE; 1994. 239p.
28. Ministerio de Ganadería, Agricultura y Pesca, DIEA (UY). Anuario Estadístico Agropecuario 2021. Montevideo: MGAP; 2022. 263p.
29. Petraglia C, Dell'Acqua M, Pereira G, Yussim E. Mapa integrado de cobertura / uso del suelo del Uruguay, año 2018. In: Anuario OPYPA 2019. Montevideo: MGAP; 2019. pp. 523-31.
30. Neitsch S, Arnold JG, Kiniry JR, Williams JR. Soil and water assessment tool. Temple: Texas A&M University; 2011. 618p.

31. Infraestructura de datos espaciales [Internet]. Montevideo: IDEuy; [cited 2023 Jul 18]. Available from: https://visualizador.ide.uy/ideuy/core/load_public_project/ideuy/
32. Ministerio de Ganadería, Agricultura y Pesca, DGRN (UY). Carta de suelos escala 1:40,000 [Internet]. Montevideo: MGAP; [cited 2023 Jul 18]. Available from: https://dgrn.mgap.gub.uy/js/visores/dgrn/#
33. Mapa de estaciones del Instituto Uruguayo de Meteorología (INUMET) [Internet]. Montevideo: INUMET; [cited 2023 Jul 18]; Available from: https://www.inumet.gub.uy/clima/recursos-hidricos/mapa-de-estaciones
34. INIA. Banco de datos agroclimáticos [Internet]. Montevideo: INIA; [cited 2023 Jul 18]. Available from: https://bit.ly/2KOj2dZ.
35. Saxton KE, Rawls WJ. Soil water characteristic estimates by texture and organic matter for hydrologic solutions. Soil Sci SocAmJ.2006;70(5):1569-78.
36. Durán A. Clasificación hidrológica de los suelos del Uruguay. Agrociencia Uruguay 1997;1(1):15-29. Doi: 10.31285/AGRO.01.1009.
37. Perdomo C, Barbazán M, Durán JM. Nitrógeno [Internet]. Montevideo: Facultad de Agronomía; [cited 2023 Jul 18]. 70p. Available from: http://www.fagro.edu.uy/fertilidad/publica/Tomo%20N.pdf
38. Hernández J, Otegui O, Zamalvide JP. Formas y contenidos de fósforo en algunos suelos del Uruguay. Boletín de Investigación. 1995(43):32p.
39. Gorgoglione A, Silveira L, Eguren G, Rivas N, Hastings F, Saracho A, Rosas F, Pérez A, Basile F, Carriquiry M, Tiscornia G, Cal A, Navas R, García C, Otero A, Roel A, Vilaseca F, Rodriguez R, Pastorini M, Chreties C, Alonso J, Baethgen W, Ancev T, Vervoot RW, Nervi E, Rosas F. Plataforma para el soporte a la toma de decisión en el desarrollo de la agricultura irrigada sostenible (DAIS-STD) [Internet]. [Place unknown]: OSF; 2023 [cited 2023 Dec 18]. Available from: https://osf.io/ytn9g/
40. Ministerio de Ambiente, DINAGUA (UY). Visualizadores geográficos de DINAGUA [Internet]. Montevideo: MA; [cited 2023 Jul 18]. Available from: https://www.ambiente.gub.uy/informacion_hidrica/

41. Sikorska AE, Renard B. Calibrating a hydrological model in stage space to account for rating curve uncertainties: general framework and key challenges. Adv Water Resour. 2017;105:51-66.
42. Genta JL, Failache N, Alonso J, Bellón D. Balances hídricos superficiales en cuencas del Uruguay. Montevideo: Universidad de la República; 2001. 115p.
43. Tchobanoglous G, Burton FL; Metcalf & Eddy. Wastewater engineering: treatment, disposal and reuse. New York: McGraw-Hill; 1991. 1334p.
44. Ministerio de Ganadería, Agricultura y Pesca, SNIG (UY). Datos basados en la declaración jurada de existencias [Internet]. Montevideo: MGAP; [cited 2023 Jul 18]. Available from: https://www.snig.gub.uy/principal/snig-principal-institucional-indicadores
45. Ministerio de Vivienda, Ordenamiento Territorial y Medio Ambiente, DINAMA (UY). Evolución de la calidad de agua en la cuenca del río San Salvador: período 2014-2019. Montevideo MVOTMA; 2020. 77p.
46. Gorgoglione A, Gregorio J, Ríos A, Alonso J, Chreties C, Fossati M. Influence of Land Use/Land Cover on Surface-Water Quality of Santa Lucía River, Uruguay. Sustainability. 2020;12(11):4692. Doi: 10.3390/su12114692.
47. Wischmeier WH, Smith DD. Predicting rainfall-erosion losses from cropland east of the Rocky Mountains: guide for selection of practices for soil and water conservation. Washington: USDA; 1965. 47p.
48. Her Y, Frankenberger J, Chaubey I, Srinivasan R. Threshold effects in HRU definition of the soil and water assessment tool. Trans ASABE. 2015;58(2):367-78.
49. Williams JR. Sediment yield predictions with universal equation using runoff energy factor. In: Present and prospective technology for predicting sediment yield and sources. Washington: USDA; 1975. pp. 244-52.
50. Sadeghi SHR, Gholami L, Khaledi Darvishan A, Saeidi P. A review of the application of the MUSLE model worldwide. Hydrol SciJ. 2014;59(2):365-75.
51. Clericci C, Préchac F. Aplicaciones del modelo USLE/RUSLE para estimar pérdidas de suelo por erosión en Uruguay y la región sur de la cuenca del Río de la Plata. Agrociencia. 2001;5(1):92-103.

52. Brown L, Barnwell T. The Enhanced Stream Water Quality Models QUAL2E and QUAL2E-UNCAS (EPA/600/3-87-007). Athens: Environmental Research Laboratory; 1987. 188p.
53. Nair SS, King KW, Witter JD, Sohngen BL, Fausey NR. Importance of crop yield in calibrating watershed water quality simulation tools1. J Am Water Resour Assoc. 2011;47(6):1285-97.
54. Saltelli A, Tarantola S, Chan KPS. A Quantitative model-independent method for global sensitivity analysis of model output. Technometrics. 1999;41(1):39-56.
55. Abbaspour KC, Johnson CA, van Genuchten MTh. Estimating uncertain flow and transport parameters using a sequential uncertainty fitting procedure. Vadose Zone J. 2004;3(4):1340-52.
56. Kennedy J, Eberhart R. Particle swarm optimization. In: Proceedings of ICNN'95 - International Conference on Neural Networks; 1995 Nov 27 – Dec 1; Perth, WA, Australia. Perth: IEEE; 1995. pp. 1942-8.
57. Abbaspour KC, Rouholahnejad E, Vaghefi S, Srinivasan R, Yang H, Kløve B. A continental-scale hydrology and water quality model for Europe: calibration and uncertainty of a high-resolution large-scale SWAT model. J Hydrol. 2015;524:733-52.
58. Nossent J, Bauwens W. Multi-variable sensitivity and identifiability analysis for a complex environmental model in view of integrated water quantity and water quality modeling. Water Sci Technol. 2012;65(3):539-49.
59. Schuerz C. SWATrunR: Running SWAT2012 and SWAT+ Projects in R. R package version 0.2.7 [Internet]. California: Github; 2019 [cited 2023 Aug 23]. Available from: https://github.com/chrisschuerz/SWATplusR
60. Nash JE, Sutcliffe JV. River flow forecasting through conceptual models part I: a discussion of principles. J Hydrol. 1970;10(3):282-90.
61. Gupta HV, Kling H, Yilmaz KK, Martinez GF. Decomposition of the mean squared error and NSE performance criteria: implications for improving hydrological modelling. J Hydrol. 2009;377(1-2):80-91.

62. Moriasi DN, Arnold JG, Liew MW Van, Bingner RL, Harmel RD, Veith TL. Model evaluation guidelines for systematic quantification of accuracy in watershed simulations. Trans ASABE. 2007;50(3):885-900.
63. Knoben WJM, Freer JE, Woods RA. Inherent benchmark or not? Comparing Nash-Sutcliffe and Kling-Gupta efficiency scores. Hydrol Earth Syst Sci. 2019;23(10):4323-31. Doi: 10.5194/hess-2019-327.
64. Perdomo C. Metodología de estimación de aportes difusos de nitrógeno y fósforo a aguas superficiales desde suelos bajo uso agropecuario. Montevideo: MA; 2013. 6p.
65. Ministerio de Ganadería, Agricultura y Pesca, DGRN. Estimación de fósforo index [Internet]. Montevideo: MGAP; 2022 [cited 2023 Dec 18]. Available from: https://bit.ly/4aM1tCO
66. U.S. Environmental Protection Agency. An approach for using load duration curves in the development of TMDLs [Internet]. Washington: Watershed Branch; 2007 [cited 2023 Dec 18]. 68p. Available from: https://bit.ly/3TEtjKQ
67. Aubriot L, Chalar G, De León L, Goyenola G, Lizarralde C, Míguez B, Perdomo C, Quintans F, Rodó E, Teixeira de Mello F. Establecimiento de niveles guía de estado trófico en cuerpos de agua superficiales. Montevideo: MA; 2017. 48p.
68. Seibert J. On the need for benchmarks in hydrological modelling. Hydrol Process. 2001;15(6):1063-4.
69. Her Y, Yoo SH, Cho J, Hwang S, Jeong J, Seong C. Uncertainty in hydrological analysis of climate change: multi-parameter vs. multi-GCM ensemble predictions. SciRep.2019;9(1):4974. Doi:10.1038/s41598-019-41334-7
70. Liu L, Wang QJ, Xu YP. Temporally varied error modelling for improving simulations and quantifying uncertainty. J Hydrol. 2020;586:124914. Doi: 10.1016/j.jhydrol.2020.124914.
71. García JA. Producción de forraje de pasturas cultivadas en la Región Litoral Sur. In: Risso D, Berretta E, Morón A, editors. Producción y manejo de pasturas. Montevideo: INIA; 1996. pp. 163-8.

3.6 SUPPLEMENTARY MATERIAL

Table S 3-1: Data description and sources.

Dataset	Format	Resolution	Period	Source
Digital Elevation Model	Raster	0.32 m/ pixel resized to 120 m/pixel	2019	Spatial Data Infrastructure - Agency for the Development of Electronic Management and the Information and Knowledge Society (IDE-AGESIC).
Land Use/Cover Map	Raster	30 m/ pixel resized to 120 m/pixel	1990	Hastings and others[20]
Land Use/Cover Map	Raster	10 m/ pixel resized to 120 m/pixel	2018	Petraglia and others[29]
Soil Map and soil physical-chemical properties	Shape fille and table	esc.: 1:40,000	---	General Directorate of Natural Resources of the Ministry of Livestock, Agriculture, and Fisheries (DGRN-MGAP)
Precipitation Data	Time series	Daily, 13 stations	1988-2021	Uruguay Meteorological Institute (INUMET)
Meteorological Data	Time series	Daily, 1 station	1988-2021	National Agricultural Research Institute (INIA)
Streamflow	Time series	Daily, 1 station	1990-2000	National Water Directorate of the Ministry of Environment (DINAGUA-MA).
Water Quality	Time series	Semesterly, 11 station	2014-2021	National Environmental Observatory of the Ministry of Environment (OAN-MA)
Agricultural and irrigation management	Table	Annual	---	Consultation with local stakeholders and the group United Irrigators of Uruguay
Crop yields	Time series	Annual	2010-2021	Uruguayan Federation of Regional Agricultural Experimentation (FUCREA)
Irrigated crop yields	Time series	Annual	2010-2021	Consultation with the group United Irrigators of Uruguay.
Grassland biomass	Time series	Annual	2010-2021	DIEA-MGAP[28]
Production and native forest biomass	Value	Annual mean	---	Consultation with technicians of the General Forestry Directorate of the Ministry of Livestock, Agriculture, and Fisheries (DGF-MGAP)
Pasture biomass	Value	Annual mean	---	García[71]
Sediment yields	Table	Mean annual	2000-2020	General Directorate of Natural Resources of the Ministry of Livestock, Agriculture, and Fisheries (DGRN-MGAP)
Nitrogen and phosphorus yields	Table	Mean annual	Different periods	Perdomo[64]

Table S 3-2: Crop rotations associated with Land Use of 1990. AGR1, AGR2, AGR3, AGR4, and AGRP belong to rainfed agriculture with the proportions indicated in the table; AGRP includes a three-year grazing pasture, and AGRI represents irrigated agriculture.

ID	Type	% rainfed area	1		2		3	4
AGRC	Rainfed - grazing	14%	Corn	Barley	Sorghum	Winter wheat	Pasture	Pasture
AGRP		86%	Pasture	Winter wheat	Pasture	Winter wheat	Pasture	Pasture

Table S 3-3: Crop rotations associated with Land Use of 2018. *1st and 2nd refer to the fact that a cover crop and a winter crop, respectively, were planted before this crop.

ID*	Type	% rainfed area	1		2		3		4	5
AGR1	Rainfed	37%	W. wheat	Soyb. 2nd	Oats	Soyb. 1st				
AGR2		18%	Barely	Soyb. 2nd	W. wheat	Soyb. 2nd				
AGR3		27%	Oats	Corn 1st	Oats	Soyb. 1st				
AGR4		9%	W. wheat	Soyb. 2nd	Oats	Corn 1st	Oats	Soyb. 1st		
AGRP	Rainfed -grazing	9%	Pasture	Soyb. 1st	Oats	Soyb. 1st	Pasture	Pasture	Pasture	Pasture
AGRI	Irrigated	---	Oats	Soyb. 1st	Oats	Soyb. 1st	Oats	Corn 1st		

Table S 3-4 Operations for the management of crops.

*1st and 2nd refer to the fact that a cover crop and a winter crop, respectively, were planted before this crop. **The pasture has a duration of three years, is fertilized at planting as indicated in the table and then re-fertilized each year with 14 kg N/ha and 37 kg P/ha, and also receives additional organic fertilizer through grazing.

				Fertilization (Kg/ha/season)	
Crop*	Planting	Harvest	Irrigation	Nitrogen	Phosphorus
Barley / Winter wheat	14 Jun	25 Nov	No	92	46
Corn 1st	23-Sep	20-Feb	No	119	69
Corn 2nd	10-Dec	15-May	No	119	69
Soybean 1st	12-Nov	21-Apr	No	0	20
Soybean 2nd	10-Dec	1-May	No	0	20
Corn	23-Sep	20-Feb	Yes	215	79
Soybean	12-Nov	21-Apr	Yes	0	24
Pasture**	22-Apr	11-Nov	No	27	69

Table S 3-5: Parameters for soft calibration of plants. Bibliographic ranges, default values in SWAT, and final set parameters. Part 1.

		Production forest			**Native forest**			**Pasture**			**Native grasses**		
Parameter	**Definition**	Biblio.	Default	Final	Biblio.	Default	Final	Biblio.	Default	Final	Biblio.	Default	Final
BIO_E	Biomass/Energy Ratio ((kg/ha)/(MJ/m^2)).	7-75	15	75	---	25	40	2.3-7	35	10	4-12	34	8.5
HVSTI	Harvest index.	0.7	0.76	0.7	---	0.1	0.1	0-0.6	0.9	0.9	---	0.9	0.9
BLAI	Max leaf area index.	3.5	5	3.5	---	5	5	---	4	4	---	2.5	4
CHTMX	Max canopy height (m).	20	6	20	---	5.9	6.2	---	0.5	0.6	---	1	0.4
RDMX	Max root depth (m).	3	3.5	3	---	2.5	2.5	---	2	2	---	2	2
T_OPT	Min temp plant growth (°C).	20	30	19	---	17	17	20-25	25	19	---	25	17
T_BASE	Optimal temp for plant growth (°C).	7	10	6	---	1	1	2-5	12	6	---	12	2.5

Table S 3-6: Parameters for soft calibration of plants. Bibliographic ranges, default values in SWAT, and final set parameters. Part 2.

	Soybean 1st and 2nd				**Corn 1st**				**Winter Wheat**			**Spring Barley**			**Oats**		
Parameter	Biblio.	Default	Final	Final Irr.	Biblio.	Default	Final	Final Irr.	Biblio.	Default	Final	Biblio.	Default	Final	Biblio.	Default	Final
BIO_E	14-29	25	20	22	17-49	39	32	45	17-36	30	22	12-35	35	23	14-47	35	25
HVSTI	0.3-0.5	0.31	0.35	0.35	0.45 0.47	0.5	0.45	0.45	0.35 0.43	0.4	0.4	0.4-0.5	0.54	0.4	0.4-0.7	0.42	0.42
BLAI	6-6.5	3	6	6.5	5.7-6.5	6	5.8	6.5	7	4	6	7	4	6		4	4
CHTMX	---	0.8	0.8	0.8	---	2.5	2.5	2.5	---	0.9	0.8	---	1.2	0.8		1.5	1.25
RDMX	---	1.7	0.75	0.75	---	2	2	2	---	1.3	0.8	---	1.3	0.7		2	1
T_OPT	27.5-28	25	27.8	27.8	34	25	30	30	8-25	18	18	24.5	25	24.5	26	15	15
T_BASE	5-7	10	6	6	8	8	8	8	0	0	0	0	0	0	2	0	0

Table S 3-7: SWAT parameters considered for the flow sensitivity analysis.

Parameter	**Definition**	**Process**	**Filter LU***	**Default values**	**Sensitivity range**
CN2.mgt	SCS runoff curve number for moisture condition II.	Surface runoff	A	49 - 87	-20 - 15%
			B	45 - 83	-20 - 15%

Parameter	Definition	Process	Filter LU*	Default values	Sensitivity range
ESCO.hru	Soil evaporation compensation factor.	Evapotranspiration	A	0.95	0.3 - 1
			B	0.95	0.3 - 1
OV_N.hru	Manning's "n" value for overland flow.	Surface runoff	A	0.15 - 0.3	-90 - 500%
			B	0.1 - 0.14	-90 - 500%
HRU_SLP .hru	Average slope steepness (m/m).	Surface runoff	---	0.0001 - 0.1007	-30 a 30%
SLSUBBSN .hru	Average slope length (m).	Concentration time, erosion	---	61, 91, 122	-70% - 200%
CANMX.hru	Maximum canopy index (mm).	Evapotranspiration	A	1.5	1 - 3
			B	3.5	3 - 8
ALPHA_BF.gw	Baseflow recession factor (1/day)	Groundwater	---	0.1	0 - 1
GW_DELAY .gw	Groundwater delay (days).	Groundwater	---	31	0 - 300
GW_REVAP .gw	Groundwater 'revap' coefficient.	Groundwater	---	0.02	0.02 - 0.2
GWQMN .gw	Threshold depth of water in shallow aquifer for return flow to occur (mm).	Groundwater	---	1000	100 - 5000
REVAPMN .gw	Threshold depth of water in the shallow aquifer for 'revap' (mm).	Groundwater	---	750	100 - 1000
RCHRG_DP .gw	Groundwater recharge to deep aquifer (fraction).	Groundwater	---	0.02	0 - 0.15
SOL_AWC .sol	Available water capacity of the soil layer (mm/mm soil).	Soil water	---	0.08 - 0.19	0 - 300%
SURLAG .bsn	Surface runoff lag coefficient.	Surface runoff	---	4	0 - 72
CH_N2.rte	Manning coefficient for channel.	Routing	---	0.05	0.015 - 0.150
CH_L2.rte	Length of main channel. (km).	Routing	---	8 - 59	-50 - 100%
CH_S2.rte	Average slope of main channel (m/m).	Routing	---	0.0006 - 0.0021	-50 - 100%
CH_K2.rte	Effective hydraulic conductivity in main channel alluvium (mm/h).	Routing	---	6	0.0001 - 25

Table S 3-8: Observed water quality, 2014-2021. #: quantity of samples.

		TP (mg/L)				TN (mg/L)				TSS (mg/L)			
Station	**Start**	#	Mean	Max.	Min.	#	Mean.	Max.	Min.	#	Mean.	Max.	Min.
SS10	May-14	38	0.20	0.59	0.04	18	1.5	3.8	0.3	40	17	210	3
SS20	May-14	36	0.32	0.80	0.08	18	1.6	4.7	0.8	40	20	110	3
SS30	May-14	35	0.35	0.73	0.13	17	1.4	2.0	0.7	39	16	97	3
SS40	May-14	38	0.36	0.63	0.15	19	1.6	2.8	0.8	39	18	84	4
SS50	May-14	38	0.39	1.40	0.13	18	2.7	16.0	1.0	40	36	670	5
SS60	May-14	36	0.37	0.77	0.13	19	1.8	3.5	0.8	40	19	160	3
SS70	May-14	36	0.39	0.78	0.17	20	1.8	3.5	1.0	40	20	130	3
AG100	May-19	13	0.42	1.19	0.11	2	3.1	4.2	1.9	14	14	50	4
MA90	May-19	14	0.41	0.71	0.13	1	4.0	4.0	4.0	14	19	73	5
MG110	May-19	13	0.22	0.57	0.05	2	3.6	6.1	1.1	14	15	84	3
SMA80	May-19	14	0.31	0.62	0.10	2	2.1	3.3	0.9	14	12	66	3

Table S 3-9: Simulated (2014-2021) mean and standard deviation of yields from Sediments (SYLD), Total Nitrogen (NT) and Total Phosphorus, for each sub-basin and land use category.

	Subbasin												
Land use	**1**	**2**	**3**	**4**	**5**	**6**	**7**	**8**	**9**	**10**	**11**	**12**	**13**
SYLD (ton/ha/yr)													
Irrigated cropland	1.43	---	3.66	4.35	---	2.74	2.86	---	2.99	1.56	3.26	2.18	3.94
Rain-fed cropland	2.14	1.82	2.65	2.06	2.05	2.96	2.45	2.96	2.66	2.37	2.63	2.72	2.28
Cropland with grazing	2	2.2	2.35	2.43	2.05	3.7	2.3	3.52	2.74	3.1	2.25	3.29	2.21
Production forest	---	---	0.15	0.14	---	0.29	0.28	0.29	0.06	0.13	---	---	0.16
Native forest	0.03	0.03	0.04	0.03	---	0.15	0.11	0.16	0.04	0.12	0.11	0.04	0.04
Native grassland	0.66	0.66	0.81	0.59	0.95	1.54	1.07	1.62	1.03	1.06	1.31	1.01	0.85
Urban area	---	2.6	---	---	---	---	---	1.06	---	---	---	---	2.25
PT exported (kg/ha/yr)													
Irrigated cropland	1.43	---	3.66	4.35	---	2.74	2.86	---	2.99	1.56	3.26	2.18	3.94
Rain-fed cropland	2.14	1.82	2.65	2.06	2.05	2.96	2.45	2.96	2.66	2.37	2.63	2.72	2.28
Cropland with grazing	2	2.2	2.35	2.43	2.05	3.7	2.3	3.52	2.74	3.1	2.25	3.29	2.21
Production forest	---	---	0.15	0.14	---	0.29	0.28	0.29	0.06	0.13	---	---	0.16
Native forest	0.03	0.03	0.04	0.03	---	0.15	0.11	0.16	0.04	0.12	0.11	0.04	0.04
Native grassland	0.66	0.66	0.81	0.59	0.95	1.54	1.07	1.62	1.03	1.06	1.31	1.01	0.85
Urban area	---	2.6	---	---	---	---	---	1.06	---	---	---	---	2.25

	Subbasin												
Land use	**1**	**2**	**3**	**4**	**5**	**6**	**7**	**8**	**9**	**10**	**11**	**12**	**13**
NT exported (kg/ha/yr)													
Irrigated cropland	9.1	---	21.5	22.7	---	16.1	18.2	---	19.2	8.5	19.9	11.7	23.7
Rain-fed cropland	11.6	9.4	13.9	10.4	11.1	15.5	12.8	13.7	14.7	11.4	14	13.4	12.1
Cropland with grazing	7.2	8.3	8.8	9	6.2	14.6	7.6	12.5	9.6	11.3	7.9	12.6	8
Production forest	---	---	0.2	0.2	---	0.4	0.5	0.4	0.1	0.2	---	---	0.1
Native forest	0	0	0	0	---	0	0	0.1	0	0	0	0	0
Native grassland	1.3	1.1	1.6	1	1.6	3.2	2.1	3.2	2.1	2.1	2.6	2.2	1.8
Urban area	---	0.5	---	---	---	---	---	7	---	---	---	---	6.5
Area (ha)													
Irrigated cropland	85	---	619	30	---	439	338	---	72	1	293	747	200
Rain-fed cropland	7111	3128	16954	9942	3924	9856	19694	16454	1684	9262	14536	14864	8154
Cropland with grazing	703	309	1677	983	388	975	1948	1627	166	916	1438	1470	806
Production forest	---	---	3607	876	---	849	436	838	589	566	---	---	1
Native forest	322	346	604	587	---	272	421	371	251	725	863	681	284
Native grassland	1976	535	8252	6885	1567	8038	11296	12701	1956	8533	8523	3382	1296
Urban area	---	529	---	---	---	---	---	1	---	---	---	---	1

Table S 3-10: Point sources of nutrients, annual mean loads of total nitrogen (TN) and total phosphorus (TP).

	Subbasin												
Land use	1	2	3	4	5	6	7	8	9	10	11	12	13
PT (ton/yr)													
Domestic sewage	0.00	3.29	0.00	0.00	0.00	0.00	0.00	0.00	0.00	0.00	0.00	0.00	0.00
Dairies	0.96	0.24	1.82	0.78	1.38	2.47	3.52	6.67	0.08	0.31	0.44	1.42	0.80
Fattening farms	0.51	0.18	1.11	1.02	0.00	0.22	1.65	0.46	0.10	0.41	0.65	1.27	0.20
NT (ton/yr)													
Domestic sewage	0.0	42.0	0.0	0.0	0.0	0.0	0.0	0.0	0.0	0.0	0.0	0.0	0.0
Dairies	3.7	1.0	6.8	3.3	5.3	9.6	13.9	25.6	0.4	1.5	2.3	5.2	2.9
Fattening farms	2.6	1.0	5.7	5.3	0.0	1.2	8.5	2.4	0.5	2.1	3.3	6.5	1.0

Table S 3-11: Direct sources of nutrients (from unrestricted cattle access to watercourses), annual mean loads of total nitrogen (TN) and total phosphorus (TP).

	Subbasin												
Land use	1	2	3	4	5	6	7	8	9	10	11	12	13
PT (ton/yr)													
Native grassland	0.51	0.14	2.13	1.78	0.40	2.08	2.92	3.28	0.51	2.20	2.20	0.87	0.33
Cropland with grazing	0.67	0.30	1.61	0.94	0.37	0.93	1.87	1.56	0.16	0.88	1.38	1.41	0.77
NT (ton/yr)													
Native grassland	4.0	1.1	16.8	14.0	3.2	16.4	23.0	25.9	4.0	17.4	17.4	6.9	2.6
Cropland with grazing	5.3	2.3	12.7	7.4	2.9	7.4	14.7	12.3	1.3	6.9	10.9	11.1	6.1

Table S 3-12: Proportional contribution of each source to nutrient loading by flow condition, 2014-2021.

Source type	**Flow condition Source**	**TN (%)**					**TP (%)**				
		High	Moist	Mid-range	Dry	Low	High	Moist	Mid-range	Dry	Low
Diffuse	Rain-fed cropland	80.6%	59.8%	4.2%	0.6%	0.1%	69.1%	58.5%	2.4%	0.1%	0.0%
	Native grasslands	8.7%	4.7%	2.8%	0.6%	0.1%	19.9%	10.0%	0.3%	0.0%	0.0%
	Cropland with grassland	6.2%	3.8%	0.4%	0.1%	0.1%	7.5%	5.3%	0.1%	0.0%	0.0%
	Irrigated cropland	2.2%	1.8%	0.1%	0.0%	0.0%	1.7%	1.5%	0.1%	0.0%	0.0%
	Other land uses	0.3%	0.0%	0.0%	0.1%	0.0%	0.5%	0.1%	0.0%	0.0%	0.0%
Direct	Grazing on native grasslands	0.9%	12.7%	38.6%	41.0%	41.7%	0.5%	8.2%	31.8%	32.4%	32.3%
	Grazing on cropland	0.5%	7.6%	23.8%	25.0%	25.0%	0.3%	4.9%	19.5%	19.8%	19.4%
Point	Dairies	0.4%	6.3%	19.7%	21.0%	21.2%	0.5%	8.3%	32.7%	33.7%	34.3%
	Fatenning farms	0.2%	3.3%	10.4%	11.6%	11.8%	0.2%	3.3%	13.1%	14.0%	14.0%

4 IMPACTS OF IRRIGATION DEVELOPMENT ON WATER QUALITY IN THE SAN SALVADOR WATERSHED (PART 2): IMPLEMENTATION OF SCENARIOS IN SWAT.[3]

IMPACTOS DEL DESARROLLO DEL RIEGO EN LA CALIDAD DE AGUA EN LA CUENCA DEL RÍO SAN SALVADOR (PARTE 2): IMPLEMENTACIÓN DE ESCENARIOS EN SWAT.

IMPACTOS DO DESENVOLVIMENTO DA IRRIGAÇÃO NA QUALIDADE DA ÁGUA NA BACIA HIDROGRÁFICA DE SAN SALVADOR (PARTE 2): IMPLEMENTAÇÃO DE CENÁRIOS NO SWAT.

Hastings, Florencia[1]; Perez-Bidegain, Mario[1]; Navas, Rafael[2]; Gorgoglione, Angela[3]

[1]*Universidad de la República, Facultad de Agronomía, Montevideo, Uruguay*. *ORCID F.H.* https://orcid.org/ 0000-0002-7861-4702, M.P-B. https://orcid.org/ 0000-0002-5501-064X .
[2]*Universidad de la República, Centro Universitario Regional Norte, Departamento del Agua, Salto, Uruguay. ORCID* https://orcid.org/0000-0001-8559-9523.
[3]*Universidad de la República, Facultad de Ingeniería, Montevideo, Uruguay*. ORCID https://orcid.org/0000-0002-2476-2339.

ABSTRACT

Intensive agricultural activities pose a significant threat to water quality as critical non-point sources of pollution. Effective mitigation strategies demand understanding of the causes and processes of water pollution. This study aimed to quantify the impacts of irrigation development on water quality and assess best management practices for sustainable agriculture intensification. Employing the calibrated SWAT model for the San Salvador watershed (baseline scenario), two scenarios were implemented and evaluated: the first depicted irrigation development from a future reservoir, and the second integrated riparian buffer zones to minimize nutrient and sediment losses. Notably the baseline scenario did not achieve nutrient water quality objectives. Results revealed that irrigation development increases nutrient yields, driving the future reservoir toward eutrophication. Implementing riparian buffer zones reduced nutrient loss, but additional measures are necessary for sustainable environmental goals at the basin scale. This research contributes valuable

[3] Publicado en: Agrociencia Uruguay [Internet], 27(NE1):e1199. doi: 10.31285/AGRO.27.1199.

insights for formulating effective management strategies to minimize nutrient pollution in water and safeguard water quality and biodiversity in the basin.

Keywords: sustainable agriculture, water quality, supplementary irrigation, SWAT

RESUMEN

La intensificación agrícola representa una importante fuente de contaminación que amenaza la cantidad y calidad del agua. Estrategias de mitigación efectivas requieren comprensión de las causas y procesos de la contaminación del agua Este estudio tiene como objetivo cuantificar los impactos del desarrollo del riego en la calidad del agua y evaluar las buenas prácticas de manejo para la intensificación agrícola sostenible. Se utilizó el modelo SWAT calibrado para la cuenca de San Salvador (escenario base), se implementaron y evaluaron dos escenarios: el primero representa el desarrollo de riego a partir de un futuro embalse, y el segundo incorpora zonas buffer ribereñas para minimizar las pérdidas de nutrientes y sedimentos. Se destaca que en el escenario base no se alcanzan los objetivos de calidad del agua. Los resultados revelaron que el desarrollo del riego aumenta la exportación de nutrientes, llevando al futuro embalse a un estado de eutrofización. La implementación de zonas buffer ribereñas redujo los nutrientes exportados, pero se necesitan medidas adicionales para alcanzar objetivos ambientales sostenibles en la cuenca. Esta investigación aporta conocimientos valiosos para formular estrategias de gestión eficaces que minimicen la contaminación por nutrientes y protejan la calidad del agua y la biodiversidad en la cuenca.

Palabras clave: agricultura sostenible, calidad de agua, riego complementario, SWAT.

RESUMO

A intensificação das atividades agrícolas é uma importante fonte de poluição que ameaça a qualidade da água. Estratégias eficazes de mitigação requerem compreensão das causas e processos da poluição da água. Este estudo visa quantificar os impactos

do desenvolvimento da irrigação na qualidade da água e avaliar as melhores práticas de manejo para intensificação sustentável da agricultura. Utilizando o modelo SWAT calibrado para a bacia de San Salvador (cenário base), dois cenários foram implementados e avaliados: o primeiro representava o desenvolvimento da irrigação a partir de um reservatório futuro, e o segundo integrava zonas de proteção ripária para minimizar as perdas de nutrientes e sedimentos. Note-se que o cenário base não atinge os objetivos de qualidade da água para nutrientes. Os resultados revelaram que o desenvolvimento da irrigação aumenta a exportação de nutrientes, levando o futuro reservatório a um estado de eutrofização. A implementação de zonas de proteção ripária reduziu a perda de nutrientes, mas medidas adicionais são necessárias para objetivos ambientais sustentáveis na escala da bacia. Esta pesquisa fornece conhecimentos valiosos para a formulação de estratégias eficazes de gestão para minimizar a poluição por nutrientes na água e proteger a qualidade da água e a biodiversidade na bacia.

Palavras chave: agricultura sustentável, qualidade de água, irrigação, SWAT.

4.1 INTRODUCTION

According to some projections, global crop production will need to at least double by 2050 to meet projected food demand, leading to new concerns and stresses on the Earth's natural resources[1-2]. To achieve global food security and environmental sustainability, FAO promotes climate-smart agriculture with three main objectives: sustainably increasing agricultural productivity and income, adapting and building resilience to climate change, and reducing or eliminating greenhouse gas emissions[3].

Globally, differences between observed and potential crop yields suggest the presence of 'yield gaps' where management constrained productivity; in recent decades, agricultural intensification (e.g., through the use of irrigation, fertilizers, biocides, and mechanization) has accounted for the majority of yield increases[1]. Sustainable expansion of irrigation on rainfed croplands could close global yield gaps and secure food production to feed the world's population[4-6]. For a sustainable irrigation expansion, water resources must not be depleted, and environmental flows must be maintained[7-8]. Environmental flows refer to the quantity and quality of water

required for ecosystem conservation and resource protection[9]. Water infrastructure development is important as a long-term adaptation strategy to climate change[10]; the irrigation demand can be sustainably satisfied through water storage infrastructure[11].

Agricultural cropland is considered a critical source of nutrients to nearby water bodies; high concentrations of total nitrogen (TN)and total phosphorus (TP) were associated with agricultural watersheds[12-13]. Excessive nutrient levels can affect the health of water bodies by promoting rapid algal growth or eutrophication[14].

Riparian buffer zones represent a best management practice to protect waterbodies from diffuse nutrient, sediment, and chemical losses[15]. A riparian buffer zone is an area adjacent to a water body where a combination of trees, shrubs, and /or other perennial plants grow. When a buffer zone is implemented, the soil is stabilized, fertilizers and pesticides are retained, and pollutants that are washed off with runoff are trapped by the vegetation and soil[15]. Merriman and others[16] reported average nutrient reductions of 47% and 57% for riparian buffers for TN and TP, respectively. While Calvo[17] reported average reductions of nutrients of 25% to 78% for TP and -11% to 62% for TN, and suggested that a buffer zone composed of herbaceous and woody vegetation had the best overall efficiency.

Based on these considerations, this study used the Soil Water Assessment Tool (SWAT)[18] model to simulate and analyze the impact of irrigation development on agricultural production, water quantity, and water quality. SWAT is a physically based, continuous-time model at the watershed scale. It is widely used to predict the effects of land use and land management on nutrient loading and soil erosion in agricultural watersheds. Key components of the model include hydrology, weather, soil erosion, plant growth, nutrients, pesticides, land management, and stream routing.

This study represents the second part of a master's thesis aimed at developing a modeling tool to support sustainable land use and planning in an irrigation development scenario. The model implementation, calibration, and validation were reported in the paper “Impacts of irrigation development on water quality in the San Salvador watershed (Part 1): Assessment of current nutrient delivery and transport using SWAT”[19].

4.2 MATERIALS AND METHODS

4.2.1 Study area

The San Salvador watershed is located in the department of Soriano, Uruguay (Figure 4-1), and has an area of 2,413 km^2. The mean elevation is 79 m and ranges from 1 to 171 m, and the average slope is 2.3%. Land use (2018) is predominantly rainfed agriculture (62%) and native grassland (31%), while irrigated cropland accounts for only a small portion of the area (1.2%). The mean annual temperature and precipitation for the period 1961-1990 were 17.5 °C and 1100 mm, respectively [20].

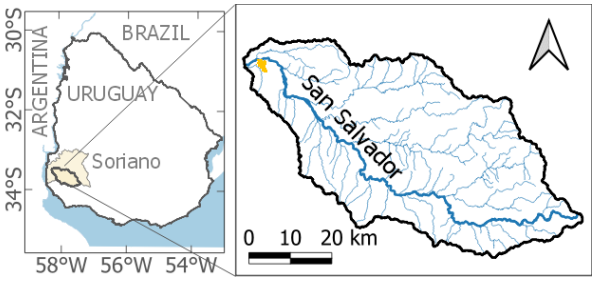

Figure 4-1: Location of San Salvador watershed (Soriano department, Uruguay). Coordinate Reference System: World Geodetic System 1984 (WGS84)

4.2.2 Brief model description

. A model setup with land uses from 2018 and daily time step simulation 1992-2021 (and three years of warm-up 1989-1992) was considered. The model scheme included 13 sub-basins and 1354 hydrologic response units (HRUs), which are units with the same soil, slope, and land use. No filters were used in delineating the HRUs; this level of detail allows for the simulation of the hydrologic process using a semi-distributed approach (Figure 4-2). The model input data included a Digital Elevation Model (DEM), land use, soil, management practices, and climatic data for the period 1990-2021; a detailed description of the input data can be found in Hastings and others[19].

The version of the model used in this study is SWAT 2012, including SWAT Editor (2020 Revision 681) and QSWAT interface (version 1.9), available for QGIS (version 2.6.1).

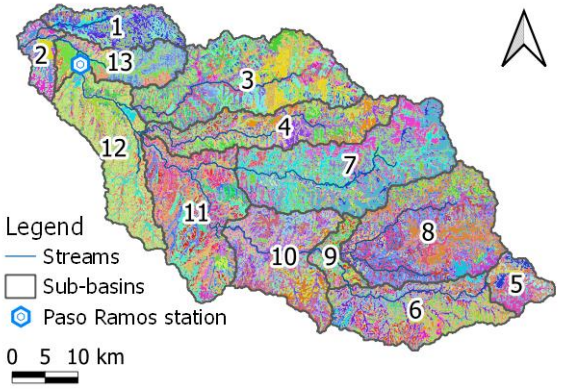

Figure 4-2: Sub-basins and Hydrologic Response Unit (HRU) delineated in SWAT.

4.2.3 Hard and soft model calibration

The calibration approach included hard and soft data[21]. A detailed description of the procedures and results can be found in Hastings and others[19].

Time series of discharge at the Paso Ramos station were used as hard data for calibration and validation of hydrological processes. Calibration and validation were performed for the 1990-1998 and 1999-2000 periods, respectively. Particle swarm optimization (PSO)[22], available in the SwatPlusR tool[23] was used for model optimization and Nash-Sutcliffe efficiency (NSE)[24] was chosen as the objective function. Furthermore, percent bias (pbias) and Kling-Gupta efficiency (KGE) were calculated for model verification. According to Moriasi and others[25], calibration performance was satisfactory (NSE 0.55, pbias -9, and KGE 0.47); although, NSE decreased to an unsatisfactory level during the validation period, KGE remained at a satisfactory level (NSE 0.37, pbias -12.5, and KGE 0.5). It was concluded that the performance of the hydrological model was adequate according to the available data.

Crop, sediment, and nutrient yields were verified using local data (observed crop yields and biomass 2010-2021, average annual sediment yield of Uruguay 2000-2020, and nutrient yields bibliographic review). Also, water quality (TN, TP, and total suspended solids, TSS) was soft-calibrated due to the low sampling frequency. Simulation averages were verified against observed averages at Paso Ramos station in the period 2014-2021.

4.2.4 Scenarios in SWAT

Two additional scenarios were implemented to compare to the baseline scenario representative of the current situation (1992-2021). The first scenario represents irrigation development (Scenario 1), and the second scenario adds riparian buffer zones to minimize export from diffuse nutrient, sediment, and chemical losses (Scenario 2).

4.2.4.1 Scenario 1: irrigation development

The irrigation scenario implemented in this study consists of considering the construction of a reservoir on a tributary to the San Salvador River and the associated increase in irrigated croplands. The reservoir's location and size and the location and extent of irrigated cropland areas were determined by a previous study that considered economic, social, and environmental criteria to select the most interesting scenario for irrigation development in the Salvador basin[26].

The scenario provides water for the irrigation of 6,950 ha of summer crops through central pivots, representing a 2.5 times increase in the irrigated area compared to the baseline scenario. There are two irrigation zones simulated (Figure 4-4): the first is in sub-basin 3, where water from the reservoir is pumped to irrigate 2,100 ha near the lake; the second zone is in sub-basin 12, and water is transported 14.5 km downstream via Aguila Creek and then pumped to irrigate 4,850 ha.

The simulated reservoir, in sub-basin 3 (Figure 4-4), has a capacity of 26.5 hm^3, a lake of 587 ha, and a contributing watershed of 27,048 ha. Table 4-1 shows the volume and area of the projected reservoir, the volume to fill the emergency spillway is 5% greater than that of the principal spillway.

Table 4-1: SWAT input variables related to reservoirs.

Variable	Value	Definition
RES_ESA	650	Area of the reservoir when filled to the emergency spillway (ha)
RES_EVOL	2783	Volume of water needed to fill to the emergency spillway (10^4 m^3).
RES_PSA	628	Area of the reservoir when filled to the principal spillway (ha).
RES_PVOL	2650	Volume of water needed to fill to the principal spillway (10^4 m^3).

An environmental flow was assumed to be daily discharged from the reservoir, whose volume was calculated as the monthly discharge with a 60% probability of exceedance for the baseline scenario ((Figure 4-3)), in accordance with the requirements of Uruguayan law [27].

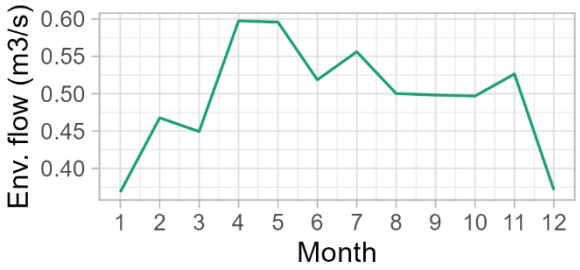

Figure 4-3: Monthly environmental flows.

The SWAT model assumes the reservoir is completely mixed and the only transformation in the water body is sediment and nutrient settling. A mass balance is computed to calculate nutrient discharge. Settling losses of phosphorous and nitrogen are estimated as a mass flux proportional to the apparent settling velocity[28]. Table 4-2 shows the settling velocities of phosphorus and nitrogen. Because reservoir water quality is very sensitive to these velocities and they are site-specific, default velocities and minimum and maximum values were used. In the case of sediment settling, the median particle diameter was set to 26 μm based on data from another local reservoir named Baygorria, located on Río Negro River[29]. The equilibrium sediment concentration was set at 40 mg/L, resulting from an iteration until obtaining a mean concentration in the water body of 5.5 mg/L (mean TSS observed in a local reservoir named Paso Severino, located on Santa Lucía River [29]).

Table 4-2: SWAT input variables that control settling in the reservoir. The minimum and maximum values are given in parentheses.

Variable	Default value	Final value	Definition
PSETLR	10 (2-20)	10 (2-20)	Phosphorous settling rate (m/yr).
NSETLR	5.5 (1-15)	5.5 (1-15)	Nitrogen settling rate (m/yr).
RES_D50	10 (0-10^5)	26	Median particle diameter of sediment (mm).
RES_NSED	4000 (1-5000)	40	Equilibrium sediment concentration (mg/l).

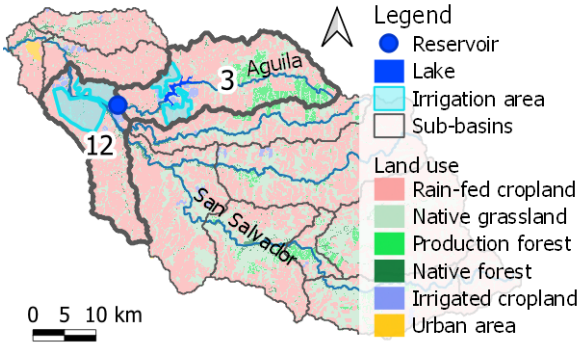

Figure 4-4: Irrigation scenario: location of the proposed reservoir and irrigated area.

This scenario entails a change in land use with respect to the baseline scenario: most (84%) of the projected irrigated area (6,950 ha) is converted from rain-fed agriculture to irrigated agriculture, while the remaining area (16%) is converted from native grassland to irrigated agriculture. An irrigated crop rotation of three years was considered: two years of soybeans and one year of corn (with a cover crop between summer crops). Simulated fertilizer applications per season were 215 kg N/ha for corn and 79 and 24 kg P/ha for corn and soybeans, respectively. Irrigation of crops in the model was based on crop demand during the season; irrigation occurs whenever the plant reaches a stress level of AUTO_WSTRS=0.9 (this value ranges from 0 to 1, where 1 means that plant growth is not affected by water stress). Once the irrigation scenario was implemented, the SWAT model was run using the 30-year climate database (from 1992 to 2021 and considering a warm-up period from 1989 to 1992).

4.2.4.2 Scenario 2: Riparian buffer zones

The second scenario consist of incorporating riparian buffer zones into Scenario 1 for the entire watershed. In this study, the design of the riparian buffer zones followed the guidelines proposed in the Santa Lucía River Protection Action Plan[30]. That plan proposes riparian buffer zones to mitigate nutrient delivery from agricultural areas in another Uruguayan watershed. The riparian buffer zones proposed have a width of 40 m in the main river, 20 m in streams with a minimum watershed of 10 km^2, and 100 m around reservoirs. Quantum GIS was used to delineate watersheds with a minimum size of 10 km^2 and their drainages. Buffer zones of 20, 40, and 100 m were then drawn. In the Plan[30], a buffer zone is defined as an area without crop cultivation and

agrochemical application, with the purpose of containing the transport of soil contaminants to water and restoring the hydro-morphological condition of the river. The native forest, defined as a natural buffer zone due to its inherent characteristics, was not considered part of the buffer zone scenario if it overlapped with the buffer area delineated in GIS (at a fixed distance from watercourses). Finally, the buffer area of the Scenario was uniformly distributed among all HRUs with land use in agriculture, livestock production, or urban areas. This calculation was performed on a sub-basin basis.

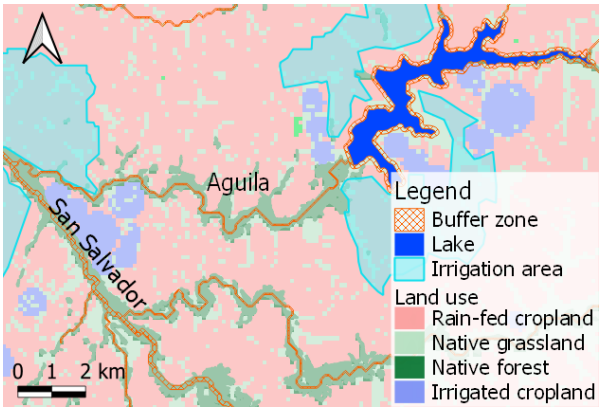

Figure 4-5: Scenario 2: Location of the riparian buffer zones implemented.

The delineated buffer covers an area of 2,703 ha and represents 1.1% of the total watershed area. Figure 4-5 shows the different widths of the riparian buffer zones in Scenario 2: 100 m around the reservoir, 40 m in the San Salvador River, and 20 m in Aguila Creek. The riparian buffer zones scenario entails a change in land use and/or management compared to the baseline scenario, where half (50%) of the buffer zone area is currently native grassland, 28% is native forest (which is already considered a buffer zone), 21% is rainfed agriculture, and the remaining 1% is production forest. Table S 4-3 shows the buffer area per sub-basin and its current land use.

In SWAT, the filter strip algorithm (VFS) is used to model riparian buffer zones; it reduces sediment and nutrients without affecting surface runoff. The VFS is based on 22 publications of measured data collected by researchers in several countries[31]. The algorithm includes three parameters: FILTER_RATIO, which was calculated for each sub-basin as the ratio of the sub-basin area to buffer area and varied from 42 to 148 (Table S 4-3); FILTER_CON, where the default value of 0.5 was used, meaning

that 50% of the HRU drains into the most concentrated 10% of the buffer; FILTER_CH, where the default value of 0.5 was used, meaning that there is no fully channelized flow[32].

4.3 RESULTS AND DISCUSSION

After implementing the scenarios in SWAT, daily simulations (1992-2021) were compared to the baseline scenario. Sub-basins 3 and 12 were selected for analysis because that is where the projected irrigated area develops. For inland processes, changes in crop yields, irrigation volume, and sediment and nutrient yields were evaluated. In addition, the construction of the reservoir changes the flow regime and affects water quantity and quality. Therefore, streamflow, TN, TP, and TSS were evaluated at the outlet of sub-basin 3 (in Aguila Creek, at the location of the reservoir) and the outlet of sub-basin 12 (after the confluence of Aguila Creek with the San Salvador River) (Figure 4-4). SWAT assumes that the reservoir is fully mixed so that water quality in the water body is equivalent to water quality at the outlet of sub-basin 3. Local water quality objectives (TN < 0.65 mg/L and TP < 0.05 mg/L)[33]. were considered to evaluate the simulated water quality.

4.3.1 Scenario 1: Irrigation development

The implementation of the irrigation development scenario showed that the flow of sub-basin 3, at the location of the reservoir, changed. Figure 4-6 compares the flow duration curves for the irrigation and baseline scenarios, and Table S 4-1 shows some flow percentile values. In the irrigation scenario, the flow duration curve has a flattened middle portion attributable to environmental flow discharge (with a 60% exceedance rate). The interquartile range (IQR), which explains the spread of 50% of the data, has also decreased from 1.9 m^3/s to 0.4 m^3/s. Downstream (sub-basin 12), flow impacts are lesser as Aguila Creek joins the mainstream. However, low flows (q10 and q25) seem slightly increased, again likely due to environmental flow requirements.

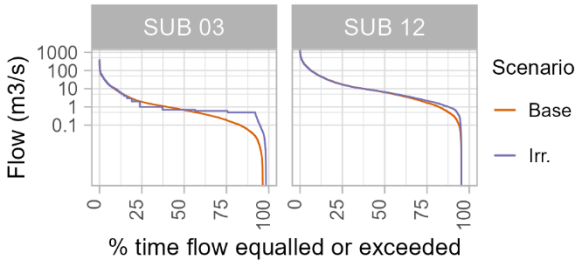

Figure 4-6: Flow-duration curve for the baseline and irrigation scenarios, 1992-2021.

Table 4-3 presents rainfall, irrigation, and irrigation deficit statistics for soybeans and corn during each growing season. Irrigation supplements precipitation but is highly variable; for example, simulated soybean irrigation averaged 115 mm but varied from 20 to 244 mm per season (1992-2021), while cumulative seasonal precipitation varied from 297 to 1,272 mm. These results are consistent with the observed irrigation average for 2016-2019[34], which was 133 and 183 mm for soybean and corn, respectively, and with a local study[35] that reported a simulated irrigation average of 204 mm for soybean and 225 mm for corn (1984-2007). The irrigation deficit is the difference between the amount irrigated with an unlimited water source and the amount with the reservoir as the water source. The average irrigation deficit is about 10% of the irrigated water.

Table 4-3: Precipitation (Pcp.), irrigation (Irr.), and irrigation deficit (Deficit) (mm) per cropping season, 1992-2021, average of sub-basins 3 and 12.

	Soybean				**Corn**			
	mean	**sd**	**min.**	**max.**	**mean**	**sd**	**min.**	**max.**
Pcp.	710	243	297	1272	579	243	215	1306
Irr.	115	61	20	244	118	61	40	224
Deficit	14	20	0	81	13	26	0	105

In this scenario, irrigation had a positive effect on crop yields and reduced the coefficient of variation compared to the baseline scenario (Table 4-4). The results showed a 39% and 32% increase in average yields for corn and soybeans, respectively. The coefficient of variation also decreases by more than half. This decrease in the coefficient of variation suggests that production is more stable over time under irrigation; similar results are reported by Rosas and others[36]. In absolute terms, considering all crops in the rotation, the average yield in sub-basins 3 and 12 increased by 13% under the irrigation scenario (from 164,155 Mg/yr to 185,316 Mg/yr).

Table 4-4: Average yields (kg/ha), standard deviation, and variation coefficient, 1992-2021, of sub-basins 3 and 12.

	Rain-fed		Irrigated	
	Corn	**Soybean**	**Corn**	**Soybean**
Mean	6683	2551	10980	3753
Std.	1011	992	809	498
CV (%)	15%	39%	7%	13%

As a result of the land use change, there was an increase in sediment, nitrogen, and phosphorus yields in this scenario compared to the baseline. Table 4-5 shows the results of the annual mean values of sediment, nitrogen, and phosphorus yields and their standard deviation. Sediment, nitrogen, and phosphorus yields increased by 2.3%, 5.6%, and 2.4%, respectively.

Table 4-5: Annual sediment (SYLD), nitrogen (NYLD), and phosphorus (PYLD) yields, 1992-2021, sub-basins 3 and 12.

	SYLD (Mg/ha/yr)		NYLD (kg/ha/yr)		PYLD (kg/ha/yr)	
Scenario	**mean**	**sd**	**mean**	**sd**	**mean**	**sd**
Base	4.34	2.29	11.49	5.97	2.65	1.45
Irr.	4.44	2.36	12.14	6.34	2.71	1.49
Irr.Buff.	1.17	0.85	5.89	3.35	1.14	0.69

The construction of the reservoir changed hydraulic conditions and nutrient transport. As mentioned before, there was an increase in sediment, nitrogen, and phosphorus yields, some of which were trapped in the reservoir. The mean sedimentation rate for 1992-2021 was 19,845 Mg/yr with a trapping efficiency of 94%. The mean sedimentation rate of nitrogen was 44 Mg/yr when NSETLR=5.5 m/yr and varied from 15 to 66 Mg/yr when NSETLR varied between 1 and 15 m/yr. Nitrogen trapping efficiency was 17% and ranged from 5% to 25%. The mean phosphorus sedimentation rate was 17 Mg/yr when PSETLR=10 m/yr and varied from 6 to 25 Mg/yr when PSETLR varied from 2 to 20 m/yr. Phosphorous trapping efficiency was 25% and ranged between 8% and 37%.

For nitrogen, phosphorus, and sediment loads transported by water (Table 4-6), total amounts were lower for the irrigation scenario (Irr.) than for the baseline scenario (Base) for sub-basins 3 and 12. Results for loads of TN and TP varied in magnitude as PSETLR and NSETLR varied, but the trend was the same.

Table 4-6: Annual mean loads (Mg/yr) of nitrogen, phosphorus, and sediment transport by water, 1992-2021. Values in parentheses are the results when NSETLR and PSETLR vary, as indicated in Table 4-2.

Sub	Scenario	NT	PT	SED
3	Base	294	76	21,316
	Irr.	258 (237-288)	60 (52-71)	1,516
	Irr.Buff.	120 (110-133)	25 (22-29)	1,516
12	Base	1,849	490	170,664
	Irr.	1,787 (1,768-1,813)	463 (456-473)	169,474
	Irr.Buff.	855 (846-867)	196 (193-200)	103,299

Water quality was affected by changes in the streamflow and nutrient loads. Figure 4-7 shows the daily nutrient and sediment duration curves in the water for the baseline and irrigation scenarios at the outlets of the sub-basins 3 and 12. Significant changes were observed at the discharge of the reservoir (sub-basin 3); while there were slight changes at the outlet of sub-basin 12 as Aguila Creek flows into the San Salvador River. In sub-basin 3, the median concentration of TN increased from 0.47 to 1.63 mg/L and the median concentration for TP increased from 0.10 to 0.36 mg/L. In the case of TSS, the median concentration at the outlet of sub-basin 3 decreased from 35.1 to 1.6 mg/L (Table S 4-2).

Based on these results, conservation measures would be needed to reduce nutrient concentrations in the reservoir (water quality in the fully mixed reservoir is equivalent to water quality at the outlet of sub-basin 3). It would be desirable to reduce TP to at least mesotrophic levels (TP < 0.04 mg/L, classification by Salas & Martino[37]). Measures may include practices that minimize nutrient inputs to surface waters, such as establishing riparian buffer zones and limiting nutrient loading upstream through less intensive agriculture, practices to reduce erosion, and moving cropland downstream.

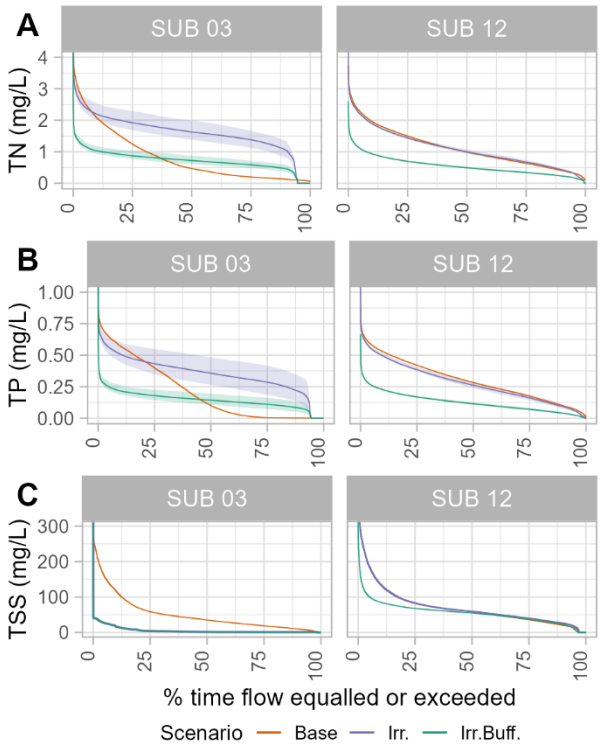

Figure 4-7: Daily duration curves in water for the baseline (Base), irrigation (Irr.), and irrigation with riparian buffer zone (Irr.Buff.) scenarios, 1992-2021. (A) Total nitrogen concentration, (B) total phosphorus concentration, and (C) total suspended solids. Ribbons represent the results of considering that PSETLR and NSETLR vary in a range of 2-20 m/yr and 1-15 m/yr.

4.3.2 Scenario 2: Riparian buffer zone

Implementing the riparian buffer zone resulted in a high reduction in nutrient and sediment yields compared to the irrigation scenario. Table 4-6 shows the results (Irr.Buff. scenario) of annual mean sediment, nitrogen, and phosphorus yields in sub-basins 3 and 12, and their standard deviation. Sediment, nitrogen, and phosphorus yields decreased by 74%, 51%, and 58%, respectively.

As a result, nutrient and sediment loads in water (Table 4-6) decreased compared to the irrigation scenario. The buffer zone has an overall retention efficiency of 52%, 57%, and 46% for TN, TP, and sediment, respectively, evaluated at the watershed outlet (sub-basin 2). These results are comparable with a study on the Paso Severino reservoir (Uruguay), where nutrient retention was measured within riparian buffers of different compositions (herbaceous, shrublands, and woodlands). In this study,

nutrient retention efficiency ranged from 25% to 78% for TP and from -11% to 62% for TN[17].

Figure 4-7 shows the daily nutrient and sediment concentration duration curves for the baseline, irrigation, and riparian buffer zone scenarios at the outlets of the sub-basins 3 and 12. At the reservoir outlet (sub-basin 3), the median concentrations of TN and TP decreased from 1.63 to 0.72 mg/L and from 0.36 to 0.14 mg/L, respectively. There was no change in TSS because its concentration was very low after settling in the reservoir. Although the median TP concentration decreased by 61% in the buffer scenario compared to the irrigation scenario, the water body remains classified as eutrophic.

It is crucial to note that achieving and maintaining the retention efficiency of riparian buffer zones requires proper design, including the selection of appropriate plant species, as well as effective management, which may involve harvesting products[17]. If not properly designed and managed, the buffer can be saturated and become a nutrient source rather than a sink, particularly during high-flow events[17]. Another related conservation practice is preventing animal access to water bodies, a measure observed to result in the revegetation of banks and the re-establishment of forested buffers[38-39].

4.4 CONCLUSIONS

The evaluation of the scenarios allowed us to understand the main processes affecting the export, transport, and transformation of nutrients and to quantify the impact at the watershed level, which is crucial for evaluating and proposing best management practices consistent with sustainable agricultural intensification.

The results of the irrigation development scenario showed increased sediment, nitrogen, and phosphorus yields compared to the baseline scenario. Additionally, heavy sedimentation occurs in the reservoir, with 17%, 25%, and 94% retention of the upstream of TN, TP, and sediment, respectively. As a result, the average load of nutrients and sediment in water would decrease compared to the baseline scenario. However, the reservoir would be classified as eutrophic due to the predicted median

concentration of TP. Therefore, conservation measures would be required to reduce nutrient concentrations in the reservoir and achieve an environmentally sustainable scenario.

Implementation of the scenario with riparian buffer zones resulted in reduced nutrient and sediment loads in water with overall retention efficiencies of 52%, 57%, and 46% for TN, TP, and sediment, respectively. These results are consistent with local studies. Although the average concentration of TP in the reservoir has decreased by 58%, it remains classified as eutrophic. On the other hand, the riparian buffer zone improves the overall water quality of the watershed. In sub-basin 12, the concentrations of TN and TP decreased by 52% and 58%, respectively, compared to the baseline scenario. This means that the median concentration of TN is 0.49 mg/L and meets the water quality objective (TN < 0.65 mg/L), while the median concentration of TP is 0.11 mg/L and does not meet the water quality objective (TP < 0.05 mg/L).

Although the riparian buffer zone improves water quality in the watershed, additional conservation measures would be required to achieve an environmentally sustainable scenario. It is worth noting that in the current situation (baseline scenario), the nutrient water quality standards are not accomplished, as the median concentrations in Paso Ramos (sub-basin 12) were 0.99 mg/L and 0.51 mg/L for TN and TP, respectively. However, the construction of the reservoir involves transitioning from a lotic water body to a lentic one, accompanied by high nutrient availability, which could potentially increase the risk of algae growth.

Acknowledgments

This study is part of the master's thesis of Florencia Hastings from FAGRO-UdelaR. It was partially supported by the National Research and Innovation Agency [grant numbers: POS_NAC_2020_1_164287 and FSA_PI_2018_1_148628].

Transparency of data

The models with the scenarios implemented in this work are freely available on the OSF platform: https://osf.io/ytn9g/

Author contribution statement

HF: Methodology, Software, Validation, Formal analysis, Investigation, Data Curation, Writing - Original Draft, Visualization, Funding acquisition.

PBM, NR and GA: Conceptualization, Methodology, Writing - Review & Editing, Supervision, Funding acquisition.

4.5 REFERENCES

1. Foley J, Ramankutty N, Brauman K, Cassidy E, Gerber J, Johnston M, Mueller N, O'Connell C, Ray D, West P, Balzer C, Bennett E, Carpenter S, Hill J, Monfreda C, Polasky S, Rockström J, Sheehan J, Siebert S, Zaks D. Solutions for a Cultivated Planet. Nature. 2011;478(7369):337-42.
2. Godfray HCJ, Beddington JR, Crute IR, Haddad L, Lawrence D, Muir JF, Pretty J, Robinson S, Thomas SM, Toulmin C. Food security: the challenge of feeding 9 billion people. Science. 2010;327(5967):812-8.
3. The state of food security and nutrition in the world: transforming food systems for food security, improved nutrition and affordable healthy diets for all. Rome: FAO; 2021. 240p.
4. Schmitt RJP, Rosa L, Daily GC. Global expansion of sustainable irrigation limited by water storage. Proc Natl Acad Sci U S A. 2022;119(47):e2214291119. Doi: 10.1073/pnas.2214291119.
5. Beltran-Peña A, Rosa L, D'Odorico P. Global food self-sufficiency in the 21st century under sustainable intensification of agriculture. Environ Res Lett. 2020;15:095004. Doi: 10.1088/1748-9326/ab9388.
6. Rosa L, Rulli MC, Davis K F, Chiarelli DD, Passera C, D'Odorico P. Closing the yield gap while ensuring water sustainability. Environ Res Lett. 2018;13:104002. Doi: 10.1088/1748-9326/aadeef.
7. Rosa L, Chiarelli DD, Tu C, Rulli MC, D'Odorico P. Global unsustainable virtual water flows in agricultural trade. Environ Res Lett. 2019;14:114001. Doi: 10.1088/1748-9326/ab4bfc.

8. Oduor BO, Campo-Bescós MÁ, Lana-Renault N, Echarri AA, Casalí J. Evaluation of the impact of changing from rainfed to irrigated agriculture in a Mediterranean Watershed in Spain. Agriculture. 2023;13(1):106. Doi: 10.3390/agriculture13010106.
9. Tharme R. A global perspective on environmental flow assessment: Emerging trends in the development and application of environmental flow methodologies for rivers. River Res Appl. 2003;19(5-6):397-441. Doi: 10.1002/rra.736.
10. Hansen Z, Libecap G, Lowe S. Climate variability and water infrastructure: historical experience in the Western United States. In: Libecap GD, Steckel RH, editors. The economics of climate change: adaptations past and present. Chicago: University of Chicago press; 2011. pp. 253-80.
11. Rosa L. Adapting agriculture to climate change via sustainable irrigation: biophysical potentials and feedbacks. Environ Res Lett. 2022;17:063008. Doi: 10.1088/1748-9326/ac7408.
12. US Environmental Protection Agency. The quality of our Nation's waters: summary of the national water quality inventory: 1998 report to Congress. Washington: US EPA; 2000. 20p.
13. Gorgoglione A, Gregorio J, Ríos A, Alonso J, Chreties C, Fossati M. Influence of Land Use/Land Cover on Surface-Water Quality of Santa Lucía River, Uruguay. Sustainability. 2020;12(11):4692. Doi: 10.3390/su12114692.
14. United States Environmental Protection Agency Protecting and Restoring America's Watersheds [Internet]. Washington: US EPA; 2001 [cited 2023 Jul 18]. 56p. Available from: https://bit.ly/48y5hFO
15. United States Department of Agriculture, NRCService. Core4 conservation practices training guides: the common sense approach to natural resource conservation. Washington: USDA; 1999. 395p.
16. Merriman KR, Gitau MW, Chaubey I. A tool for estimating best management practice effectiveness in Arkansas. Appl Eng Agric. 2009;25(2):199-213.

17. Calvo C. Rol ecosistémico de la zona riparia en sistemas dulceacuícolas en un escenario de cambio global [doctoral's thesis]. Montevideo (UY): Universidad de la República, Facultad de Agronomía; 2022. 146p.
18. Arnold JG, Srinivasan R, Muttiah RS, Williams JR. Large area hydrologic modeling and assessment part I: model development. J Am Water Resour Assoc. 1998;34(1):73-89. Doi: 10.1111/j.1752-1688.1998.tb05961.x.
19. Hastings F, Perez-Bidegain M, Navas R, Gorgoglione A. Impacts of irrigation development on water quality in the San Salvador watershed (Part 1): assessment of current nutrient delivery and transport using SWAT. Agrociencia Uruguay [Internet]. 2023 [cited 2024 Feb 13];27(NE1):e1198. doi: 10.31285/AGRO.27.1198.
20. Instituto Uruguayo de Meteorología. Clasificación climática [Internet]. Montevideo: INUMET; [cited 2023 Jul 18]. Available from: https://www.inumet.gub.uy/clima/estadisticas-climatologicas/clasificacion-climatica
21. Arnold JG, Youssef MA, Yen H, White MJ, Sheshukov AY, Sadeghi AM, Moriasi AM, Steiner JL, Amatya D, Skaggs RW, Haney EB, Jeong J, Arabi M, Gowda PH. Hydrological processes and model representation: impact of soft data on calibration. Trans ASABE. 2015;58(6):1637-60.
22. Kennedy J, Eberhart R. Particle swarm optimization. In: Proceedings of ICNN'95 - International Conference on Neural Networks; 1995 Nov 27 – Dec 1; Perth, WA, Australia. Perth: IEEE; 1995. pp. 1942-8.
23. Schuerz C. SWATrunR: Running SWAT2012 and SWAT+ Projects in R. R package version 0.2.7 [Internet]. California: Github; 2019 [cited 2023 Aug 23]. Available from: https://github.com/chrisschuerz/SWATplusR
24. Nash JE, Sutcliffe JV. River flow forecasting through conceptual models part I: a discussion of principles. J Hydrol. 1970;10(3):282-90.
25. Moriasi DN, Arnold JG, Liew MW Van, Bingner RL, Harmel RD, Veith TL. Model evaluation guidelines for systematic quantification of accuracy in watershed simulations. Trans ASABE. 2007;50(3):885-900.

26. BRL Ingenierie SA, SIGMAPLUS SRL. Caracterización de las cuencas del río San Salvador, río Yí y río Arapey para fines de riego [Internet]. Montevideo: MGAP; 2017 [cited 2023 Dec 20]. Available from: https://bit.ly/3GUJOLs
27. Aprobación de medidas para que los usos de las aguas públicas aseguren el caudal Ambiental que permita la protección del ambiente y criterios de manejo ambientalmente adecuados de las obras hidráulicas. Decreto N° 368/018. Publicada D.O. 13 Nov/018 - N°30.068.
28. Neitsch S, Arnold JG, Kiniry JR, Williams JR. Soil and water assessment tool. Temple: Texas A&M University; 2011. 618p.
29. Ministerio de Ambiente, OAN (UY). Extracción de datos [Internet]. Montevideo: MA; [cited 2023 Jul 18]. Available from: https://www.ambiente.gub.uy/iSIA_OAN/
30. Plan de Acción Santa Lucía: medidas de segunda generación. Montevideo: GNA; 2018. 95p.
31. White MJ, Arnold JG. Development of a simplistic vegetative filter strip model for sediment and nutrient retention at the field scale. Hydrol Process. 2009;23(11):1602-16.
32. Arnold J, Kiniry J, Srinivasan R, Williams J, Haney E, Neitsch S. Water Assessment Tool, input / output documentation. Temple: Texas A&M University; 2012. 654p.
33. Aubriot L, Chalar G, De León L, Goyenola G, Lizarralde C, Míguez B, Perdomo C, Quintans F, Rodó E, Teixeira de Mello F. Establecimiento de niveles guía de estado trófico en cuerpos de agua superficiales. Montevideo: MA; 2017. 48p.
34. Regadores Unidos del Uruguay. Cultivos regados RUU [Internet]. Message to: Florencia Hastings. 2020 Jul 8 [cited 2023 Dec 19]. [1 paragraphs].
35. Giménez L, García Petillo M. Summer crops evapotranspiration for two climatically constrating regions of Uruguay. Agrociencia. 2011;15(2):100-8. Doi: 10.31285/AGRO.15.598.
36. Rosas F, Sans M, Arana S. The effect of irrigation on income volatility reduction: a prospect theory approach [Internet]. Montevideo: ORT; 2018

[cited 2023 Dec 19]. 32p. Available from: https://dspace.ort.edu.uy/bitstream/handle/20.500.11968/3890/documentodeinvestigacion118.pdf?sequence=1&isAllowed=y

37. Salas HJ, Martino P. Metodologías simplificadas para la evaluación de la eutrofización en lagos cálidos tropicales [Internet]. Lima: OPS; 2001 [cited 2023 Dec 19]. 63p. Available from: https://iris.paho.org/handle/10665.2/55330
38. Tomer MD, Sadler EJ, Lizotte RE, Bryant RB, Potter TL, Moore MT, Veith TL, Baffaut C, Locke MA, Walbridge MR. A decade of conservation effects assessment research by the USDA Agricultural Research Service: progress overview and future outlook. J Soil Water Conserv. 2014;69(5):365-73.
39. Moriasi DN, Steiner JL, Arnold JG. Sediment measurement and transport modeling: impact of riparian and filter strip buffers. J Environ Qual. 2011;40(3):807-14. Doi: 10.2134/jeq2010.0066.

4.6 SUPPLEMENTARY MATERIAL

Table S 4-1: Flow (m3/s) quantiles and averages for the baseline and irrigation scenarios, 1992-2021.

Sub	Scenario	mean	q10	q25	q50	q75	q90
3	Base	4.3	0.1	0.2	0.8	2.1	9.2
	Irrigation	4.4	0.5	0.6	0.7	1.0	10.0
12	Base	30.4	0.9	2.7	7.6	19.1	67.0
	Irrigation	30.2	1.4	3.4	7.8	18.4	65.6

Table S 4-2: Total nitrogen (TN), total phosphorus (TN) and total suspended solids (TSS) concentrations quantiles and averages for the baseline and irrigation scenarios, 1992-2021.

Sub	Scenario	mean	q10	q25	q50	q75	q90
			TN (mg/l)				
3	Base	0.82	0.13	0.20	0.47	1.25	2.08
	Irr.	1.60	1.04	1.38	1.63	1.92	2.19
	Irr.Buff.	0.72	0.45	0.58	0.72	0.87	1.03
12	Base	1.11	0.40	0.63	0.99	1.50	1.96
	Irr.	1.09	0.43	0.67	1.00	1.44	1.89
	Irr.Buff.	0.55	0.23	0.34	0.49	0.69	0.93
			TP (mg/l)				
3	Base	0.209	0.001	0.005	0.099	0.399	0.571
	Irr.	0.351	0.205	0.285	0.357	0.432	0.506
	Irr.Buff.	0.144	0.078	0.11	0.143	0.179	0.216
12	Base	0.301	0.098	0.175	0.282	0.42	0.527
	Irr.	0.278	0.091	0.161	0.262	0.386	0.493
	Irr.Buff.	0.125	0.039	0.07	0.114	0.169	0.225
			TSS (mg/l)				
3	Base	49.8	9.9	18.8	35.1	58.3	117.4
	Irr.	5.5	1.0	1.0	1.6	4.1	16.8
	Irr.Buff.	5.5	1.0	1.0	1.6	4.1	16.8
12	Base	70.4	20.0	35.9	59.0	83.4	136.2
	Irr.	71.6	25.7	39.6	59.2	82.7	134.8
	Irr.Buff.	55.2	22.7	37.2	55.0	68.0	85.0

Table S 4-3: Riparian buffer zone design, projected area per sub-basin, and current land use. *FILTER RATIO = Sub. Area (ha) / Scenario buffer area (ha)

Sub.	Sub. Area (ha)	Current (2018) land use of GIS delineated buffer zone (ha)						GIS deli-neated buffer area (ha)	Scenario buffer area (ha)	FILTER RATIO *
		Rain-fed croplan d (ha)	Native grasslan d (ha)	Producti on forest (ha)	Native forest (ha)	Irrigated cropland (ha)	Urban area (ha)			
1	10198	34	34		34	1		103	69	148
2	4848	43	24		60		4	131	71	68
3	31713	181	279	8	66	5		539	473	67
4	19303	13	126	4	59			202	143	135
5	5880	35	106					141	141	42
6	20431	80	311	7	58			456	398	51
7	34132	45	211	1	47			304	257	133
8	31992	72	195	4	25			296	271	118
9	4717	19	57	2	75			153	78	60
10	20004	17	189	13	151			370	219	91
11	25654	68	221		219			508	289	89
12	21145	97	82		183	2		364	181	117
13	10744	75	38		51			164	113	95
Total	**240761**	**779**	**1873**	**39**	**1028**	**8**	**4**	**3731**	**2703**	**89**

5 SÍNTESIS, CONCLUSIONES GENERALES Y REFLEXIONES FINALES

Este capítulo se inicia con una breve síntesis que resalta los principales hallazgos de la investigación y su contribución al campo de estudio. Con base en los resultados obtenidos, se formulan las conclusiones generales, respaldadas por los fundamentos, hipótesis y objetivos establecidos en la introducción. Por último, se presentan algunas reflexiones finales y se proponen futuras líneas de investigación.

5.1 SÍNTESIS

Para alcanzar el objetivo general de la investigación, de cuantificar el impacto del desarrollo del riego en la cantidad y calidad del agua en la cuenca del río San Salvador mediante el modelo SWAT, se llevaron a cabo tres etapas documentadas en tres artículos científicos que se enfocan en (1) la identificación del uso del suelo mediante imágenes satelitales para la conceptualización del modelo (Hastings et al., 2020), (2) la implementación del modelo y la caracterización de flujos (Hastings et al., 2023a) y (3) la aplicación del modelo en la simulación de escenarios (Hastings et al., 2023b).

El primer artículo (capítulo 2), titulado *Land-cover mapping of agricultural areas using machine learning in Google Earth Engine* (Hastings et al., 2020), ha proporcionado un mapa de la cobertura y uso del suelo para el año 1990 en la cuenca del río San Salvador. Este mapa sirvió de base para definir la conceptualización del modelo a través de las unidades de respuesta hidrológica y está disponible para futuros usos. Además, a partir de este mapa, se analizó la transformación del uso del suelo en la cuenca entre 1990 y 2018, donde se evidenciaron cambios significativos, como la conversión de áreas de campo natural en tierras de cultivo y el desarrollo de la forestación. La metodología utilizada en este estudio puede aplicarse en la elaboración de mapas históricos de cobertura y uso del suelo en otras cuencas, aprovechando herramientas de código abierto y gratuitas, como Google Earth Engine. Esta herramienta demuestra un excelente potencial en la cartografía de la cobertura del suelo, gracias a su eficiencia en el procesamiento y a los algoritmos de aprendizaje automático que son de fácil aplicación. Además, la disponibilidad de imágenes

satelitales gratuitas, como las de Landsat, facilita la creación de series temporales de mapas desde aproximadamente 1984.

El segundo artículo (capítulo 3), titulado *Impactos del desarrollo del riego en la calidad de agua en la cuenca del río San Salvador (Parte 1): Análisis de la exportación y transporte de nutrientes actual mediante SWAT* (Hastings et al., 2023a), tiene por objetivo caracterizar tanto la cantidad como la calidad del agua en la cuenca de San Salvador utilizando el modelo SWAT. La calibración del caudal se realiza en el período 1990-1998 y se valida en 1999-2000 en la estación hidrométrica Paso Ramos. Los indicadores de desempeño, como el coeficiente de eficiencia de Nash (Nash), el índice Kling-Gupta Efficiency (KGE) y el sesgo (pbias), reflejan un ajuste satisfactorio entre las simulaciones y los datos observados durante la calibración y validación, con valores de Nash de 0,55 y 0,37, KGE de 0,47 y 0,50, pbias de -9 % y -12,5 % para la calibración y validación, respectivamente. La biomasa, el rendimiento en grano de los cultivos, los sedimentos y nutrientes exportados concuerdan con los datos cualitativos locales. Además, la calidad del agua simulada se ajusta satisfactoriamente con la calidad observada, lo que se confirma mediante un análisis cualitativo, incluyendo gráficos de boxplots, curvas de frecuencia y gráficos en ventanas temporales centradas en los muestreos. Es importante destacar que se obtuvieron mejores resultados en los puntos con área de cuenca más grande. Se aplicó la metodología de US EPA (2007) para analizar las cargas de nutrientes simuladas en comparación con las cargas objetivo[4] y en función del caudal de agua, lo que reveló que las cargas de nutrientes superan las cargas objetivo bajo todas las condiciones de caudal (desde picos hasta estiaje), tanto en cargas observadas como simuladas. La mayor parte de la carga total de nutrientes proviene de fuentes difusas, siendo la agricultura de secano para grano, el campo natural bajo pastoreo y la agricultura con pastoreo los principales contribuyentes. No obstante, el análisis también muestra que las cargas difusas predominan solo el 40 % del tiempo durante las condiciones de caudales altos y picos. En condiciones de caudales moderados a estiaje (el 60 % restante del tiempo), la

[4] Las cargas objetivo se refieren a las cargas de nutrientes admisibles, calculadas considerando los niveles de concentración especificados en las guías locales de calidad del agua.

calidad del agua se explica principalmente por la contribución de excreciones directas de ganado a los cuerpos de agua y fuentes puntuales (efluentes de tambos y encierros de engorde a corral). De lo anterior se desprende que, para lograr una intensificación agrícola sostenible que se refleje en la calidad del agua en la cuenca, es necesario implementar un conjunto integral de medidas de conservación y buenas prácticas agrícolas. Esto incluye (pero no se limita a): la reducción de las fuentes difusas mediante el control de la erosión, la retención de nutrientes mediante zonas *buffer* ribereñas, medidas para evitar el acceso de animales a los cuerpos de agua y disminuir así las cargas directas, así como el tratamiento y la gestión de efluentes de tambos y encierros de engorde a corral.

El tercer artículo (capítulo 4), titulado *Impactos del desarrollo del riego en la calidad de agua en la cuenca del río San Salvador (Parte 2): Implementación de escenarios en SWAT* (Hastings et al., 2023b), evalúa los principales cambios en la cantidad y calidad de agua en la cuenca en un escenario de desarrollo del riego. Este análisis es esencial para proponer alternativas de buenas prácticas de manejo en el contexto de la intensificación agrícola sostenible. En el escenario de riego, se simula un nuevo reservorio sobre el arroyo del Águila, un afluente del río San Salvador, junto con dos zonas de riego suplementario de cultivos de verano con pivot, una aguas arriba y la otra aguas abajo del reservorio, después de la confluencia del arroyo con el río San Salvador. La implementación del reservorio tiene un efecto significativo en los caudales de la subcuenca donde se ubica, al aumentar los caudales bajos y disminuir los caudales altos con respecto al escenario base (mismo punto sin reservorio), dado que eroga el caudal ambiental con 60 % de excedencia según la normativa vigente. Esto se traduce en una curva de excedencia con una porción central aplanada y una disminución en el valor del rango intercuartil. Tras la confluencia con el río San Salvador, el efecto en los caudales disminuye, aunque se observa un aumento de los caudales bajos. Los resultados de las simulaciones muestran que el riego tiene un efecto positivo en los rendimientos de los cultivos, con aumentos del 39 % y 32 % en los rendimientos promedio de maíz y soja, respectivamente, durante el período 1992-2021. Además, se observa una reducción del coeficiente de variación de los rendimientos, lo que sugiere una mayor estabilidad en la producción bajo riego. Sin

embargo, la implementación del riego conlleva un aumento en la exportación de sedimentos, nitrógeno y fósforo en comparación con el escenario base. El reservorio retiene una parte significativa de estos nutrientes y sedimentos, pero la concentración mediana de fósforo total en el embalse lo clasifica como eutrófico. Esto indica la necesidad de implementar medidas de conservación y buenas prácticas agrícolas para reducir las concentraciones de nutrientes en el reservorio y lograr un escenario ambientalmente sostenible. En un segundo escenario, se incorporan zonas *buffer* ribereñas con el propósito de retener nutrientes y mejorar la calidad de agua en la cuenca. Estas zonas muestran eficiencias de retención para nitrógeno, fósforo y sedimentos del 52 %, 57 % y 46 % respectivamente, lo que se traduce en concentraciones medianas más bajas de TP y TN en comparación con el escenario base. A pesar de que mejora la calidad general del agua en la cuenca, la concentración mediana de PT en el reservorio aún lo clasifica como eutrófico. Por lo tanto, se requieren medidas adicionales de conservación y buenas prácticas agrícolas para lograr un escenario ambientalmente sostenible. Es importante destacar que en el escenario base no se cumplen los objetivos de calidad del agua para nutrientes. Sin embargo, la construcción de un reservorio implica una transición de un cuerpo de agua lótico a uno léntico, junto con una alta disponibilidad de nutrientes podría aumentar el riesgo de crecimiento de algas.

5.2 CONCLUSIONES GENERALES

El objetivo general de este trabajo, que implica la implementación del modelo SWAT para cuantificar el impacto del desarrollo del riego en la cantidad y calidad del agua en la cuenca del río San Salvador, así como el primer objetivo específico de implementar, calibrar, validar y evaluar este modelo han sido alcanzados con éxito. Como resultado, el modelo SWAT se ha implementado, calibrado y validado en la cuenca, utilizando tanto datos cuantitativos como información cualitativa en un proceso de calibración rigurosa y blanda (*hard and soft calibration*). El modelo muestra su capacidad para representar adecuadamente varios procesos, incluyendo el crecimiento de los cultivos, la exportación de sedimentos, y la cantidad y calidad de

agua. Estos resultados confirman que SWAT es una herramienta apropiada para evaluar y predecir los efectos del uso del suelo y las prácticas agrícolas en la cantidad y calidad del agua en esta cuenca. De esta manera, se confirma la primera hipótesis planteada en este estudio, que sostiene que el modelo SWAT es capaz de representar de manera adecuada los procesos biofísicos y la calidad del agua de esta cuenca.

El segundo objetivo específico plantea evaluar la idoneidad y el desempeño del modelo SWAT para ser aplicado en Uruguay, e identificar oportunidades y limitaciones. Los resultados indican que el modelo SWAT es una herramienta adecuada para representar los cultivos y las prácticas de manejo del suelo en la cuenca del río San Salvador, así como los caudales y flujos de sedimentos y nutrientes derivados de estas actividades. Los principales tipos de cobertura y uso del suelo en Uruguay, como campo natural, cultivos, pasturas, ganadería y áreas urbanas, se han modelado con éxito en esta cuenca. Además, las características topográficas y climáticas presentan una relativa homogeneidad a lo largo del territorio uruguayo. Las fuentes puntuales de contaminación pueden incorporase en el modelo en función de las actividades específicas de cada zona. Por lo tanto, se identifica una oportunidad para utilizar el modelo SWAT en otras cuencas del territorio uruguayo. Sin embargo, es crucial reconocer las limitaciones que surgen de la falta de datos sobre la cantidad y calidad del agua. En Uruguay, las instituciones gubernamentales responsables del monitoreo a nivel nacional de caudales y calidad del agua son DINAGUA y DINACEA. Actualmente, existen 42 estaciones de monitoreo de caudal activas, lo que implica un promedio de una estación cada 4200 km^2. La mayoría de estas estaciones comenzaron a operar en la década de 1980, con una frecuencia de medición diaria o subdiaria. Por otro lado, la red de monitoreo de la calidad del agua superficial (sin incluir el monitoreo de playas) consta de 176 estaciones, lo que determina un promedio de una estación cada 1400 km^2. Esta red se desarrolló en su mayoría en la década de 2000, en general con una frecuencia de monitoreo trimestral. Aunque la red de monitoreo de calidad tiene una mayor densidad de estaciones en comparación con la de caudales, la serie histórica es de menor duración y no captura las variaciones rápidas de calidad de agua producto de descargas puntuales intermitentes o de variaciones en el caudal. Los datos de caudal y calidad de agua no siempre están disponibles en forma

conjunta, como en el presente estudio, donde, a pesar de existir el monitoreo de calidad de agua en varias subcuencas, la única estación de monitoreo de caudal se encuentra fuera de operación. En este sentido, la estrategia empleada en esta investigación para la calibración del caudal incluye la construcción de un mapa de uso del suelo del año 1990, dado que los datos observados se limitan al año 2000, junto con el ajuste de los caudales base. La falta de datos representa una limitación significativa en la evaluación de la calidad del agua y sugiere la necesidad de promover una mayor recopilación de datos tanto por los organismos gubernamentales como en futuros proyectos de investigación. Para mejorar la precisión de los resultados de los modelos, sería deseable disponer de muestreos de calidad de agua con frecuencia diaria en algunos sitios estratégicos complementando a la red de monitoreo existente, lo que permitiría capturar las variaciones de los parámetros que no se observan en un monitoreo trimestral. Sin embargo, la aplicación exitosa de la calibración blanda del modelo ha permitido validar los procesos biofísicos y de calidad de agua, incluso en ausencia de datos directos o cuando los datos observados son escasos, como el caso de los muestreos de calidad de agua trimestrales. Este enfoque ha resultado efectivo para abordar los desafíos derivados de la disponibilidad limitada de datos, al tiempo que ha contribuido a mejorar la precisión y confiabilidad del modelo. La segunda hipótesis planteada en este estudio, que sostiene la posibilidad de superar la limitación de datos y desarrollar un modelo confiable que aborde la gestión en la cantidad y calidad del agua teniendo en cuenta el impacto del uso del suelo, ha sido confirmada. Aunque existen incertidumbres asociadas a cualquier modelo de simulación, estas deben identificarse y considerarse al interpretar los resultados y tomar decisiones. En este contexto, el modelo SWAT ha demostrado ser una herramienta confiable para identificar tendencias generales y evaluar escenarios de alto impacto en la cuenca del río San Salvador.

El tercer objetivo específico plantea evaluar los potenciales impactos en la cantidad y calidad del agua en la cuenca del río San Salvador bajo diferentes escenarios, que incluyen el desarrollo de la agricultura irrigada y la aplicación de buenas prácticas agrícolas y medidas de conservación. Se ha logrado implementar en SWAT un escenario de desarrollo del riego en la cuenca del río San Salvador, que

incorpora un nuevo reservorio destinado a este fin. En la modelación del reservorio se ha considerado la erogación del caudal ambiental de acuerdo con la legislación vigente. Se han cuantificado las variaciones en la exportación de sedimentos y nutrientes en este escenario en comparación con el escenario base. Además, se han evaluado las variaciones en los caudales a la salida del reservorio en términos de curvas de frecuencia, así como la retención de nutrientes y sedimentos en el reservorio. La implementación del escenario de riego aumenta la exportación de sedimentos, nitrógeno y fósforo en comparación con el escenario base. Aunque el reservorio retiene una parte significativa de estos nutrientes y sedimentos, según la concentración promedio de fósforo del reservorio este se clasificaría como eutrófico. Por lo tanto, se recomienda la implementación de medidas de buenas prácticas agrícolas y de conservación que reviertan esta situación. Es importante señalar que SWAT tiene una representación simplificada de los reservorios, para obtener un mayor detalle en las dinámicas del reservorio, es posible utilizar modelos específicos acoplados. En un segundo escenario, se han incorporado zonas *buffer* ribereñas al escenario de riego con el objetivo de mejorar la calidad del agua en la cuenca. Los resultados de la simulación de escenarios muestran que existen opciones viables para disminuir los impactos negativos de la agricultura irrigada en la calidad del agua, mediante la implementación de zonas *buffer* ribereñas. Es importante notar que las zonas *buffer* deben tener un diseño y un manejo adecuado para alcanzar las eficiencias simuladas, de lo contrario podrían transformarse en una fuente de nutrientes. Las zonas *buffer* han demostrado ser efectivas en disminuir la exportación de nutrientes a los cursos de agua y mejorar en general la calidad del agua en la cuenca. Sin embargo, de acuerdo con la concentración promedio de fósforo modelada en el nuevo reservorio, este seguiría clasificándose como eutrófico. La tercera hipótesis plantea la viabilidad de encontrar una combinación de buenas prácticas agrícolas y medidas de conservación que minimicen los efectos negativos de la agricultura irrigada en la calidad del agua. Los resultados de esta investigación respaldan esta hipótesis al demostrar que la implementación *buffer* ribereñas contribuye significativamente a la mitigación de los impactos ambientales del riego agrícola en la cuenca del río San Salvador.

Sin embargo, es esencial considerar la aplicación de otras medidas aguas arriba del reservorio para mejorar la calidad de agua de manera integral.

5.3 REFLEXIONES FINALES

Esta investigación ha proporcionado una base científica sólida para abordar los desafíos que enfrenta la cuenca del río San Salvador en su búsqueda de un desarrollo de la agricultura irrigada sostenible y la preservación de sus recursos hídricos. Los logros alcanzados en la implementación y validación del modelo SWAT respaldan su utilidad en la evaluación de los efectos del uso del suelo y las prácticas agrícolas a escala de cuenca. Además, el enfoque de calibración blanda se presenta como una estrategia efectiva para superar las limitaciones de datos. Esta investigación no solo contribuye al entendimiento de la relación entre el uso del suelo y la calidad del agua, sino que también pone a disposición una herramienta práctica para la planificación y gestión de recursos naturales en la cuenca del río San Salvador.

Sin embargo, esta investigación identifica algunas limitaciones, como la escasez de datos de calidad del agua y la disponibilidad de datos de caudales solo hasta el año 2000 en una única estación hidrométrica. Es esencial considerar la incertidumbre asociada a los resultados del modelo al interpretar los hallazgos y tomar decisiones. En este contexto, el modelo SWAT ha demostrado ser una herramienta confiable para identificar tendencias generales y evaluar escenarios de alto impacto en la cuenca del río San Salvador.

Finalmente, de la experiencia recogida durante la investigación surgen algunas recomendaciones y propuestas para futuras líneas de investigación:

1. El modelo de la cuenca del río San Salvador demuestra ser apropiado para evaluar otros escenarios de alto impacto, algunos de los cuales no fueron abordados en esta investigación. Como se mencionó anteriormente, para lograr una intensificación agrícola sostenible que se refleje en la calidad del agua en la cuenca, es necesario implementar un conjunto integral de medidas de conservación y buenas prácticas agrícolas, las que pueden ser modeladas mediante escenarios. Entre los escenarios adicionales que pueden ser modelados en SWAT se encuentran: la

reducción de las fuentes difusas mediante el control de la erosión, la aplicación de medidas para prevenir el acceso de animales a los cuerpos de agua con el fin de reducir las cargas directas, así como el tratamiento y la gestión de los efluentes generados por tambos y encierros de engorde a corral. En esta línea, el modelo ofrece la posibilidad de abordar otros escenarios de interés que puedan surgir en el futuro.

2. El monitoreo y la modelación son complementarios. Por un lado, los modelos dependen de datos para su calibración y validación; por otro lado, los modelos permiten obtener información adicional, tanto en términos temporales como espaciales, a partir de los datos de monitoreo. Los esfuerzos de monitoreo, incluyendo la cantidad de puntos, las variables monitoreadas y la frecuencia, deben estar alineados con las preguntas que se buscan responder a través de la modelación. En este caso, para disminuir la incertidumbre del modelo, se recomienda mejorar la disponibilidad y calidad de datos. Se recomienda reanudar el monitoreo de los caudales, incluyendo, en la medida de lo posible, otras estaciones de medición y con tecnología que sea adecuada para la medición de caudales pico y de estiaje. En cuanto al monitoreo de calidad del agua, se recomienda incluir campañas de monitoreo continuo en algunos sitios estratégicos, complementando a la red de monitoreo existente, con el objetivo de capturar los rangos de variación de los parámetros que no son capturados con las campañas de monitoreo trimestrales.

3. Los aportes de las cargas directas (excreciones del ganado en los cuerpos de agua) y cargas puntuales (efluentes de tambos y encierros de engorde a corral) han mostrado ser de relevancia en el balance general de nutrientes en la cuenca. Este estudio proporciona estimaciones iniciales de ambas cargas que pueden ser perfeccionadas. En el caso de las cargas directas, es necesario determinar qué proporción del ganado en la cuenca accede libremente a los cursos de agua, y, en estos casos, se debería medir la cantidad de excretas que llega a los cuerpos de agua. En el caso de los efluentes de los encierros de engorde a corral, donde la gestión de los efluentes implica su almacenamiento en lagunas, se podría mejorar la caracterización de dichos efluentes (en este estudio se realizó una caracterización con un único análisis). Además, sería beneficioso desarrollar un modelo de vertido que tenga en

cuenta la escorrentía o el clima (en este estudio, se considera un vertido promedio continuo).

4. El modelo es una representación de la realidad construida a partir de la mejor información disponible en un momento dado. La incertidumbre asociada está relacionada con un propósito de modelación específico. En caso de que surja nueva información relevante de los procesos modelados, el modelo debe actualizarse, y puede requerir una nueva calibración y validación.

6 BIBLIOGRAFÍA

Arnold JG, Srinivasan R, Muttiah RS, Williams JR. 1998. Large-area hydrologic modeling and assessment Part I: model development. Journal of the American Water Resources Association, 34(1): 73-89. doi: 10.1111/j.1752-1688.1998.tb05961.x.

Aubriot LE, Delbene L, Haakonsson S, Somma A, Hirsch F, Bonilla S. 2017. Evolución de la eutrofización en el Río Santa Lucía: influencia de la intensificación productiva y perspectivas. INNOTEC, 14:07-16. doi: 10.26461/14.04Barreto P, Dogliotti S, Perdomo C. 2017. Surface Water Quality of Intensive Farming Areas Within the Santa Lucia River Basin of Uruguay. Air, Soil and Water Research, 10:1-8. doi:10.1177/1178622117715446

Beltran-Peña A, Rosa L, D'Odorico P. 2020. Global food self-sufficiency in the 21st century under sustainable intensification of agriculture. Environmental Research Letters, 15(9). doi: 10.1088/1748-9326/ab9388.

BRLI, SIGMAPLUS. 2017. Caracterización de las cuencas del río San Salvador, río Yí y río Arapey para fines de riego. Informe para el proyecto Desarrollo y Adaptación al Cambio Climático (DACC), Ministerio de Ganadería, Agricultura y Pesca (MGAP), Préstamo Banco Mundial 8099-UY. [En línea]. Consultado 13 de febrero de 2024. Disponible en: https://www.gub.uy/ministerio-ganaderia-agricultura-pesca/politicas-y-gestion/proyecto-caracterizacion-cuencas-del-rio-san-salvador-rio-yi-rio-arapey-para

Carpenter SR, Caraco NF, Correll DL, Howarth RW, Sharpley AN, Smith VH. 1998. Nonpoint pollution of surface waters with phosphorous and nitrogen. Ecological Applications, 8(3): 559-568. doi: 10.2307/2641247.

Foley J, Ramankutty N, Brauman K, Cassidy E, Gerber J, Johnston M, Mueller N, O'Connell C, Ray D, West P, Balzer C, Bennett E, Carpenter S, Hill J, Monfreda C, Polasky S, Rockström J, Sheehan J, Siebert S, Zaks D. 2011. Solutions for a Cultivated Planet. Nature, 478: 337–342. doi: 10.1038/nature10452.

FAO (Food and Agriculture Organization). 2013. Climate-Smart Agriculture Sourcebook (1st ed.). Rome. 557 p.

Goyenola G, Kruk C, Mazzeo N, Nario A, Perdomo C, Piccini C, Meerhoff M. 2021. Producción, nutrientes, eutrofización y cianobacterias en Uruguay: armando el rompecabezas. INNOTEC, 22: e558. doi: 10.26461/22.02

Goyenola G, Meerhoff M, Teixeira-de Mello F, González-Bergonzoni I, Graeber D, Fosalba C, Vidal N, Mazzeo N, Ovesen NB, Jeppesen E, Kronvang B. 2015. Phosphorus dynamics in lowland streams as a response to climatic, hydrological and agricultural land use gradients. Hydrology and Earth System Sciences Discussions, 12(3):3349-90. doi:10.5194/hessd-12-3349-2015

Hansen Z, Libecap G, Lowe S. 2009. Climate Variability and Water Infrastructure: Historical Experience in the Western United States. En: Libecap GD, Steckel RH. (eds.) The Economics of Climate Change: Adaptations Past and Present. Cambridge: University of Chicago Press. doi:10.3386/w15558.

Hastings F, Fuentes I, Perez-Bidegain M, Navas R, Gorgoglione A. 2020. Land-Cover Mapping of Agricultural Areas Using Machine Learning in Google Earth Engine. En: Gervasi O, et al. (eds.) Computational Science and Its Applications – ICCSA 2020: 20th International Conference, Cagliari, Italy, July 1–4, 2020, Proceedings, Part IV. Springer, Cham. 721–736. doi: 10.1007/978-3-030-58811-3_52

Hastings F, Perez-Bidegain M, Navas R, Gorgoglione A. 2023a. Impacts of irrigation development on water quality in the San Salvador watershed (Part 1): Assessment of current nutrient delivery and transport using SWAT. Agrociencia Uruguay [Internet], 27(NE1):e1198. doi: 10.31285/AGRO.27.1198.

Hastings F, Perez-Bidegain M, Navas R, Gorgoglione A. 2023b. Impacts of irrigation development on water quality in the San Salvador watershed (Part 2): Implementation of scenarios in SWAT. Agrociencia Uruguay [Internet], 27(NE1):e1199. doi: 10.31285/AGRO.27.1199.

Ketchum D, Hoylman ZH, Huntington J, Brinkerhoff D, Jencso KG. 2023. Irrigation intensification impacts sustainability of streamflow in the Western United States. Commun Earth Environ, 4: 479. doi: 10.1038/s43247-023-01152-2

Lizarralde C, Ciganda V, Baethgen W, Quincke A. 2016. Pérdida de nutrientes en agua de escurrimiento en sistemas de rotaciones contrastantes. Revista INIA, 46:41-3.

Merchán D, Causapé J, Abrahão R, García-Garizábal I. 2015. Assessment of a newly implemented irrigated area (Lerma Basin, Spain) over a 10-year period. II: Salts and nitrate exported. Agric. Water Manage. doi: 10.1016/j.agwat.2015.04.019

MGAP (Ministerio de Ganadería, Agricultura y Pesca). 2015. Estrategia de fomento del desarrollo de la agricultura regada en Uruguay: resumen ejecutivo. Montevideo, Uruguay. 40p. Consultado 13 de febrero de 2024. Disponible en: https://www.gub.uy/ministerio-ganaderia-agricultura-pesca/comunicacion/publicaciones/estrategia-fomento-agricultura-regada-uruguay-2015

MGAP-DIEA (Ministerio de Ganadería, Agricultura y Pesca-Oficina de Estadísticas Agropecuarias). 1994. Censo general agropecuario 1990. Montevideo, Uruguay. 239 p.

Naciones Unidas. 2018. La Agenda 2030 y los Objetivos de Desarrollo Sostenible: una oportunidad para América Latina y el Caribe. Santiago. 96 p.

Pinardi M, Soana E, Laini A, Bresciani M, Bartoli M. 2018. Soil system budgets of N, Si and P in an agricultural irrigated watershed: surplus, differential export and underlying mechanisms. Biogeochemistry, 140(2):175–197. doi: 10.1007/s10533-018-0484-4

Rodríguez-Gallego L, Achkar M, Defeo O, Vidal L, Meerhoff E, Conde D. 2017. Effects of land use changes on eutrophication indicators in five coastal lagoons of the Southwestern Atlantic Ocean. Estuarine, Coastal and Shelf Science, 188:116-126. doi: 10.1016/j.ecss.2017.02.010.

Rosa L. 2022. Adapting agriculture to climate change via sustainable irrigation: Biophysical potentials and feedbacks. Environmental Research Letters, 17(6). doi: 10.1088/1748-9326/ac7408.

Scanlon BR, Jolly I, Sophocleous M, Zhang L. 2007. Global impacts of conversions from natural to agricultural ecosystems on water resources: Quantity versus quality. Water Resources Research, 43(3). doi: 10.1029/2006wr005486.

Scholz R, Ulrich A, Eilittä M, Roy A. 2013. Sustainable use of phosphorus: A finite resource. Science of the Total Environment, 461: 799-803. doi: 10.1016/j.scitotenv.2013.05.043.

Shuman, LM. 2001. Leaching of phosphate and nitrate from simulated golf green. En: Proceedings of the 2001 Georgia Water Resources Conference, 26–27 de marzo, 2001. Atenas, GA, pp. 194–197.

Sigua GC, Stone KC, Bauer PJ, Szogi AA. 2020. Efficacy of Supplemental Irrigation and Nitrogen Management on Enhancing Nitrogen Availability and Urease Activity in Soils with Sorghum Production. Sustainability, 12(20):8358. doi: 10.3390/su12208358

Sigua GC, Stone KC, Bauer PJ, Szogi AA, Shumaker PD. 2017. Impacts of irrigation scheduling on pore water nitrate and phosphate in coastal plain region of the United States. Agricultural Water Management, 186:75–85. doi: 10.1016/j.agwat.2017.02.016

Smilovic M, Gleeson T, Adamowski J, Langhorn C. 2019. More food with less water – Optimizing agricultural water use. Advances in Water Resources, 123:256–261. doi: 10.1016/j.advwatres.2018.09.016

Uruguay. Poder Legislativo. 2017. Ley n.° 19.553. Modificación de la Ley 16.858, relativo al riego con destino agrario. [En línea]. Consultado 13 de febrero de 2024. Disponible en: https://www.impo.com.uy/bases/leyes/19553-2017.

Uruguay. Poder Legislativo. 2018. Decreto n.° 366. Reglamentación de la Ley 16.858, referente al riego con destino agrario y regulación del aprovechamiento de las aguas de dominio público. [En línea]. Consultado 13 de febrero de 2024. Disponible en: https://www.impo.com.uy/bases/decretos/366-2018.

US EPA (U. S. Environmental Protection Agency). 2007. An Approach for Using Load Duration Curves in the Development of TMDLs. Washington, DC. 68 p. [En línea]. Consultado 13 de febrero de 2024. Disponible en: https://www.epa.gov/sites/default/files/2015-07/documents/2007_08_23_tmdl_duration_curve_guide_aug2007.pdf

Van Dijk M, Morley T, Rau ML, Saghai Y. 2021. A meta-analysis of projected global food demand and population at risk of hunger for the period 2010–2050. Nature Food, 2: 494–501. doi:10.1038/s43016-021-00322-9.

Wang G-Y, Hu Y-X, Liu Y-X, Ahmad S, Zhou X-B. 2021. Effects of Supplement Irrigation and Nitrogen Application Levels on Soil Carbon–Nitrogen Content and Yield of One-Year Double Cropping Maize in Subtropical Region. Water, 13(9):1180. doi: 10.3390/w13091180